Water Quality Decay

and Pathogen Survival in Drinking Water

Distribution Systems

by

Precious Thabisile Biyela

A Dissertation Presented in Partial Fulfillment
of the Requirements for the Degree
Doctor of Philosophy

Approved October 2010 by the
Graduate Supervisory Committee:

Bruce E Rittmann, Chair
Morteza Abbaszadegan
Caitlyn Butler

ARIZONA STATE UNIVERSITY

December 2010

ABSTRACT

The deterioration of drinking-water quality within distribution systems is a serious cause for concern. Extensive water-quality deterioration often results in violations against regulatory standards and has been linked to water-borne disease outbreaks. The causes for the deterioration of drinking water quality inside distribution systems are not yet fully understood. Mathematical models are often used to analyze how different biological, chemical, and physical phenomena interact and cause water quality deterioration inside distribution systems. In this dissertation research I developed a mathematical model, the Expanded Comprehensive Disinfection and Water Quality (CDWQ-E) model, to track water quality changes in chloraminated water. I then applied CDWQ-E to forecast water quality deterioration trends and the ability of *Naegleria fowleri* (*N.fowleri*), a protozoan pathogen, to thrive within drinking-water distribution systems. When used to assess the efficacy of substrate limitation versus disinfection in controlling bacterial growth, CDWQ-E demonstrated that bacterial growth is more effectively controlled by lowering substrate loading into distribution systems than by adding residual disinfectants. High substrate concentrations supported extensive bacterial growth even in the presence of high levels of chloramine. Model results also showed that chloramine decay and oxidation of organic matter increase the pool of available ammonia, and thus have potential to advance nitrification within distribution systems. Without exception, trends predicted by CDWQ-E matched trends observed from experimental studies. When CDWQ-E was used to evaluate the ability *N. fowleri* to survive in finished drinking water, the model predicted that *N. fowleri* can survive for extended periods of time in distribution systems. Model results also showed that *N. fowleri* growth depends on the availability of high bacterial densities in the 10^5 CFU/mL range. Since HPC levels this high are rarely reported in bulk water, it is clear that in

distribution systems biofilms are the prime reservoirs *N. fowleri* because of their high bacterial densities. Controlled laboratory experiments also showed that drinking water can be a source of *N. fowleri*, and the main reservoir appeared to be biofilms dominated by bacteria. When introduced to pipe-loops *N. fowleri* successfully attached to biofilms and survived for 5 months.

DEDICATION

To my mother, Princess Tholakele Biyela (uMaGonya), for teaching me that life has no aspiration too great that I can not achieve with hard work and dedication and for modeling how to tackle all challenges, big and small, with the right combination of grace, strength, and tenacity.

ACKNOWLEDGMENTS

I am greatly indebted to Dr Bruce Rittmann, my advisor and committee chair, whose commitment to the success of every student under his wing, passion for research, and unparalleled professionalism helped me stay on course. I am humbled to have learnt from one of the greatest leaders in the field of environmental engineering.

I am grateful to the members of my PhD Advisory Committee, Drs. Morteza Abbaszadegan and Caitlyn Butler, for their valuable contribution to my research as well as general support. Not only did Dr Abbaszadegan recruit me to come and study at Arizona State University, he is also one of the people who opened my eyes to the reality that all things more exciting than microbiology occur at a place where microbiology intersects engineering. For that I thank him. I can not thank Dr Butler enough for agreeing to serve on my committee towards the end of my program.

During the course of my dissertation research I was privileged to work with and receive assistance from several individuals whom I owe thanks. Special thanks to Dr Seongjun Park for helping me with all the modeling aspects of my project. The amount of time and energy that Dr Park put to my work can only be surpassed by his patience and resourcefulness. He simply is the best. I also thank Drs Andrew Marcus and Randhir Deo for additional tips modeling and computer programming. The work on *Naegleria fowleri* was also a collaborative effort. Albert Brown and his students, including the late Daniel Kennedy, coordinated all field sampling for the study. Dr Abbaszadegan and his team, Drs Ryu and Absar, did all the microbiological analysis. I am particularly grateful to Dr Ryu for seeing all the microbiological work to completion.

My time and experience at the Center for Environmental Biotechnology (CEB) would have been very different without the support and camaraderie of my dear friend and colleague, Prathap Parameswaran. Not only did we join CEB at the same time, in the

spring of 2006, we also received adjacent desk spaces. It was great to prepare for and go through some of the major milestones in our program together. I can hardly do justice to the CEB team because of its size and ever-changing nature. But some of my co-workers deserve special mention. Cesar Torres, David Jackermeyer, Jon Badalamenti, Michal Ziv-El, and Youneng Tang all deserve special mention for their 'sunny' side. I am also grateful to the scholarly and emotional support I received from many CEB alumni including Dr Ahn, Astrid Zayas-Santiago, Ilsu lee, John Schloondorn, Kelvin Wong, Lijing Jiang, Linda Powell, Pei Zhang, and Dr Yongming Zhang among many others.

So many other people made my time at CEB easy and I owe them gratitude. Diana Hagner, our lab manager, was always available to help whenever needed. Dr Rittmann's office assistants: Dana Aguilar (current), Kyla Anderson (former), and Saunia Calloway (former), all rose to the occasion whenever I needed help.

Besides my colleagues at CEB I also received tremendous support from my friends, Andelline Moller, Ngoc Trung, Jane Ganda, Bella De-LaGarza, Chaya Dwarkanath, Fauzia Karim, Ayla Kiser, Elsy Escobar, Dalton and Khosi Lunga, Edwin Moshia, and Monica Joyi among many others. I am also grateful to my family at Mesa Baptist Church in general and particularly my 'Friday Family': Chandan Sood, Andre and Carolyn Bunnitt, Diana Jerowitz, Dolly Garcia, Jeanette Chervenka, Rachel Bush and her two boys, Gabe and Seun, Carl and Julie Fitchner, Josh, Grady, and many others who were a part of our home group at different points in time and whose love and support always lifted my morale. Also deserving of special mention are Bev, Carol, Diane, Esten, Gireh, Judy, Marge, Maureen, Mona, Nancy, Peggy, Sandra, and other members of DKG's Alpha Beta Chapter for all their support.

Finally, I owe a debt of gratitude to my family: my mother; my sisters, Sbuko, Philile, Zo, and Thale; my brother, Lindo, and all my nieces and nephews. Their love

and support helped me stay focused and motivated at all times. If I could have a chance to start life all over again and choose my own family, I would still choose my family, every single person in my family.

Fellowships from the Fulbright Educational and Cultural Exchange Program, Delta Kappa Gamma Society International, the National Research Foundation of South Africa, and the Oppenheimer Memorial Trust as well as a grant from the Arizona Water Institute made it financially possible for me to finish this work and I am thankful to each one of these organizations.

TABLE OF CONTENTS

Page

LIST OF TABLES

LIST OF FIGURES

Figure Page

Chapter 1

Background and Significance

Access to good quality drinking water is essential for the protection, promotion, and maintenance of public health. Historically, the bulk of drinking water regulations in the United States (US) focused on treatment plant effluent quality (USEPA, 1974, 1975, 1979, 1989). This approach to drinking water regulation was based on the assumption that once treated, water remains potable until the time of use. Recent studies have shown that the quality of drinking water can deteriorate significantly between the treatment plant and the point of use (LeChevallier et al., 1996; Li et al., 2000; Momba et al., 2000; Norton and LeChevallier, 2000; Pontius, 2000; Szewzyk et al., 2000; Woolschlager, 2000; Le Dentec et al., 2002; Zhang and DiGiano, 2002; Camper et al., 2003; Uber et al., 2003; Le Puil, 2004; Woolschlager et al., 2005; Krasner et al., 2006; D'Souza and Kumar, 2010; Grigorescu and Hozalski, 2010; Zhang and Edwards, 2010). This realization has resulted in a shift towards a multi-barrier approach to drinking water quality monitoring and regulation (USEPA, 1996, 1998, 2002, 2003, 2005, 2010). Within this framework drinking water regulations can be divided into two distinct branches, one branch dealing with treatment plant effluent quality and the other branch dealing with the maintenance of the quality of treated water during distribution.

Table 1.1 is a summary of key US federal drinking water regulations. The majority of regulations passed after 1996 deal with the maintenance of drinking water quality after the treatment barrier. Issues addressed in these regulations include enhanced protection from microbial pathogens while complying with requirements for minimizing disinfection by-product (DBP) formation. For example, the Interim Enhanced Surface Water Treatment Rule (IESWTR), amalgamated in 1998, and the Long Term 1 Enhanced Surface Water Treatment Rule (LT1ESWTR), amalgamated in 2002, provides guidelines

to enhance protection from microbial pathogens while complying with requirements set out in Disinfection By-Product Rule Stage 1 (DBPR1). Other regulations provide treatment recommendations for the removal of specific microbial pathogens. For example, the Long Term 2 Enhanced Surface Water Treatment Rule (LT2ESWTR), amalgamated in 2005, mandates at risk public water systems to monitor their water sources to determine treatment requirements for the removal of Cryptosporidium, a protozoan pathogen. Regulations aimed at controlling disinfection by-products formation have also gotten more stringent. For example, DBPR1, amalgamated in 1998, requires monitoring of total trihalomethanes (TTHMs) at selected sites along a distribution network but determines compliance by estimating a running annual average for all monitoring sites across the entire distribution system. Its successor, Disinfection By-Product Rule Stage 2 (DBPR2), amalgamated in 2005, requires compliance with the maximum contaminant levels for TTHM and haloacetic acids (HAAs) at each monitoring site in the distribution system.

Table 1.1 Evolution of US Federal Drinking Water Regulations

Regulation	Key Distribution System Requirements	Passed
SDWA	gives EPA authority to establish national primary and secondary drinking water regulations	1974
NIPDWR	requires that representative coliform samples be collected throughout the distribution system	1975
TTHM Rule	established a standard for TTHMs as 0.1 mg/L	1979
TCR	regulates coliform bacteria which are used as surrogate organisms to indicate whether or not treatment is effective and if system contamination is occurring	1989
SWTR	requires using chlorine or some other disinfectant	1989
96SDWAA	several provisions dealing with distribution systems, including role that source water quality plays in influencing the quality of distributed water	1996
IESWTR	provisions to enhance protection from microbial pathogens for large systems while they comply with the DBPR1	1998
DBPR1	lowered the standard for TTHMs from 0.1 mg/L to 0.08 mg/L and requires monitoring at selected points along distribution network	1998
LT1ESWTR	provisions to enhance protection from pathogens for systems serving less than 10,000 people while they comply with the DBPR1	2002
DBPR2	requires compliance with the maximum contaminant levels for TTHM and HAAs at each monitoring location in the distribution system instead of determining compliance by calculating the running annual average of samples from all monitoring locations across the system as required by DBPR1	2005
LT2ESWTR	requires all public water systems that use surface water or ground water under the direct influence of surface water to monitor their water sources to determine treatment requirements for the removal of Cryptosporidium	2005
Proposed Revisions to the Total Coliform Rule	requires public water systems that are vulnerable to microbial contamination to identify and fix problems. Also establishes criteria for systems to qualify for and stay on reduced monitoring, thereby providing incentives for improved water system operation	2010 proposed

Acronyms: SDWA, Safe Drinking Water Act; NIPDWR, National Interim Primary Drinking Water Regulation; TTHM Rule, Total Trihalomenthane Rule; TCR, Total Coliform Rule; SWTR, Surface Water Treatment Rule; 96SDWAA, 1996-Safe Drinking Water Act Amendment; IESWTR, Interim Enhanced Surface Water Treatment Rule; DBPR1, Disinfection By-Product Rule Stage 1; LT1ESWTR, Long Term 1 Enhanced Surface Water Treatment Rule; DBPR2, Disinfection By-Product Rule Stage 2; LT2ESWTR, Long Term 2 Enhanced Surface Water Treatment Rule.

Several factors have led to the increased attention being placed on the investigation, protection, and control of drinking water quality as it is distributed after treatment.

First, consumer expectations about the quality of treated water are rising. The amended Safe Drinking Water Act (USEPA, 1996), under the right-to-know provisions, mandates drinking water utilities to prepare and disseminate annual drinking water quality reports. Above and beyond letting consumers know what is in their water, these reports seek to (i) promote dialogue between consumers and water utilities, (ii) raise consumer awareness about water quality issues and their implications, (iii) promote confidence in municipal water quality, and (iv) help consumers make informed decisions about water use issues (USEPA, 2003). A 2003 Gallup poll reported that 37% of respondents residing within municipalities that disseminate annual drinking water quality reports acknowledged receiving these reports. Furthermore 78% of the respondents who recalled receiving the reports took time to read them (USEPA, 2003).

Ironically, improved awareness about water quality issues is happening at the same time that water suppliers are being forced to use sources that have poorer quality. A 2006 report by the Environmental News Service (ENS) revealed that between July 2003 and December 2004 two thirds of industrial and municipal facilities across the US discharged more pollution into the country's waterways than their Clean Water Act permits allowed for that time period (ENS, 2007). While the ENS report offered no details about the extent to which this increased pollution impacts drinking water or the connection to distribution systems, this is a cause for concern. First, technologies conventionally used to treat drinking water are not always capable of removing some of the chemicals often found in industrial wastes. If by any chance some of these industrial pollutants bypass the treatment barrier and end up in distribution systems they may alter

the rates and even types of chemical and biological reactions that occur inside distribution systems and potentially lead to a myriad of water quality issues within distribution systems.

While chronic contamination, typified by effluent discharges from local and regional industrial facilities is a serious course for concern it is not the only form of industrial contamination that ends up in waterways. There is also an ever present threat of contamination from man-made environmental disasters, such as the 1989 Exxon Valdez oil spill and the 2010 BP spill along the Gulf of Mexico, both of which released exceedingly large volumes of crude oil into waterways over relatively short periods of time. Again, the presence of any pollutant in high concentrations in source waters increases the likelihood for that pollutant to find its way into drinking water distribution systems.

Second, the development of new analytical techniques, especially bacterial enumeration techniques such as fluorescence microscopy (Hobie *et al.*, 1977) and heterotrophic plate counts using low nutrient R2A agar (Reasoner and Geldreich, 1985), coupled with the growing degree of drinking water regulations (USEPA 1989, 1996, 1998, 2002, 2005, 2010) are placing more pressure on water purveyors to produce and deliver high-quality water.

Third, in the aftermath of the September 11 (2001) terrorist attacks, the US has experienced resurgence in concerns about the vulnerability of drinking water distribution networks to intentional contamination. 2002 saw the enactment of the Public Health Security and Bioterrorism Preparedness and Response Act (PL 107-188). This law requires that all community water systems serving upwards of 3,300 people set up

vulnerability assessments and emergency response plans (Bioterrorism Act, 2002; USEPA 2003, 2004, 2005).

To meet existing and future regulations on water quality, drinking water utilities ought to adopt more advanced approaches to water treatment and distribution systems management. This is only possible if processes that affect water quality within the distribution system are well-understood. While individual processes can be easily monitored and analyzed, multiple, interrelated processes need to be considered simultaneously in order to grasp the full extent of water quality deterioration within distribution systems.

Because of their ability to handle large amounts of data mathematical models provide a valuable tool for studying water quality deterioration within distribution systems. Not only do models allow the simultaneous analysis of biological, chemical, and hydraulic processes, they also allow the analysis of all processes and changes across space and time dimensions.

The general goal of this dissertation research was to develop and utilize a dynamic model for examining biological and chemical processes that control water quality and the growth of *Naegleria fowleri* (*N.fowleri*), a protozoan pathogen, inside distribution systems. The model developed in this research is called the Expanded-Comprehensive Disinfection and Water Quality Model (CDWQ-E).

This project was divided into two core parts. The first part was the development of the CDWQ-E model. This involved five steps, defining key processes that affect water quality decay in chloraminated water, writing mass-balance equations to represent these processes, writing a computer code to solve the equations, debugging the code, and validating the code to ensure mass-balance closure on all modeled species.

The second part was the application of the CDWQ-E model to investigate water quality deterioration and *N. fowleri* growth after the treatment barrier. This involved three steps: (i) using CDWQ-E to compare the efficacy of nutrient substrate limitation and disinfection to control heterotrophic growth in chloraminated drinking water, (ii) measuring water quality parameters, such as chlorine residuals, dissolved organic carbon (DOC), biodegrabable dissolved organic carbon (BDOC), dissolved oxygen (DO), total ammonia ($CtNH_3$), ammonium (NH_4^+), nitrite (NO_2^-), nitrate (NO_3^-), heterotrophic plate counts (HPC), and detecting general amoebic activity and *N. fowleri* in water and biofilm samples obtained from two full-scale distribution systems and two laboratory scale pipe–loop systems, (iii) using CDWQ-E to analyze water quality decay trends and occurrence and survival of *N. fowleri* within distribution systems.

The experimental work on *N. fowleri* involved a three-way research partnership among three research groups at Arizona State University. The first team (Albert Brown, Daniel Kennedy, and Samrath Madan) collected all water and biofilm samples from two participating distribution systems. This also included on-site measurement of temperature, pH, dissolved oxygen, and chlorine residuals. The second team (Drs Morteza Abbaszadegan, Hodon Ryu, and Absa Alum) set up and ran the pipe loop simulator and assayed all (field and laboratory) water and biofilm samples for general amoebic activity and the presence of live *N. fowleri*. The third team (Dr Bruce Rittmann and I) assayed all water and biofilm samples for chemical water quality parameters (DOC, BDOC, ammonia, nitrate, nitrite, and HPC). I also developed the CDWQ-E model, gathered and interpreted all field and laboratory data from the three groups, and helped with the overall coordination of the project.

Finally, the CDWQ-E model was used to interpret and analyze water quality trends observed in full-scale distribution systems and pipe-loops as well the ability of

introduced *N. fowleri* to survive within pipe-loop systems. This confirmed the power of the CDWQ-E model to provide a refined interpretation of water quality trends and *N.fowleri* survival observed in distribution systems and pipe-loops.

Due to its prognostic capability, the CDWQ-E model has potential for use in treatment process design and optimization as well distribution system operation to ensure that the quality of water that reaches consumers conforms to set regulations.

1.1. Introduction to Drinking water Distribution Systems

1.1.1 Distribution System Design and Operation

Distribution systems (DS) are a major part of water utilities. From a design point of view, a distribution system must deliver water from a treatment plant to customers in the required quantity and quality at a satisfactory pressure at all times (Mays, 2001; Walski et al., 2003). To be able to meet the requirements for pressure and quantity, a typical distribution system requires the following: (i) A network of pipes to carry water from the treatmnet plant, or another source such as a well, to consumers (ii) Storage reservoirs to provide storage facility to meet variations in water demand. (iii) Pumps to apply energy to the water in order to boost it to high elevations as well as to increase pressure. (iv)Valves to isolate sections of distribution system for maintenance and repair (isolation valves) and to regulate water pressure within the distribution system (control valves). (v) Fire Hydrants – to support fire flows when needed (Fair and Geyer, 1971; Mays, 2001; Walski et al., 2003; ISO, 2003).

1.1.2 Distribution Systems as Dynamic Reactors

The way in which distribution systems are designed and operated provides numerous opportunities for the quality of treated water to degrade between the treatment

plant and the point of use (Gelderich et al., 1972; LeChevallier et al., 1987; Maul et al., 1985; LeChevallier et al., 1996; Momba et al., 2000; Zhang and DiGiano, 2002; Camper et al., 2003; Le Puil, 2004, Woolschlager et al, 2005; MSU-CBE, 2010). Inside distribution systems, numerous physical, biological, and chemical reactions occur as a result of interactions among dissolved chemical species, deposits, pipe materials, and water-wall and water-air interfaces in the pipes.

Figure 1.1 shows some of the main interactions that affect water quality decay inside distribution systems, including reactions that occur in the bulk water, on pipe surfaces, and in biofilms that form on pipes. Over time and space, these interactions can lead to bacterial growth, biofilm formation, loss of residual disinfectants, formation of disinfection by-products, coloration, and many other undesired changes (Geldreich et al., 1972; LeChevallier et al., 1987; Maul et al., 1985; LeChevallier et al., 1996; Li et al., 2000; Momba et al., 2000; Zhang and DiGiano, 2002; Camper et al., 2003; Le Puil, 2004, Woolschlager et al, 2005; Grigorescu and Hozalski, 2010; Zhang and Edwards, 2010).

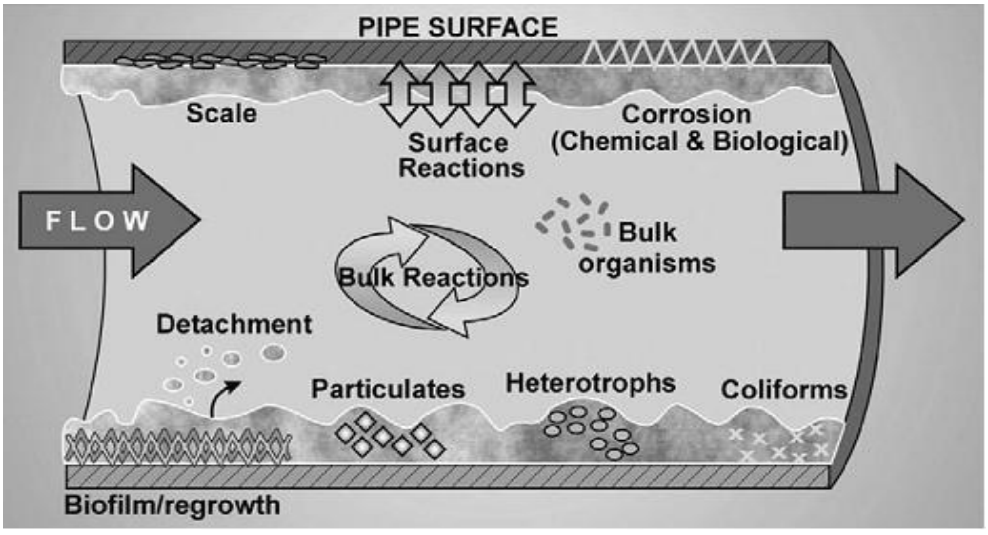

Fig1.1 Main Interactions Affecting Water quality decay Inside Distribution Systems (MSU-CBE, 2010)

1.2 Reasons for Water quality decay Inside Distribution Systems

While distribution system design makes water quality decay inevitable during distribution design alone does not account for the full extent of water quality decay that is reported in some distribution systems. The reasons for the extensive deterioration of the quality of treated drinking water within distribution systems are not yet fully understood, but five of the main factors that play a role in this have been studied and are discussed below, they are water age, type of treatment and the quality of treated water at the time that it enters the distribution system, type of pipe materials with such attendant problems as susceptibility to corrosion and the propensity to support biofilm formation, bacterial growth and accumulation, and loss of residual disinfectant and the formation of disinfection by-products (Geldreich et al., 1972; LeChevallier et al., 1987; Maul et al., 1985; Momba et al., 2000; Zhang and DiGiano, 2002; Camper et al., 2003; Le Puil, 2004, Woolschlager et al, 2005).

1.2.1 Water Age

The length of time that water is retained within the distribution system depends on the size of the physical distribution infrastructure, water demand, and such system operational parameters as pressure and flow rate (Mays, 2001). A well-designed distribution system is one that can maintain pressures and quantities needed to meet future needs and to provide reserve flows for fire fighting, power outages, and other emergencies. As a result, most drinking water distribution systems are hydraulically over-sized (Mays, 2001; Grayman et al., 2004; AWWA 2005; USEPA, 2005).

In an average municipal distribution system less than 25% of the water in storage reservoirs is used daily under normal conditions. The other 75% is set apart for emergencies and fire fighting (USEPA, 2005). The average distribution system has a mean detention time of 1.3 days and a maximum detention time of 3.0 days (AWWA,

2005). Hence, detention times less than 1.3 days can be considered short, while detention times longer than 3.0 days can be considered long. Long detention times are typical of dead-ends and other areas within the distribution network where water tends to stagnate (DiGiano et al., 2000; Prentice, 2000; Acker and Krasa, 2001; Vandermeyden and Hartman, 2001). Table 1.2 below shows a summary of water age evaluations from a survey done by AWWA (2005) on more than 800 US utilities. Clearly, systems serving small populations are more prone to have "old" water.

Table 1.2 Water Age Estimations (AWWA, 2005)

Population Served	Water Mains (Miles)	Ranges of Age (Days)
750,000	1,100	<1 – 3
800,000	2,750	3 - 7+
87,900	358	>16
24,000	86	12 – 24

Water age is arguably the most vital determinant of the extent to which the quality of treated water deteriorates within distribution systems.

Reactions that affect the deterioration of water quality within distribution systems occur between the water and the pipe walls, as well as in the bulk water as it moves through networks of pipes from the treatment plant to the point of use. Examples of such reactions include microbial oxidation of organic matter, microbial growth and decay, biofilm formation and detachment, disinfectant decay, and oxidation of organic matter by disinfectant residuals among others. Longer detention times can provide greater opportunity for all chemical and biological interactions known to affect water quality within the distribution system (Geldreich et al., 1972; LeChevallier et al., 1987; Maul et al., 1985a and b; Zhang and DiGiano, 2002; Camper et al., 2003; AWWA, 2005). Table 1.3 below is a summary of water quality problems associated with water age. This table

clearly shows that water-age is the most over-arching influence in distribution system water quality exerting an influence on several biological, chemical, and physical water quality issues.

Table 1.3 Water Quality Problems Associated with Prolonged Residence Times (AWWA, 2005)

Biological issues	Chemical issues	Physical issues
microbial growth and pathogen protection	disinfectant decay and DBP formation	biofilm accumulation
nitrification and denitrification	corrosion control effectiveness	temperature increases
taste and odor	taste and odor	Color

1.2.2 Water Treatment

In the United States and most developed countries, surface water is generally treated using flocculation, sedimentation, filtration, and disinfection.

The aim of disinfecting water is to kill pathogenic microorganisms and also to lower levels of heterotrophic bacteria in the treatment plant effluent. Disinfection at the treatment plant, called primary disinfection, is usually achieved by ozonation, UV radiation, and chlorination (Hack, 1984; AWWA, 1990; Hall and Dietrich, 1999; Woolschlager 2000; Le Puil, 2004). Primary disinfection ensures that the water is free of pathogenic microorganisms and that the levels of non-pathogenic, nuisance, organisms are also low when the water leaves the treatment plant (LeChevallier et al., 1987; Zhang and DiGiano, 2002; Camper et al., 2003; Le Puil, 2004; USEPA, 2005).

Residual disinfection takes place after treatment and as the water enters the distribution system. Some distribution systems have booster chlorination stations, where chlorine or chloramine is injected to the water as it passes through. Maintaining a

disinfectant residual suppresses bacterial growth during distribution and acts as a sentinel to detect intrusions or breaches within the distribution system. Failure to maintain recommended concentrations of residual disinfectant may lead to increased health risks if the distribution system is contaminated by pathogenic microorganisms downstream of the treatment process (White, 1986; Le Puil, 2004; Richards et al., 2005). Most water utilities in the United States use free chlorine or chloramine, chlorine combined with ammonia, for residual disinfection. Other chlorine species, such as chlorine dioxide, also work as residual disinfectants, but are less widely used (Woolschlager, 2000). Treating drinking water prior to distribution can help alleviate water quality problems associated with long detention times by improving the biological stability of finished water (AWWA, 2005).

1.2.3 Type of Pipe Materials

The type of materials used for pipe infrastructure also influences water quality decay. Corrosion, massive system failure, and biofilm formation have been linked to certain types of pipe materials (Momba et al., 2001; Woolschlager, 2000; Le Puil, 2004; Zhang et al., 2008; Zhang and Edwards, 2010). Pipes made entirely of cast iron, for example, are more prone to corrosion than ductile iron, vinyl, and reinforced concrete pipes (Woolschlager, 2000; Zhang et al., 2008; Zhang and Edwards, 2010).

Pipe corrosion products adversely affect the quality of water being transported. Corroding metal, usually thought of in terms of rust, may take many forms. In the case of buried cast iron pipes, the corroded material is a hard, graphitic substance that temporarily maintains the shape of the pipe wall and looks like iron, but provides minimal strength if any. Later, the material forms pits, which, in some cases, penetrate the wall, exposing water to potential contamination, leakage, and premature failure.

Corrosion of iron pipes is also known to exert significant amounts of chlorine demand through the reactions of chlorine with corrosion products, as well as the concentrated biomass that is found in corrosion zones. Ductile iron, vinyl, and reinforced concrete pipes are not as much prone to corrosion, and they now represent the bulk of pipelines being used in the United States (Woolschlager, 2000; Mays, 2001; Le Puil, 2004; Zhang et al., 2008; Zhang and Edwards, 2010).

Another water quality phenomena related to types of pipe materials is biofilm formation (Vasconcelos et al., 1997; Kiene et al., 1998; Woolschlager, 2000; Dubiel et al., 2002; Momba et al., 2002; Richardson, 2005). Again, iron pipes, particularly in corrosion zones, tend to support more biofilm accumulation than pipes made of plastic materials. There are four possible explanations for this. First, corrosion zones provide an environment in which electron donor substrates, such as dissolved ferrous iron, may be available in high enough concentrations to support the growth and proliferation of fastidious microbial communities such as iron oxidizing bacteria that may not otherwise do well in conditions typical of distribution system environments. Second, concrete and iron pipes surfaces support more biofilm accumulation than plastic pipes, because their rougher surface protects biofilms from detachment. Third, solid corrosion products, such as scale and tubercles, may shelter microorganisms from disinfection and detachment, thus leading to further bacterial accumulation. Fourth, chlorine is consumed in the oxidation of Fe^{2+} produced by corrosion processes to Fe^{3+}. This increases the demand for chlorine leaving relatively less chlorine available for microbial disinfection (Woolschlager, 2000; Dubiel et al., 2002; Momba et al., 2002).

In a study comparing two distribution systems, one with iron pipes and the other with synthetic plastic pipes, Kiene and co-workers (1998) showed that corrosion of iron-pipe surfaces was alone responsible for 57% of total chlorine demand. Deposits on pipes

accounted for a further 25% of the total chlorine demand. Since pipe deposits (in iron pipes) are mostly composed of corrosion products, the total chlorine demand that can be attributed to iron pipe wall corrosion in this study was upwards of 80%. This is not the only study in which reactions on the pipe surfaces were shown to have a significantly greater chlorine demand than reactions occurring in the bulk water. Woolschlager (2000) reported that more chloramine is lost due to surface catalysis reaction on cement pipes than is lost through reactions in bulk water (Woolschlager, 2000).

1.2.4 Bacterial Growth and Accumulation

Bacterial growth in drinking water distribution systems is not desired. Since one essential objective of drinking water treatment is to protect consumers from infectious diseases, drinking water treatment provides multiple barriers to ensure that pathogenic microorganisms are not present in the treated water. However, drinking water and distribution systems are not sterile. Growth and accumulation of bacteria in the distribution system opens up the possibility that pathogens can be present at the consumer's tap, even when the treated water is pathogen free at the point of entry to the distribution system (Rose, 1997, Momba et al., 2000, Norton and LeChevallier, 2000, Szewzyk et al., 2000, Le Dentec et al., 2002, Le Puil, 2004).

Bacterial growth inside drinking water distribution system can arise due to the presence of bio-available electron-donor substrates and the absence of sufficient disinfectant residual. In general, growth substrate and disinfectant residuals are counter forces to each other. A higher substrate concentration demands a higher disinfectant concentration to suppress growth (Woolschlager, 2000; Le Puil, 2004).

The presence of electron-donor substrates, such as biodegradable dissolved organic matter (BOM) and ammonium, in finished water is the most fundamental cause of bacterial growth and accumulation in distribution systems. Other relevant electron

donors can be nitrite (NO_2^-), ferrous iron (Fe^{2+}), and manganese (Mn^{2+}) (Bourbigot *et al.*, 1984; Rittmann and Snoeyink, 1984; Rittmann and Huck, 1989; LeChevallier *et al.*, 1991; van der Kooij, 1992; Block *et al.*, 1993; Servais *et al.*, 1993; Rittmann et al., 1994; Mathieu *et al.*, 1995; Prevost *et al.*, 1997; Chandy and Angles, 1999; Woolschlager 2000, Regan et al., 2002; Le Puil, 2004). These and any other bio-available electron donors are called biological instability. Water is said to be biologically stable when it contains electron donor substrates at concentrations that are below the levels required to support significant bacterial growth or when it contains residual disinfectants at concentrations that are high enough to kill or inactivate bacteria at a rate that is equal to or exceeds the overall rate of synthesis.

Bacterial growth also can be increased by such factors as the presence of open storage reservoirs, pipeline breaks, construction work, back-siphonage of soil organic matter due to transiently low pressure within the distribution system, and the revival of microorganisms that have been injured by disinfection but not killed (Geldreich, 1996; Le Chavallier et al., 1996; D'Souza and Kumar, 2010).

Whatever its cause may be, proliferation of microorganisms in drinking water distribution systems may result in non-compliance to government-set quality standards, increased likelihood of waterborne illness, enhanced corrosion, increased turbidity, and taste and odor problems (Le Chavallier et al., 1996; Momba et al., 2000; Woolschlager, 2000; Le Puil, 2004; D'Souza and Kumar, 2010).

1.2.5 Loss of Residual Disinfectant and Formation of Disinfection By-Products

The purpose of adding residual disinfectants is to minimize overall bacterial activity in treated water during distribution, as well as to kill pathogenic microorganisms that might enter the distribution system downstream of the treatment process (LeChevallier et al., 1998a; LeChevallier et al., 1998b; Norton and Le Chavallier 2000).

In the past, high concentrations of chlorine were applied to achieve these goals in the face of chlorine decay and biological instability. Nowadays, regulations to control the formation of harmful disinfection by-products (DBPs) limits how much chemical disinfectant can be used in treating water that is meant for human consumption (USEPA 1998, 2002, 2005). As a result, the ability to maintain adequate control over microbial contaminants while minimizing the health risks associated with DBPs has emerged as one of the most important challenges that water supply professionals must deal with (Li et al., 2000; Woolschlager 2000; Le Puil, 2004; Zhang et al., 2004; Krasner et al., 2006; Grigorescu and Hozalski, 2010; USEPA, 1998, 2002).

The need to balance disinfection efficacy and DPB control has caused some US utilities to switch from using chlorine as both primary and secondary disinfectant to using chloramine as secondary disinfectant and only keeping chlorine as a primary disinfectant. This change was mainly triggered by an increase in reports showing evidence of the formation of high levels of total trihalomethanes (TTHMs) from chlorine in drinking water distribution systems. Because TTHMs are linked to certain types of cancers, the EPA now mandates drinking water utilities to reduce TTHMs along with haloacetic acids (HAAs) and many other chlorine derived by-products from drinking water supplies (USEPA 1998, 2002). While chlorine still remains the most used widely used residual disinfectant, a significant percentage of US utilities now use chloramine as residual disinfectant following the passage of this mandate (Neden *et al.*, 1992; Norton and LeChevallier, 1997; Woolschlager, 2000; Richardson, 2005). On top of aiding with the reduction of TTHMs and HAAs chloramine has also been shown to be more effective at controlling distribution system biofilms than free chlorine.

Chloramine is formed by combining chlorine and ammonia via an electrophilic substitution reaction. Chloramine retains the oxidizing power of free chlorine, but is less

reactive with organic matter. On the one hand, being less reactive makes chloramine more persistent than chlorine; therefore, relatively smaller doses can be used to maintain a sufficient disinfectant residual throughout the distribution system in some cases. The longer persistence of chloramine residuals within distribution systems also results in more effective biofilm control, as well as better control of offensive tastes and odors, in chloraminating systems versus chlorinating systems. Also, because they react less with organic matter, chloramines form less THMs and HAAs than chlorine (LeChevallier et al., 1988; Neden *et al.,* 1992; Chen *et al*., 1993; Norton and LeChevallier, 1997; Woolschlager, 2000).

While chloramination offers certain water quality benefits, its increased use presents a different set of problems to the water-supply industry. First, the reduction in THMs and HAAs has been coupled with increased levels of chloral hydrate and nitrogen-based DBPs, such as iodo-acids, iodo-THMs, NDMA, and other nitrosamines. Already, toxicity studies have revealed that several of these DBPs are more genotoxic (in isolated cells) than many of the DBPs currently regulated, and new occurrence data has revealed that many of these DBPs can, in some cases, be present at levels comparable to regulated DBPs i.e. 0.08 mg/L (Nikolaou et al., 1999; California, 1999; WHO, 2000; Richardson, 2005). Second, chloramination triggers nitrification events that may support algal blooms in reservoirs and increase overall bacterial activity throughout the distribution system (Woolschlager, 2005). Third, some utilities failed to meet the concentration time (CT) rule when chloramines were used as a primary disinfectant, because chloramine is a weaker disinfectant than chlorine and needs a higher CT for the same degree of disinfection. Finally, the long term persistence of chloramine could potentially depend more on pipe materials than previously thought. Woolschlager (2000) demonstrated that chloramine decays much faster in distribution systems or sections of distribution systems

with concrete pipes. This is because of surface catalysis reactions. These reactions alone accounted for up to 40% of total chloramine demand (Woolschlager, 2000).

1.3 Implications of Post Treatment Water Quality Decay

Post-treatment water quality decay can lead to problems ranging from nuisance complaints about unpleasant tastes and odors, through serious breaches of standing regulatory standards, to consumer exposure to serious health threats. Key among problems associated with post-treatment water quality decay are issues associated with extensive bacterial growth which could lead to violations of coliform standards, extensive biofilm formation, nitrification and denitrification, and the growth and spread of microbial pathogens and opportunistic pathogens.

1.3.1 Extensive Bacterial Growth

Enhanced microbial growth inside drinking water distribution systems is associated with violations of coliform counts, interference with coliform detection, increased biological nitrification, loss of disinfectant residuals, depletion of dissolved oxygen, and extensive biofilm formation among other things (Le Chavallier et al., 1996; Rose, 1997; Momba et al., 2000; Norton and LeChevallier, 2000, Szewzyk et al., 2000; Woolschlager, 2000; Le Dentec et al., 2002; Le Puil, 2004; D'Souza and Kumar, 2010). An over-abundance of heterotrophic bacteria inside a distribution system can mask serious health threats, such as cross-connections and other forms of bacterial intrusions that may occur downstream of the treatment plant (LeChevallier and McFeters, 1985; Geldreich, 1996; LeChevallier *et al.*, 1996; Woolschlager, 2000).

1.3.2 Extensive Biofilm Formation

Biofilms exist to varying degrees in all drinking water distribution systems. Distribution system biofilms have been implicated in problems ranging from nuisance

complaints, such as changes in taste, odor, and color, to problems that have regulatory implications (Characklis, 1981; Camper et al., 1991; Dukan et al., 1996; Murga et al., 2001; Donlan, 2002; Banning et al., 2003; Morato et al., 2004; Appenzeller et al., 2005). Extensive biofilm formation on pipe surfaces plays a role in increasing heterotrophic plate counts, nitrification, denitrification, depletion of disinfectant residuals, corrosion, and depletion of dissolved oxygen (Woolschlager, 2000; Woolschlager et al., 2005).

Also, distribution system biofilms play a major role in the sorption of planktonic microorganisms from the bulk water, including coliforms, pathogens, and opportunistic pathogens. Biofilm-bound organisms serve as a continuous source of inoculation for bulk water and pipe surfaces downstream. This phenomenon may lead to occurrence of high levels of heterotrophic plate counts, coliforms, and pathogens inside distribution networks with no obvious breaching of treatment barriers (Camper et al., 1991; Donlan, 2002; Morato et al., 2004). Understanding the role that biofilm formation plays in the survival and spread of microbial pathogens within distribution systems is vital for the protection of public health.

Whether residence within a biofilm is detrimental or beneficial to a pathogenic microorganism depends on how well the pathogen in question is able to interact with and or compete with indigenous biofilm microorganisms.

On the one hand, pathogens have been shown to have the ability to attach to surfaces and existing biofilms without being able to grow within biofilms. Banning and co-workers (2003) showed that biofilms established from indigenous river water bacteria were able to reduce the persistence of introduced *Escherichia coli* (*E.coli*) and other enteric pathogens. A similar observation was also reported by Camper and co-workers (1985) when they were studying the interactions between indigenous fresh water bacteria and enteric pathogens grown on granular activated carbon.

On the other hand, pathogens and opportunistic pathogens grown in biofilms have been shown to persist longer than their planktonic counter-parts. Banning and co-workers (2003) reported that the opportunistic pathogen, *Pseudomonas aeroginosa* (*P. aeroginosa*), survived longer in biofilms. Similar observations were reported by Momba and co-workers (2000), who showed that several opportunistic pathogens including *P. aeroginosa* and members of the mycobacterium avium complex thrived better in biofilms than when they were grown under planktonic conditions. Some of the ways in which biofilm existence may affect pathogen survival, growth, and dispersal are summarized here.

1.3.2.1 Concentration of trace nutrients

Biofilms can concentrate nutrients to levels several times the concentrations in the surrounding liquid. This is particularly true of non-substrate nutrients such as phosphorus, potassium, magnesium, calcium, cobalt and others that may be required for cell synthesis, but are neither electron donor nor electron acceptor substrates. This may benefit pathogenic microorganisms, particularly those requiring key nutrients only available in trace amounts in the bulk liquid (Camper et al., 1985, Donlan, 2002; Banning et al., 2003; Zhang and Edwards, 2010).

1.3.2.2 Creation of special micro-environments

Extensive biofilm formation can create micro-environments in which chemical and physical conditions may be radically different from conditions in the surrounding liquid. Examples of such environmental modifications include creation of anaerobic zones and zones with high iron concentrations, which may, to different degrees, advantage certain pathogenic microorganisms (Dukan et al., 1996; Murga et al., 2001; Banning et al., 2003; Appenzeller et al., 2005).

1.3.2.3 Cell-to-cell interactions

Due to their close proximity, bacteria in biofilms can produce, release, and exchange metabolites and genetic elements including pathogenicity genes. Some of these metabolites may benefit the producing microorganism at the demise of its competitors. However, in some instances these exchanges can benefit all parties involved. The importance of these cell-cell interactions is evidenced by the fact that some pathogens can only effectively survive and grow as part of biofilms that have certain microorganisms. Several authors have reported such a relationship between *Legionella* and several protozoan species (Newsome et al., 1985; Murga et al., 2001; Banning et al., 2003). Although *Legionella* are commonly found in water environments, they usually survive in environments that have non-substrate nutrient combinations that are not usual in the natural environments. The downside to this is that when these nutrient combinations are present, they tend to increase the growth of fast-growing microorganisms which compete with *Legionella*. When grown in model distribution systems, *Legionella* only grows in the presence of protozoa. When grown in biofilms in the absence of protozoa, *Legionella* can only survive, but fail to divide. While cell-to-cell interactions can occur outside of biofilms, cell-cell communication is easier when chemical signals travel "short" distances (Newsome et al., 1985; Murga et al., 2001; Banning et al., 2003).

1.3.2.4 Protection from disinfection

The idea that biofilm existence protects pathogens from residual disinfection has been known since the 1970s (Characklis, 1981). There are several plausible explanations for this. First, biofilms create concentration gradients for dissolved chemical species. These gradients cause microorganisms inside biofilms to be exposed to disinfectant concentrations lower than those available in bulk water. Since disinfection efficiency is a

function of concentration and time, low chlorine doses require relatively long periods of exposure to exert a deadly effect on pathogens. Second, exposure to sub-lethal doses of disinfectants may enhance the development of resistance even in microorganisms that are inherently susceptible to chemical disinfection. Third, biofilms enhance residual disinfectant depletion. Reactions with corrosion products, extracellular polymeric substances (EPS), and SMP, all of which tend to be high in distribution systems with extensive biofilm formation, provide sinks that eat away at the chlorine that might otherwise safeguard distribution systems against pathogens (Characklis, 1981; Camper et al., 1985; LeChevallier et al, 1998a; LeChevallier et al, 1998a; Donlan, 2000; Banning et al., 2003).

1.3.2.5 Concentration of bacterial biomass

Unlike bacteria, protozoa do not feed on substrates dissolved in the water, instead they graze on other microorganisms. The high cell densities of bacterial biomass often found in biofilms can enhance the survival and growth of protozoan predators, some of which may be pathogenic (Camper et al., 1985, Newsome et al., 1985; Sibille *et al.*, 1998; Murga et al., 2001; Banning et al., 2003; Blair and Gerba, 2006).

1.3.2.6 Dispersal and distribution through biofilm detachment and re-attachment

Biofilm existence enables pathogens to linger in the distribution system long after their initial introduction in the bulk water. These pathogens can be continuously released and spread through the distribution system through detachment, thereby infecting the bulk water, while re-attaching and colonizing pipe surfaces downstream. Certain species-specific properties, such as cell surface hydrophobicity, the presence of fimbriae/flagella, and production of EPS, influence the rate and extent of attachment of microbial cells to surfaces.

Detachment and attachment also are influenced by physical phenomena such as shear stress and turbulence (Characklis, 1981; Woolschlager, 2000). In water, cells behave as particles, and the rates of settling and association with submerged surfaces depend largely on the velocity characteristics of the liquid. With very low linear velocities, the cells must traverse the sizeable hydrodynamic boundary layer, which means that their association with the surface depends in large part on cell size and cell motility. As the water velocity increases, the boundary layer decreases, and cells are subjected to increasingly greater turbulence and mixing. Higher linear velocities would, therefore, be expected to equate to more rapid association with the surface, at least until velocities become high enough to exert substantial shear forces on the attaching cells, resulting in detachment of these cells (Characklis, 1981; Donlan, 2002). Thus, biofilms can play roles in pathogen dispersal independent of a particular pathogen's ability to actively grow inside biofilms.

From a structural point of view, the most important problem that can result from biofilm accumulation is microbially induced corrosion (MIC) of distribution pipes (Lee *et al.*, 1980). Corrosion of distribution system pipes causes significant deterioration that has monumental financial and water quality consequences, including deterioration of pipe integrity, water coloration, release of chemicals that cause offensive tastes and odors, increased demand for chlorine residuals, and extensive microbial growth (Lee *et al.*, 1980; Videla, 1989; Emde *et al.*, 1992; Little *et al.*, 1998).

1.3.3 Biological Nitrification and Denitrification

Biological nitrification is the stepwise, bacterially catalyzed, oxidation of ammonium to nitrate through nitrite (Woolschlager, 2000; Wolfe and Lieu, 2001; Zhang et al., 2009; Zhang and Edwards, 2010). The activity of nitrifying bacteria inside drinking water distribution systems depends on substrate levels, especially concentrations

of reduced nitrogen species, ammonium and nitrite (Woolschlager, 2000; Zhang et al., 2008; Zhang and Edwards, 2010). Extreme nitrification is associated with distribution systems that carry water treated with chloramines (Wolfe *et al.*, 1988, 1990; Cunliffe, 1991; Woolschlager, 2000). Nitrification accelerates the loss of residual disinfectants, increases nitrite and nitrate concentrations in the water, increases heterotrophic abundance, and decreases oxygen, alkalinity and pH (Wolfe *et al.*, 1988; Odell *et al*., 1996; Woolschlager, 2000; Douglas et al., 2004; Fleming et al., 2005; Zhang et al., 2010).

Biological denitrification is the stepwise reduction of nitrate to nitrogen gas through nitrite. In distribution systems, denitrification is usually a result of extreme nitrification. There are two reasons why this is the case. First, nitrification increases available concentrations of nitrite and nitrate, both of which can be used by denitrifying bacteria as electron acceptors. Second, nitrification lowers dissolved oxygen levels, creating an anoxic environment which promotes denitrification by heterotrophic bacteria.

While drinking water distribution systems are hardly ever reported to be anoxic system-wide, it is not unusual for distribution systems to have small 'pockets' of anoxic environments. For example, deep corrosion zones can rapidly become anoxic (Tuovinen *et al.*, 1980; Tuovinen and Hsu, 1982). Extreme oxygen depletion can occur in dead-ends, where water stagnates, in which case the bulk water itself can become anoxic (Wajon *et al.*, 1988; Jacobs *et al*., 1998). Bacterial denitrification can occur under either set of conditions, if the lack of oxygen is coupled with the availability of nitrate and or nitrite (Tuovinen *et al.*, 1980; Tuovinen and Hsu, 1982; Wajon *et al.*, 1988; Jacobs *et al*., 1998).

1.3.4 Growth and Spread of Pathogens and Opportunistic Pathogens

From a public health perspective, the most unwanted effect of post-treatment water quality decay is the survival and spread of disease causing microorganisms. Figure 1.2 summarizes outbreaks of waterborne diseases in the US from between 1974 and 2004. Two interesting trends can be seen from this table. On the one hand, incidences of outbreaks associated with untreated water groundwater, untreated surface water, and treatment inefficiencies steadily declined through the three decades represented by this data. This is without a doubt due to the advancement of drinking water treatment regulations in the US. On the other hand, incidences of outbreaks disease associated with distribution systems steadily increased. This clearly shows that, while advances in treatment technologies and more stringent regulations at the treatment plant have been useful in lowering the burden of diseases associated with drinking contaminated water and improving the general public health of the US population, unless the issues associated with the decay of water quality decay during distribution are diligently dealt with, microbially-induced, waterborne infections will continue to pose a public health risk to the US population.

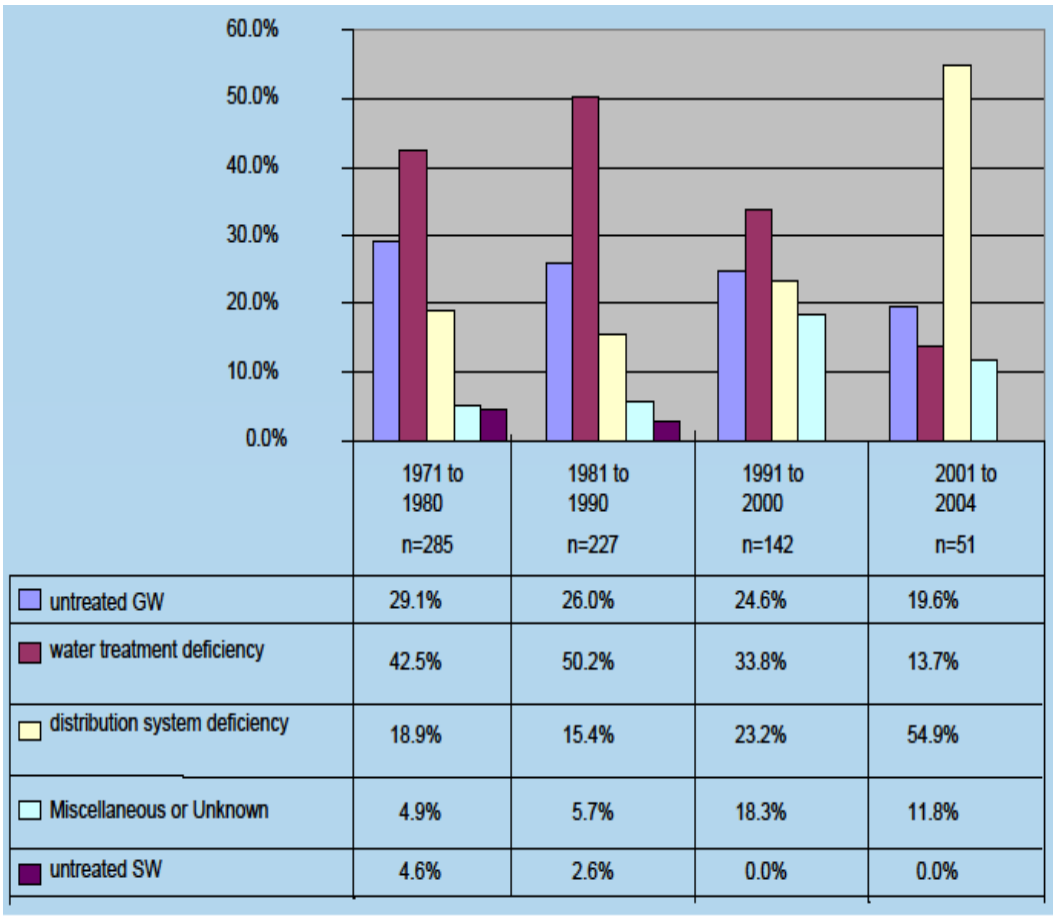

	1971 to 1980 n=285	1981 to 1990 n=227	1991 to 2000 n=142	2001 to 2004 n=51
untreated GW	29.1%	26.0%	24.6%	19.6%
water treatment deficiency	42.5%	50.2%	33.8%	13.7%
distribution system deficiency	18.9%	15.4%	23.2%	54.9%
Miscellaneous or Unknown	4.9%	5.7%	18.3%	11.8%
untreated SW	4.6%	2.6%	0.0%	0.0%

Figure 1.2 Trends in System Deficiencies for Outbreaks in Public Water Systems between 1971 and 2004 (Craun, 2007)

Despite the glaring increase in the incidences of infectious diseases associated with distribution system water-quality, the relationship between overall changes in water quality over time and the occurrence of pathogens and opportunistic pathogens remains one of the least understood aspects of distribution networks dynamics.

The bulk of research that has been carried out in the area of post-treatment water quality decay has relied on the quantification and characterization of indicator organisms such as heterotrophic plate counts and coliform bacteria (Camper et al., 1991; Camper et al., 1996; Williams and Braun-Howland, 2003), identification and characterization of the causes and effects of residual disinfectant decay and the formation of harmful

disinfection by-products (Rossman et al., 1994; Woolschlager, 2000; Richardson, 2005), and identification and characterization of the factors that play a role in the loss of biostability of potable water during transit (Rittmann and Snoeyink; 1984; Van Der Kooij, 2000; Woolschlager, 2000; Le Puil, 2004).

The apparent lack of interest in the dynamics of pathogen survival, growth, and spread within distribution systems is understandable, since the bulk of active suspended and fixed microorganisms in distribution systems are non-pathogenic. While this biomass in and of its own does not pose a direct health risk, within biofilms it can create micro-environments in which pathogenic microorganisms may be able to flourish. Understanding the extent to which pathogens and opportunistic pathogens can survive inside distribution systems is crucial to the provision of safe drinking water and by extension public health protection. Figure 1.3 shows cases of distribution system illness between 1981 and 2002. This figure shows that biological contamination accounts for 50% of all disease outbreaks associated with distribution systems, almost twice as many outbreaks as those associated with chemical contamination. The figure also shows that bacteria (16%) and protozoa (15%) account for the bulk of microbially induced non-acute gastro intestinal illnesses. Interestingly, most studies on pathogen survival and growth inside distribution systems focus on bacterial pathogens (Camper et al., 1985; Camper et al., 1991; Momba et al., 2000; Donlan, 2002; Banning et al., 2003; Morato et al., 2004).

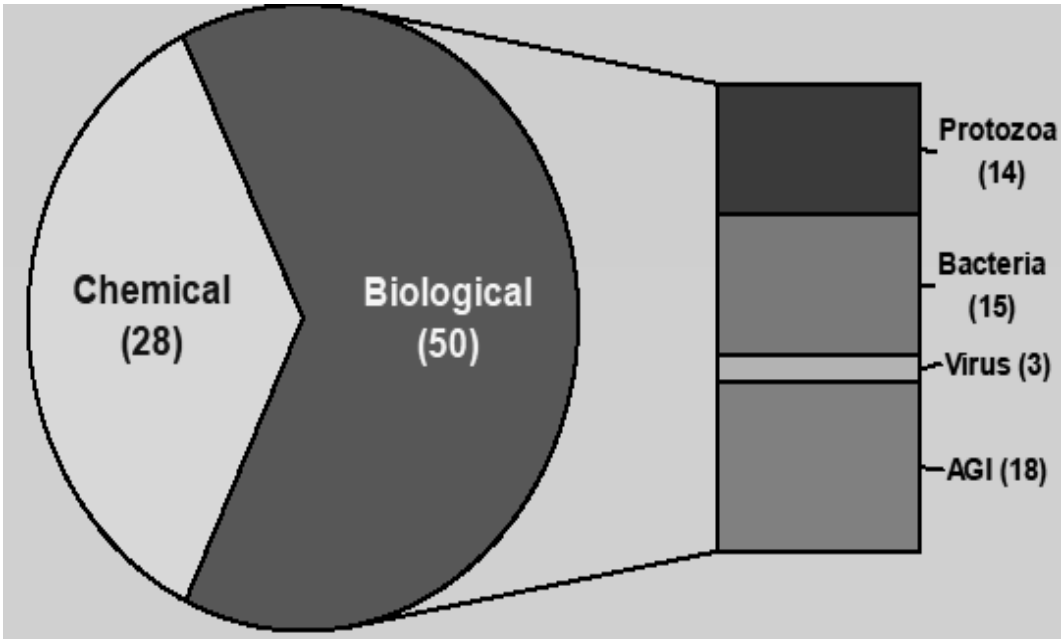

Figure 1.3 Cases of Distribution System Linked Illnesses Between1981 and 2002 (Regli, 2007)

Outbreak data, summarized in figures 1.2 and 1.3, shows several worrying trends. First, in spite of all the advances in treatment regulations, water-borne disease outbreaks continue to occur in the US. Second, water-borne disease outbreaks associated with distribution systems have increasingly become a larger fraction of the overall burden of waterborne disease outbreaks. Third, microbial pathogens cause twice as many waterborne disease outbreaks as chemical agents, in spite of stricter disinfection rules. Fourth, protozoan pathogens are responsible for nearly as many waterborne disease outbreaks as bacterial pathogens.

1.4 Water quality Modeling

Often times, the occurrence of the problems discussed in section 1.3 i.e. extensive bacterial growth, extensive biofilm formation, biological nitrification and denitrification and growth and spread of pathogens and opportunistic pathogens stirs up

urgent and strong responses from customers and regulators. The need for rapid response generates serious pressure for drinking water utility operators and managers as they are often without any swift and cost-effective fixes to these problems. Effective management of microbial activity in potable water distribution systems requires preventative and remedial strategies. It is imperative to understand the different physical, chemical, and biological phenomena that result in the deterioration of the quality of potable water during distribution. It is just as important to understand how these phenomena interact.

The ability to model the transport and fate of the different chemical and biological constituents that affect water quality in a distribution system is invaluable for efficient operation and management of water utilities. Specific examples of how data from water quality models can be used to improve the efficiency of distribution systems include: i) Determination of correct location and size for storage tanks and by extension reduction of unnecessary long water detention times. ii) Modification of system design and operation to provide a desired blend of waters and treatment regiments. iii) Identification of ideal sites for location of booster chlorination stations. iv) Assessment and minimization of point-of-use exposure to unwanted disinfectant by-products. v) Real-time assessment of systems vulnerability to incidents of external contamination, intentional or accidental (Kessler et al., 1998; Woolschlager, 2000; Uber et al., 2003; USEPA, 2003, 2004, 2005).

1.4.1 The Progression of Water Quality Modeling

Computer models that simulate the hydraulic behavior of water in distribution systems have been available for many decades. However, using computer modeling as a tool to track the transport and fate of dissolved substances and, by extension, water quality changes during distribution began only in the last 3 decades (Greyman *et al.*, 1988; Clark *et al.*, 1991; Rossman *et al.*, 1994). The early water quality models were

steady-state models describing reactions as first-order processes occurring in the bulk water over travel time. These models relied on the laws of mass conservation to determine the distribution of dissolved substances in space under static hydraulic conditions and with constant inputs.

In order to address the major limitations of the first group of models, single-species dynamic models were developed. These models differ from the first group in that they enable representation of the movement and spread of chemical and biological constituents under time-varying conditions. Biological and chemical processes that occur within distribution systems are time dependant because of variations in inputs and outputs. The most widely used model of this type is the Dynamic Water Quality Model (DWQM) first documented by Greyman *et al.* (1988). DWQM is the basis of the original water quality module in the EPANET model, arguably the most widely used hydraulic and water quality model. Because of their computational simplicity, first-order models are rapidly solved for full-scale distribution networks (Greyman *et al.*, 1988; Clark *et al.*, 1991; Rossman *et al.*, 1994). However, the application of first order models to interpret and analyze data from full-scale distribution systems is limited. All first-order models lump all reactions into single constants and therefore, cannot be reliably used to link water quality decay to specific causes. Also, the use of these models is limited to processes driven by first-order reaction kinetics.

Most limitations of first order models are somewhat overcome by the use of complex-process models. Complex-process models more accurately describe biological metabolism and disinfectant decay by using sets of complex, interconnected, multi-species, mass balance equations. A classical example of a complex-process model for distribution systems is the SANCHO model (Servais *et al.*, 1995). This model uses complex mass-balance equations to relate bacterial utilization of organic matter, bacterial

synthesis, disinfection processes, and the chlorine oxidation of organic matter. While the model accounts for the aforementioned processes in the bulk water and biofilm, an advantage over of its predecessors, it can only be solved for straight pipes. These models have one major drawback, the absence of any link between the microbial and chemical processes and hydraulic parameters within the distribution system (Woolschlager, 2000).

A uniquely important multi-species model is the Comprehensive Disinfectant and Water Quality model (CDWQ) developed by Woolschlager (2000). This model addresses water quality evolution in systems where chloramines are used. The CDWQ model includes mass balances equations that can be used to predict and analyze changes in heterotrophic counts, nitrifier counts, and chloramine decay throughout the distribution systems. Unlike its forerunners, the CDWQ model has a full hydraulic component, thus establishing a link between the microbial and chemical processes and hydraulic parameters (Woolschlager, 2000). The CDWQ is the foundation for the modeling performed in this dissertation, and Chapter 2 provides details on the components and reactions of the CDWQ model.

1.5 Research Objectives

Through this chapter, I provided background information on the issue of post-treatment water quality decay and gave a rationale for using mathematical modeling to monitor and manage water quality inside distribution systems. I use the balance of this chapter to identify the goals of this project, and I pinpoint how my work adds to the scientific knowledge in this area. The specific goals of this research are:

Objective 1: Identify the key factors that control post-treatment water quality decay. I identify and discuss key factors that influence the deterioration of the quality of chloraminated water inside distribution systems. Phenomena that I discuss includes the

depletion of chloramine residuals, utilization of biodegradable organic matter, synthesis of heterotrophic bacteria, bacterial nitrification and denitrification, production and consumption of microbial products, and the survival and growth of *N. fowleri* within distribution system biofilms.

Objective 2: Expand the CDWQ model to account for nitrification, denitrification, the effect of oxygen depletion, and the fate of introduced *N. fowleri* within distribution system biofilms. These upgrades make the CDWQ-E model a more powerful tool that can be used to manage general water quality and also, to forecast the growth and fate of *N. fowleri* within distribution systems.

Objective 3: Demonstrate the CDWQ-E model as a practical tool to analyze and interpret the water quality trends in batch experiments. I demonstrate the practical value of the model by discussing how CDWQ-E outputs show trends that can be expected in chloraminated drinking water.

Objective 4: Conduct field and laboratories studies to examine post treatment water quality decay trends, including occurrence and fate of *N. fowleri* within distribution system biofilms. I examine the role that distribution system biofilms play as reservoirs of *N.fowleri* as well as how *N.fowleri* survival and growth relates to overall water quality trends.

Objective 5: Use CDWQ-E to analyze and interpret water quality trends in two distribution systems and two pipe-loop systems. Using CDWQ-E model I identify the microbial and chemical processes beyond the water quality trends, and the long term survivability of *N.fowleri*, both seen in experimental studies.

1.6 Dissertation Organization

Here I give an overview of this dissertation by showing how each of the remaining chapters contributes toward meeting the goals outlined in section 1.5.

Chapter 2: In chapter 2, I summarize the core principles of the CDWQ model and then develop all the details of the CDWQ-E model.

Chapter 3: In chapter 3, I use a batch version of the CDWQ-E model to illustrate key features of the CDWQ-E model, including chloramine decay, nitrification, effects of oxygen limitation and heterotrophic denitrification, oxidation of organic matter, heterotrophic growth, production and loss of microbial products.

Chapter 4: In chapter 4, I use a batch version of the CDWQ-E model to fully compare the effectiveness of nutrient limitation versus disinfection in controlling bacterial growth in chloramine treated water.

Chapter 5: In chapter 5, I describe the distribution system sampling and testing methods used to collect data from the two full-scale distribution systems and two laboratory-scale pipe-loops. I then analyze these data to identify spatial and temporal trends in water quality deterioration. I also relate water quality to the occurrence and survival of *N. fowleri* and other amoeba.

Chapter 6: In chapter 6, I use CDWQ-E to investigate water quality decay trends in two distribution systems as well as examine the ability of distribution system biofilms to act as reservoirs of *N. fowleri*.

Chapter 7: In chapter 7, I summarize the major contributions of this research and provide recommendations for future studies.

Chapter 2

Developing the Expanded Comprehensive Disinfection and Water Quality Model

As stated in chapter 1, the Comprehensive Disinfectant and Water Quality model addresses water quality evolution in distribution systems where chloramines are used. The model consists of mass balance equations that can predict and analyze water quality decay throughout the distribution system. Central to the issues that the model addresses are the potential for treated water to support bacterial growth versus the potential for the water to suppress bacterial growth through disinfection (Woolschlager, 2000).

The potential to support growth is measured by concentrations of growth-supporting substrates, collectively known as biological instability (Rittmann and Snoeyink, 1984; van der Kooij, 2000; Woolschlager, 2000). The main causes of biological instability in drinking water are biodegradable organic matter (BOM) and reduced nitrogen especially ammonia (NH_3), which support the growth of heterotrophic and nitrifying bacteria, respectively.

The CDWQ model tracks heterotrophic and nitrifying bacteria independently, and, in each case, the electron donor is the sole growth-limiting substrate. The electron-donor substrate for heterotrophs, BOM, is sub-divided to BOM1 and BOM2. BOM1 includes all forms of biodegradable organic matter that are readily biodegradable. Common examples of BOM1 are ozonation by-products, such as aldehydes (formaldehyde, glyoxal, and methylglyoxal), ketones, glyoxylic acid, and pyruvic acid. BOM2 includes all forms of degradable organic matter that are not readily degradable and may require some form of prior treatment, such as hydrolysis. Common examples of

BOM2 are humic substances, such as fulvic and humic acids. The electron donor substrates for nitrifying bacteria are ammonium (NH_4^+) and nitrite (NO_2^-).

The potential to suppress bacterial growth is measured by the concentration of total chlorine available for bacterial disinfection, which is the difference between the concentration of chlorine in finished water at the time that it enters the distribution system and the net chlorine demand from non-disinfection reactions. Examples of non-disinfection reactions in which chlorine is consumed include autocatalytic chloramine decay reactions, oxidation of organic matter and microbial products, and catalytic reactions that occur at pipe surfaces. While the model tracks several species of free chlorine (HOCl, OCl^-) and combined chlorine (NH_2Cl, $NHCl_2$, and NHOHCl), it was only calibrated for a distribution system where monochloramine (NH_2Cl) is used (Woolschlager, 2000).

In expanding the CDWQ model, I merged the principles already incorporated in the original model with some of the latest developments in modeling microbial systems. In this way, I made the foundation of the model more inclusive and realistic, and I created a dynamic, multi-species model for describing processes related to bacterial growth in finished drinking water.

Following the principles laid out by Laspidou and Rittmann (2002), the expanded CDWQ model partitions the oxygen demand from an electron-donor substrate in four ways: to synthesis of new biomass, synthesis of extracellular polymeric substances (EPS), respiration of the electron acceptor, and release of utilization associated products (UAP). Once formed, active biomass is lost through endogenous respiration and disinfection to produce inert biomass. EPS hydrolyzes to form biosynthesis associated products (BAP). UAP and BAP are recycled and made available as electron donors.

While both heterotrophic bacteria and nitrifying bacteria produce UAP and BAP only heterotrophic bacteria consume them as recycled electron donors.

The original CDWQ model was intended and calibrated for distribution systems that carry chloraminated water, environments that support extensive nitrification and the consequential accumulations of NO_2^- and NO_3^- (Woolschlager 2000; Woolschlager et al, 2005). The CDWQ-E model adds the potential for anoxic respiration of NO_2^- and NO_3^-. Under aerobic conditions, heterotrophs and nitrifiers respire oxygen. However, when dissolved oxygen concentrations drop below critical levels, many heterotrophs can switch from aerobic respiration to anoxic heterotrophic denitrification, whereby they respire NO_3^- and NO_2^-. Employing dual–limitation Monod kinetics, so that the concentrations of the electron donor and the electron acceptor affect the rate of substrate utilization and biomass synthesis (Bae and Rittmann, 1996; Da Silva and Rittmann, 2000), the CDWQ-E model enables a switch from aerobic respiration to anoxic denitrification under conditions typical of drinking water distribution systems. This switch affects the fate of BOM, NO_2^-, NO_3^-, N_2; and NH_2Cl in the distribution system. Figure 2.1 is a schematic of electron flow for heterotrophic, AOB, and NOB growth in the CDWQ-E model.

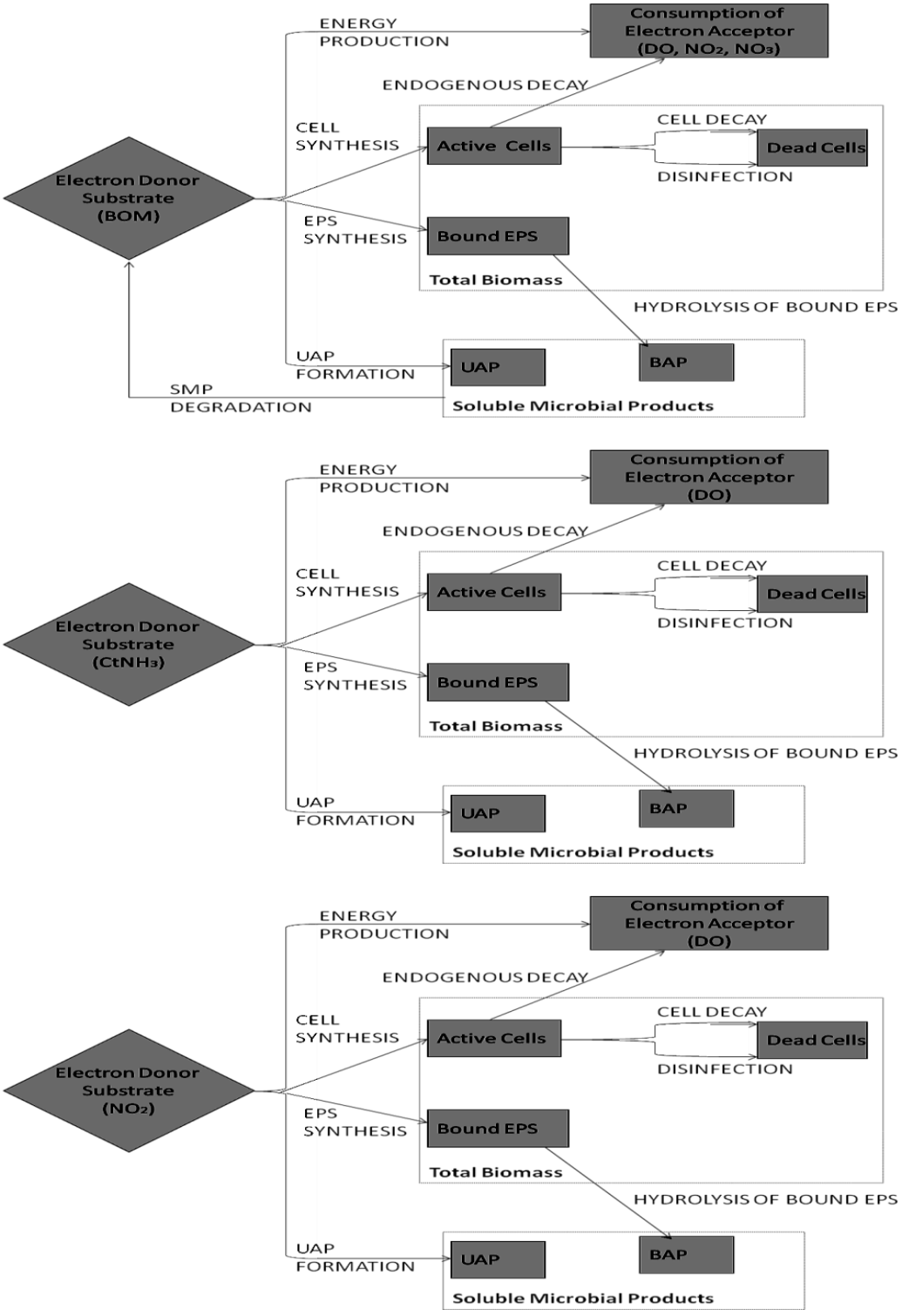

Figure 2.1 Electron Flow Schematics for Bacterial Growth. Heterotrophs (top), AOB (middle) and NOB (bottom).

In CDWQ-E, I also added the fate of *N. fowleri* in distribution system biofilms. These upgrades make the CDWQ model a more powerful tool that can be used to manage general water quality and also to monitor the occurrence of *N. fowleri* within distribution systems. By making changes to species specific growth parameters the model can be altered and reliably used to relate water quality to the occurrence and survival of other pathogenic amoeba in chloramine treated waters.

The remainder of this chapter develops the details of the batch version of CDWQ-E. An underlying principle of the batch CDWQ-E is to focus on the critical biological and chemical interactions that occur in the water and, thus, directly affect water quality. This separation allows me to focus on key processes affecting water quality decay, which in turn affords the ability to identify and characterize, in detail, interactions and processes that may be obscured when the complexities of transport are involved. Also, the batch model provides a good description of batch tests used in the water industry, such as BDOC and disinfection tests.

2.1 Model Development

2.1.1 Model Framework and Features

The key assumptions of the batch version of the CDWQ-E model are:

i. All biological and chemical reactions occur in the bulk water and without any effect from the walls of the containment system.

ii. Five types of biomass are represented: heterotrophic bacteria, ammonia-oxidizing bacteria (AOB), nitrite-oxidizing bacteria (NOB), EPS, and inert biomass.

iii. Six types of electron donor substrates are represented: BOM1, BOM2, UAP, BAP, total ammonia ($NH_4^+ + NH_3^-$), and NO_2^-.

iv. Three types of electron acceptors substrates are represented: O_2, NO_3^-, and NO_2^-.

v. Heterotrophic bacteria consume BOM1 and BOM2 as primary electron-donor substrates, UAP and BAP as recycled electron-donor substrates, O_2 as an electron acceptor under aerobic conditions, and NO_2^- and NO_3^- as electron acceptors under anoxic conditions. This consumption fuels the production of new heterotrophic biomass, UAP, EPS, and respiration of the electron acceptor.

vi. AOB consume NH_4^+ as the electron donor and O_2 as the electron acceptor. This consumption fuels the production of new AOB biomass, UAP, EPS, and respiration of the electron acceptor, which generates energy.

vii. NOB consume NO_2^- as the electron donor and O_2 as the electron acceptor. This consumption fuels the production of new NOB biomass, UAP, EPS, and respiration of the electron acceptor, which generates energy.

viii. Bacterial growth is governed by dual-limitation Monod kinetics, i.e., electron donor and electron acceptor concentrations control the substrate-utilization and biomass-synthesis rates in a multiplicative manner.

ix. EPS hydrolysis forms BAP.

x. Active biomass decay forms inert biomass, oxidizes biomass, and consumes an electron acceptor.

xi. NH_2Cl inactivates biomass through disinfection and directly oxidizes EPS, inert biomass, BOM1, BOM2, UAP, BAP, and NO_2^-.

2.1.2 Mass Balance Framework for All Species

The batch CDWQ-E model has 15 key mass balances that relate to bacterial growth and disinfection. Definitions of all symbols, subscripts, and units used in rate expressions and mass balances are given in Table 2.1.

Table 2.1 Symbols, Subscripts, and Units Used in Rate Expressions and Mass Balances

Parameters	
$X_{(j)}$	concentration of biomass [j = h, heterotroph; AOB, ammonia oxidizing bacteria; NOB, nitrite oxidizing bacteria; i, inert biomass], mg COD_x/
EPS	concentration of EPS, mg COD_x/L
BOM1	concentration of rapidly biodegradable organic matter , mg COD/L
BOM2	concentration of slowly biodegradable organic matter, mg COD/L
UAP	concentration of utilization associated products, mg COD/L
UAP	concentration of biomass associated products, mg COD/L
$NH_3+NH_4^+$	concentration of total ammonia, mg NH_4^+–N/L
NO_2^-	concentration of nitrite, mg NO_2^-–N/L
NO_3^-	concentration of nitrate, mg NO_3^-–N/L
NH_2Cl	concentration of monochloramine, mg/L
$b_{(j)}$	endogenous decay rate, d^{-1} (j = h; AOB; NOB)
f_d	fraction of biomass that is biodegradable
$K_{(j)}$	half maximum rate concentration [j= BOM1; BOM2; NH_4; NO^{2-}; UAP; BAP; NH2Cl; Chlorohydroxylamine], mol L^{-1} or mg COD L^{-1}
$q_{(j)}$	maximum specific rate of substrate utilization, mg/mg COD_x^{-d} [j = BOM1; BOM2; NH4; NO^{2-}; UAP; BAP]
t	time, d
$Y_{(j)}$	true yield coefficient [j =h, heterotroph; AOB, ammonium oxidizing biomass; NOB, nitrite oxidizing biomass], mg COD_x/ mg/COD, mg COD_x mol^{-1}
Reaction rates (k)	
$k_{AD(j)}$	chloramine auto decay constant, mole d^{-1} [j = 1, rate of NH_2Cl autocatalysis reactions; 2, rate of reversal of NH2Cl autocatalysis reactions]
$k_{d,\,j}$	biomass disinfection rate constant, L $mole^{-1}$ d^{-1} [j = 1, h; 2, AOB; 3, NOB]
$k_{ox(j)}$	chloramine oxidation rate constant L mol^{-1} d^{-1} [j = 1, BOM1; 2, BOM2; 3, UAP; 4, BAP; 5, NO_2^-, O2; 6, Xi; 7, EPS]
k_{hydr}	rate of EPS hydrolysis, hr^{-1}
k_{BAP}	BAP formation rate constant, mg COD mg/COD_xd
$k_{UAP(j)}$	UAP formation constant mg, COD mg/COD_xd [j = h, ns, nb)
$K_{I,DO}$	trigger coefficient for denitrificaiton
Subscripts	
H, heterotrophic bacteria; AOB, ammonium-oxidizing bacteria ; NOB, nitrite-oxidizing bacteria; I, inert biomass; NiN,nitrite; NaN, nitrate	
Stoichiometry	
γ_c	carbon content of biomass = mol C μg COD^{-1} (based on $C_5H_7O_2N$)
γ_n	nitrogen content of biomass = mol N μg COD^{-1} (based on $C_5H_7O_2N$)
γ_{NiN}	stoichiometry of nitrite vs. organic substrate in denitrification, g/g
γ_{NaN}	stoichiometry of nitrate vs. organic substrate in denitrification, g/g
η	anoxic reduction factor = dimensionless = 0.6

Equation 2.1 below shows the general structure of the mass balances illustrated for the generic chemical species S:

$$\frac{dS}{dt} = R_S \qquad subject\ to\ I \tag{2.1}$$

where $\frac{dS}{dt}$ is the rate at which S accumulates, I is the initial condition for S, and R_S is the net production/utilization rate of S. The units for these terms are: S, mg COD/L; h, day^{-1}; R, mg COD/L-day. Mass balances for all model components begin with equation 13, and the rate terms that make up R_S are given in equations 2.2 – 2.12.

2.1.3 Kinetic Representation of Mass Balances

Dual-Substrate Limitation Monod kinetics. The utilization rate for an electron donor substrate S_1, with concurrent respiration of electron acceptor S_2, is represented as equation 2.2:

$$rutl = q_m \left(\frac{S_1}{K_{S_1} + S_1} \right) \left(\frac{S_2}{K_{S_2} + S_2} \right) X_a \tag{2.2}$$

Modulating between aerobic respiration and anoxic denitrification. For heterotrophs, the switch between aerobic respiration and anoxic denitrification is controlled by multiplying the Monod term by $\frac{K_{od}}{K_{od} + O}$, the switching factor, such that equation 2.2 becomes equation 2.3:

$$rutl = q_m \left(\frac{S_1}{K_{S_1} + S_1} \right) \left(\frac{S_2}{K_{S_2} + S_2} \right) \left(\frac{K_{od}}{K_{od} + O} \right) \tag{2.3}$$

BOM utilization rate for aerobic respiration. To obtain an equation that accounts for aerobic utilization of total BOM (2.4.3), I combine equations for the utilization of BOM1 (2.4.1) and BOM2 (2.4.2):

$$rutl_{H,AER} = q_{BOM1,h} \left(\frac{BOM1}{K_{BOM1,h} + BOM1} \right) \left(\frac{O}{K_{O,h} + O} \right) \tag{2.4.1}$$

$$rutl_{H,AER} = q_{BOM2,h} \left(\frac{BOM2}{K_{BOM2,h} + BOM} \right) \left(\frac{O}{K_{od} + O} \right) \tag{2.4.2}$$

$$rutl_{H,AER} = q_{BOM,h} \left(\frac{BOM1}{K_{BOM1,h} + BOM1} \right) \left(\frac{O}{K_{O,h} + O} \right) + q_{BOM2,h} \left(\frac{BOM2}{K_{BOM2,h} + BOM} \right) \left(\frac{O}{K_{od} + O} \right) \tag{2.4.3}$$

BOM utilization rates for NO_3^- respiration. To obtain an equation that accounts for anoxic utilization with NO_2^- for total BOM (2.4.3), I combine equations for the utilization of BOM1 (2.5.1) and BOM2 (2.5.2):

$$rutl_{H,NAN} = q_{BOM,h} \left(\frac{BOM1}{K_{BOM1,h} + BOM1} \right) \left(\frac{NO_3}{K_{NO_3,h} + NO_3} \right) \left(\frac{K_{od}}{K_{od} + O} \right) \tag{2.5.1}$$

$$rutl_{H,NAN} = q_{BOM2,h}\left(\frac{BOM2}{K_{BOM2,h}+BOM}\right)\left(\frac{NO_3}{K_{NO_3,h}+NO_3}\right)\left(\frac{K_{od}}{K_{od}+O}\right) \tag{2.5.2}$$

$$rutl_{H,NAN} = q_{BOM,h}\left(\frac{BOM1}{K_{BOM1,h}+BOM1}\right)\left(\frac{NO_3}{K_{NO_3,h}+NO_3}\right)\left(\frac{K_{od}}{K_{od}+O}\right)+q_{BOM2,h}\left(\frac{BOM2}{K_{BOM2,h}+BOM}\right)\left(\frac{NO_3}{K_{NO_3,h}+NO_3}\right)\left(\frac{K_{od}}{K_{od}+O}\right) \tag{2.5.3}$$

BOM utilization rates for NO_2^- respiration. To obtain an equation that accounts for anoxic utilization with NO_3^- for of total BOM for (2.6.3), I combine equations for the utilization of BOM1 (2.6.1) and BOM2 (2.6.2):

$$rutl_{H,NIN} = q_{BOM,h}\left(\frac{BOM1}{K_{BOM1,h}+BOM1}\right)\left(\frac{NO_2}{K_{NO_2,h}+NO_2}\right)\left(\frac{K_{od}}{K_{od}+O}\right) \tag{2.6.1}$$

$$rutl_{H,NIN} = q_{BOM2,h}\left(\frac{BOM2}{K_{BOM2,h}+BOM}\right)\left(\frac{NO_2}{K_{NO_2,h}+NO_2}\right)\left(\frac{K_{od}}{K_{od}+O}\right) \tag{2.6.2}$$

$$rutl_{H,NIN} = q_{BOM,h}\left(\frac{BOM1}{K_{BOM1,h}+BOM1}\right)\left(\frac{NO_2}{K_{NO_2,h}+NO_2}\right)\left(\frac{K_{od}}{K_{od}+O}\right)+q_{BOM2,h}\left(\frac{BOM2}{K_{BOM2,h}+BOM}\right)\left(\frac{NO_2}{K_{NO_2,h}+NO_2}\right)\left(\frac{K_{od}}{K_{od}+O}\right) \tag{2.6.3}$$

AOB utilization of NH_4^+ under aerobic conditions.

$$rutl_{AOB,AER} = q_{NH_4,AOB}\left(\frac{NH_4}{K_{NH_4,AOB}+NH_4}\right)\left(\frac{O}{K_{O,AOB}+O}\right) \tag{2.7}$$

NOB utilization of NO_2^- under aerobic conditions.

$$rutl_{NOB,AER} = q_{NO_{24},NOB}\left(\frac{NO_2}{K_{NO_{24},NOB}+NO_2}\right)\left(\frac{O}{K_{O,NOB}+O}\right) \tag{2.8}$$

SMP utilization by heterotrophs for aerobic respiration. To obtain an equation that accounts for aerobic utilization of total SMP (2.9.3), I combine equations for the utilization of UAP (2.9.1) and BAP (2.9.2):

$$rutl_{H,UAP,AER} = q_{UAP,h}\left(\frac{UAP}{K_{UAP,h}+UAP}\right)\left(\frac{O}{K_{O,h}+O}\right) \tag{2.9.1}$$

$$rutl_{H,BAP,AER} = q_{BAP,h}\left(\frac{BAP}{K_{o,h}+BAP}\right)\left(\frac{O}{K_{od}+O}\right) \tag{2.9.2}$$

$$rutl_{H,SMP,AER} = q_{UAP,h}\left(\frac{UAP}{K_{UAP,h}+UAP}\right)\left(\frac{O}{K_{O,h}+O}\right) + q_{BAP,h}\left(\frac{BAP}{K_{o,h}+BAP}\right)\left(\frac{O}{K_{od}+O}\right) \tag{2.9.3}$$

SMP utilization by heterotrophs for NO_3^- respiration. To obtain an equation that accounts for anoxic utilization with NO_3^- of total SMP (2.10.3), I combine equations for the utilization of UAP (2.10.1) and BAP (2.10.2):

$$rutl_{H,UAP,NAN} = q_{UAP,h}\left(\frac{UAP}{K_{UAP,h}+UAP}\right)\left(\frac{NO_3}{K_{NO_3,h}+NO_3}\right)\left(\frac{K_{od}}{K_{od}+O}\right) \tag{2.10.1}$$

$$rutl_{H,UAP,NAN} = q_{BAP,h}\left(\frac{BAP}{K_{BAP,h}+BAP}\right)\left(\frac{NO_3}{K_{NO_3,h}+NO_3}\right)\left(\frac{K_{od}}{K_{od}+O}\right) \tag{2.10.2}$$

$$rutl_{H,SMP,NAN} = q_{UAP,h}\left(\frac{UAP}{K_{UAP,h}+UAP}\right)\left(\frac{NO_3}{K_{NO_3,h}+NO_3}\right)\left(\frac{K_{od}}{K_{od}+O}\right)+q_{BAP,h}\left(\frac{BAP}{K_{BAP,h}+BAP}\right)\left(\frac{NO_3}{K_{NO_3,h}+NO_3}\right)\left(\frac{K_{od}}{K_{od}+O}\right)$$

(2.10.3)

SMP utilization by heterotrophs for NO_2^- respiration. To obtain an equation that accounts for anoxic utilization with NO_2^- of total SMP (2.11.3), I combine equations for the utilization of UAP (2.11.1) and BAP (2.11.2):

$$rutl_{H,UAPP,NAN} = q_{UAP,h}\left(\frac{UAP}{K_{UAP,h}+UAP}\right)\left(\frac{NO_2}{K_{NO_2,h}+NO_2}\right)\left(\frac{K_{od}}{K_{od}+O}\right) \quad (2.11.1)$$

$$rutl_{H,BAP,NAN} = q_{BAP,h}\left(\frac{BAP}{K_{BAP,h}+BAP}\right)\left(\frac{NO_2}{K_{NO_2,h}+NO_2}\right)\left(\frac{K_{od}}{K_{od}+O}\right) \quad (2.11.2)$$

$$rutl_{H,SMP,NAN} = q_{UAP,h}\left(\frac{UAP}{K_{UAP,h}+UAP}\right)\left(\frac{NO_2}{K_{NO_2,h}+NO_2}\right)\left(\frac{K_{od}}{K_{od}+O}\right)+q_{BAP,h}\left(\frac{BAP}{K_{BAP,h}+BAP}\right)\left(\frac{NO_2}{K_{NO_2,h}+NO_2}\right)\left(\frac{K_{od}}{K_{od}+O}\right)$$

(2.11.3)

Active biomass disinfection by chloramine. Biomass disinfection, shown by Equation 2.12.1, is based on the Chick-Watson model for any active form of biomass:

$$r_{dj} = k_{dj}[NH_2Cl]X_a$$

(2.12.1)

Disinfection of active biomass produces inert biomass according to equation 2.12.2.

$$r_{NH_2Cl} = \left[k_{d1}\left[NH_2Cl\right]X_a\right] = Xi \tag{2.12.2}$$

2.1.4 Mass Balance Equations

X_h. The change in heterotroph biomass concentration is represented as equation 2.13:

$$\begin{aligned}\frac{dX_h}{dt} &= Y_h(1-k_{ln}-K_{EPS})rutl_{H,AERh} \\ &+ Y_h(1-k_{ln}-K_{EPS})\eta_{S,NAN}\,rutl_{H,NAN}\,X_h \\ &+ Y_h(1-k_{ln}-K_{EPS})\eta_{S,NIN}\,rutl_{H,NIN}\,X_h \\ &+ rutl_{H,SMP,AER} + rutl_{H,SMP,NAN} + rutl_{H,SMP,NIN} \\ &- b_h X_h - \left[k_{d1}\left[NH_2Cl\right]X_h\right]\end{aligned} \tag{2.13}$$

From left to right, the terms in equation 2.13 are accumulation of active heterotroph biomass over time, heterotroph synthesis from BOM utilization with aerobic respiration, heterotroph synthesis from BOM utilization with nitrite respiration, heterotroph synthesis from BOM utilization with nitrate respiration, heterotroph synthesis from SMP utilization with aerobic respiration, heterotroph synthesis from SMP utilization with nitrite respiration, heterotroph synthesis from SMP utilization with anoxic nitrate respiration, loss of heterotroph biomass due to endogenous decay, and loss of heterotroph biomass due to disinfection by NH_2Cl.

X_{AOB}. The change in AOB biomass concentration is represented as equation 2.14:

$$\begin{aligned}\frac{dX_{AOB}}{dt} &= Y_{AOB}(1-k_{AOB}-K_{EPS})rutl_{AOB,AER}X_{AOB} \\ &- b_{AOB}X_{AOB} - \left[k_{d2}\left[NH_2Cl\right]X_{AOB}\right]\end{aligned} \tag{2.14}$$

From left to right, the terms in equation 2.14 are: accumulation of AOB biomass over time, AOB biomass synthesis from NH_4^+ utilization with aerobic respiration, loss of AOB biomass due to endogenous decay, and loss of AOB biomass due to disinfection by NH_2Cl.

X_{NOB}. The change in NOB biomass concentration is represented as equation 2.15:

$$\frac{dX_{NOB}}{dt} = Y_{NOB}(1 - k_{NOB} - K_{EPS})rutl_{NOB,AER}X_{NOB} - b_{NOB}X_{NOB} - [k_{d3}[NH_2Cl]X_{NOB}] \quad (2.15)$$

From left to right, the terms in equation 2.15 are: accumulation of NOB biomass over time, NOB biomass synthesis from NO_2^- utilization with aerobic respiration, loss of NOB biomass due to endogenous decay, and loss of NOB biomass due to disinfection by NH_2Cl.

X_i. The change in inert biomass concentration is represented as equation 2.16:

$$\frac{dX_i}{dt} = (1-f_d)\left(\left[b_h\left(\frac{O_2}{K_{O,h}+O_2}\right)X_h\right] + \left[b_{AOB}\left(\frac{O_2}{K_{O,n1}+O_2}\right)X_{AOB}\right] + \left[b_{NOB}\left(\frac{O_2}{K_{O,n2}+O_2}\right)X_{NOB}\right]\right) + [k_{d1}[NH_2Cl]X_h] + [k_{d2}[NH_2Cl]X_{AOB}] + [k_3[NH_2Cl]X_{NOB}] - (k_{ox6}[NH_2Cl])X_i \quad (2.16)$$

From left to right, the terms in equation 2.16 are: accumulation of inert biomass over time, production of inert biomass from the endogenous decay of heterotrophs, AOB, and NOB; production of inert biomass from the disinfection of heterotrophs NH_2Cl; production of inert biomass from the disinfection of AOB by NH_2Cl; production of inert

biomass from the disinfection of NOB by NH_2Cl; and loss of inert biomass due to oxidation by NH_2Cl.

EPS. The change in EPS concentration is represented as equation 2.17:

$$\begin{aligned}\frac{\mathrm{dEPS}}{\mathrm{dt}} &= \mathrm{K_{EPS}} rutl_{H,AER} X_h + \mathrm{K_{EPS}} \eta_{S,NAN} q_S rutl_{H,NAN} X_h \\ &+ \mathrm{K_{EPS}} \eta_{S,NIN} q_S rutl_{H,NIN} X_h + K_{EPS} rutl_{H,SMP,AER} X_h \\ &+ K_{EPS} rutl_{H,SMP,NAN} X_h + K_{EPS} rutl_{H,SMP,NIN} X_h \\ &+ K_{EPS} rutl_{AOB,AER} X_{AOB} + K_{EPS\,NOB,AER} X_{NOB} - \mathrm{k_{hyd}}[\mathrm{EPSs}] \\ &- (\mathrm{k_{ox7}}[\mathrm{NH_2Cl}])\mathrm{EPS}\end{aligned} \tag{2.17}$$

From left to right, the terms in equation 2.17 are: accumulation of EPS over time, production of EPS from BOM utilization with aerobic respiration, production of EPS from SMP utilization with aerobic respiration, production of EPS from NH_4^+ utilization with aerobic respiration, production of EPS from NO_2^- utilization with aerobic respiration, production of EPS from BOM utilization with nitrite respiration, production of EPS from BOM utilization with nitrate respiration, production of EPS from SMP utilization with NO_2^- respiration, production of EPS from SMP utilization with nitrate respiration, loss of EPS due to hydrolysis, and loss of EPS due to oxidation by NH_2Cl.

BOM1. The change in BOM1 concentration is represented as equation 2.18:

$$\begin{aligned}\frac{dBOM1}{dt} &= -rutl_{H,AER} X_h - \eta_{S,NiN} rutl_{H,NAN} X_h \\ &- \eta_{S,NaN} rutl_{H,NIN} X_h - [k_{ox1}[NH_2Cl][BOM1]]\end{aligned} \tag{2.18}$$

From left to right, the terms in equation 4.18 are: accumulation of BOM1 over time, loss of BOM1 through heterotroph utilization with aerobic respiration, loss of BOM1 through heterotroph utilization with nitrite respiration, loss of BOM1 through heterotroph utilization with nitrate respiration, and loss of BOM1 due to oxidation by NH_2Cl.

BOM2. The change in BOM2 concentration is represented as equation 2.19:

$$\frac{dBOM2}{dt} = -rutl_{H,AER} X_h - \eta_{S,NiN} rutl_{H,NAN} X_h - \eta_{S,NaN} rutl_{H,NIN} X_h + \left(k_{d1}\left[NH_2Cl\right]X_h + \left[k_{d2}\left[NH_2Cl\right]X_{AOB}\right] + \left[k_{d3}\left[NH_2Cl\right]X_{NOB}\right]\right)Xfd - \left[k_{ox2}\left[NH_2Cl\right]\left[BOM2\right]\right] \quad (2.19)$$

From left to right, the terms in equation 2.19 are: accumulation of BOM2 over time, loss of BOM2 through heterotroph utilization with aerobic respiration, loss of BOM2 through heterotroph utilization with NO_2^- respiration, loss of BOM2 through heterotroph utilization with NO_3^- respiration, production of BOM2 through the decay of heterotroph, AOB, and NOB, biomass decay from disinfection by NH_2Cl, and loss of BOM due to oxidation by NH_2Cl.

UAP. The change in UAP concentration is represented as equation 2.20:

$$\frac{\mathrm{dUAP}}{\mathrm{dt}} = \mathrm{k_{UAP}} rult_{H,AER}\, \mathrm{X_h} + \mathrm{k_{UAP}} \mathrm{rutl_{AOB,AER}} \mathrm{X_{AOB}} + \mathrm{k_{UAP}} \mathrm{rutl_{NOB,AER}} \mathrm{X_{NOB}} + \mathrm{k_{BOM}} \eta_{S,NAN} rutl_{H,NAN}\, \mathrm{X_h} + \mathrm{k_{BOM}} \eta_{S,NIN} rutl_{H,NIN}\, \mathrm{X_h} - rutl_{H,UAP,AER} - \eta_{UAP,NAN} rutl_{H,NAN}\, \mathrm{X_h} - \eta_{UAP,NIN} rutl_{H,NIN}\, \mathrm{X_h} - (\mathrm{k_{ox3}}\left[\mathrm{NH_2Cl}\right]) \cdot \left[\mathrm{UAP}\right] \quad (2.20)$$

From left to right, the terms in equation 2.20 are: accumulation of UAP over time, UAP production from BOM utilization with aerobic respiration, UAP production from NH_4

utilization with aerobic respiration, UAP production from NO_2 utilization with aerobic respiration, UAP production from BOM utilization with NO_2^- respiration, UAP production from BOM utilization with NO_3^- respiration, UAP utilization by heterotrophs with aerobic respiration, UAP utilization by heterotrophs with NO_2^- respiration, UAP utilization by heterotrophs with nitrate respiration, and loss of UAP due to oxidation by NH_2Cl.

BAP. The change in BAP concentration is represented as equation 2.21:

$$\frac{dBAP}{dt} = K_{hydr}EPS - rutl_{H,AER}X_h - \eta_{BAP,NAN}rutl_{H,BAP,NAN} - \eta_{BAP,NIN}rutl_{H,BAP,NIN} - (k_{ox4}[NH_2Cl])[BAP] \quad (2.21)$$

From left to right, the terms in equation 2.21 are: accumulation of BAP over time, BAP production from EPS hydrolysis, BAP utilization by heterotrophs with aerobic respiration, BAP utilization by heterotrophs with nitrate respiration, BAP utilization by heterotrophs with nitrite respiration, and loss of BAP due to oxidation by NH_2Cl.

NH_2Cl. The change in monochloramine concentration is represented as equation 2.22:

$$\frac{dNH_2Cl}{dt} = -k_{ox5}[NH_2Cl][NO_2^-] - \gamma_c[NH_2Cl]\left[[k_{ox1}[BOM1] + k_{ox2}[BOM2]] + [k_{d1}X_{hf} + k_{d2}X_{AOB} + k_{d3}X_{NOB}] + k_{ox6}Xi + k_{ox7}EPS + [k_{ox3}[UAP] + k_{ox4}[BAP]]\right] \quad (2.22)$$

From left to right, the terms in equation 22 are: accumulation of NH_2Cl over time, loss of NH_2Cl due to NO_2^- oxidation, loss of NH_2Cl due to BOM1 and BOM2 oxidations, loss of NH_2Cl due to the disinfection of heterotrophic, AOB, and NOB biomass, loss of NH_2Cl

due to X_i oxidation, loss of NH_2Cl due to EPS oxidation, and loss of NH_2Cl due to UAP and BAP oxidations.

$CtNH_3$ (NH_3 + NH_4^+). The change in total ammonia (NH_3+NH_4^+) concentration is represented as equation 2.23:

$$\begin{aligned}
&\frac{dCtNH_3}{dt} = -q_{NH_4} rutl_{AOB,AER} X_{n1} - \gamma_n (Y_{NOB}) rutl_{NOB,AER} X_{NOB} \\
&- \gamma_n \cdot (Y_h - \frac{1}{1.42}) \cdot rutl_{H,AER} X_h - \gamma_n Y_P (rutl_{H,UAP,AER}) X_h \\
&+ \gamma_n \left(Y_h - \frac{1}{1.42 Y_P} \right) rutl_{H,BAP,AER} X_h \\
&- \gamma_n \cdot (Y_h - \frac{1}{1.42}) \cdot (\eta_{BOM,NAN} rutl_{H,NAN} + \eta_{BOM,NiN} rutl_{H,NIN}) X_h \\
&- \gamma_n \cdot (Y_h - \frac{1}{1.42}) \cdot (\eta_{UAP} rutl_{H,UAP,NAN} + \eta_{UAP} rutl_{H,UAP,NIN}) X_h \\
&- k_{AD2} [NH_2Cl][NH_4][H] + \gamma_n f_d (b_h X_h + b_{AOB} X_{AOB} + b_{NOB} X_{NOB}) \\
&+ \gamma_n (+11 \cdot k_{ox1} [NH_2Cl])[BOM1] + \gamma_n (11 \cdot k_{ox2} [NH_2Cl])[BOM2] + \gamma_n (11 \cdot k_{ox4} [NH_2Cl])[BAP] \\
&+ \gamma_n (11 \cdot k_{ox3} [NH_2Cl])[UAP] + \gamma_n (11 \cdot k_{ox6} [NH_2Cl]) X_i + \gamma_n (11 \cdot k_{ox7} [NH_2Cl])[EPS] \\
&+ k_{ox5} [NH_2Cl][NO_2^-] + k_{AD1} [NH_2Cl]^2
\end{aligned} \tag{2.23}$$

From left to right, the terms in equation 2.23 are: accumulation of total ammonia over time, loss of NH_4 due utilization by AOB with aerobic respiration, loss of NH_4 due uptake during aerobic NOB synthesis, loss of NH_4 due uptake during BOM utilization with aerobic respiration, loss of NH_4 due uptake during SMP utilization with aerobic respiration, loss of NH_4 due uptake during BOM utilization with aerobic respiration, loss of NH_4 due to uptake during SMP utilization with aerobic respiration, loss of NH_4 due

uptake during BOM utilization with anoxic NO_2^- and NO_3^- respiration, loss of NH_4^+ due to uptake during SMP utilization with anoxic NO_2/NO_3 respiration, loss of NH_4^+ during reversal of chloramine autocatalysis reaction, release of NH_4^+ by endogenous decay of heterotrophs, AOB, and NOB, NH_4^+ release from oxidation of BOM1 by HOCl, OCl^-, and NH_2Cl + nitrogen release from oxidation of BOM2 by NH_2Cl, NH_4^+ release from oxidation of BAP by HOCl, OCl^-, and NH_2Cl, NH_4 release from oxidation of UAP by HOCl, OCl^-, and NH_2Cl + oxidation, NH_4^+ release from oxidation of inert biomass by HOCl, OCl^-, and NH_2Cl, NH_4^+ release from oxidation of EPS by NH_2Cl, NH_4^+ release from oxidation of NO_2 by NH_2Cl, and NH_4^+ release auto reaction of two NH_2Cl molecules.

NO_2^-. The change in NO_2^- concentration is represented as equation 2.24:

$$\begin{aligned}\frac{dNO_2}{dt} &= (1 - \gamma_n Y_{AOB})M_{AOB}X_{AOB} - rutl_{NOB,AER}X_{NOB} \\ &- \gamma_{NiN}\eta_{BOM,NIN}\,rutl_{H,UAP,NIN}X_h - \gamma_{NiN}\eta_{SMP,NiN}\,rutl_{H,SMP,NIN}X_h \\ &+ \gamma_{NaN}\eta_{BOM,NaN}\,rutl_{H,BOM,NaN}X_h + \gamma_{NaN}\eta_{SMP,NaN}\,rutl_{H,SMP,NaN}X_h \\ &- k_{ox5}[NH_2Cl][NO_2^-]\end{aligned} \qquad (2.24)$$

From left to right, the terms in equation 2.24 are: accumulation of NO_2^- over time, NO_2^- release from AOB synthesis, loss of NO_2^- due utilization by NOB with aerobic respiration, loss of NO_2^- due to BOM utilization with anoxic NO_2^- denitrification, loss of NO_2^- due to SMP utilization with anoxic NO_2^- denitrification, release of NO_2^- due to BOM utilization with anoxic NO_3^- denitrification, release of NO_2^- due to SMP utilization with anoxic NO_3^- denitrification, and loss of NO_2^- due to oxidation by NH_2Cl.

NO_3^-. The change in **NO_3^-** concentration is represented as equation 2.25:

$$\frac{dNO_3}{dt} = rutl_{NOB,AER}X_{NOB} - \gamma_{NaN}\eta_{BOM,NaN}rutl_{H,,NIN}X_h - \gamma_{NaN}\eta_{SMP,NaN}rutl_{H,,NIN}X_h + k_{ox5}[NH_2Cl][NO_2^-] \quad (2.25)$$

From left to right, the terms in equation 2.25 are: accumulation of NO_3^- over time, release of NO_3^- from utilization by NOB utilization with aerobic respiration, loss of NO_3^- due to BOM utilization with anoxic denitrification, loss of NO_3^- due to UAP utilization with anoxic denitrification, loss of NO_3^- due to BAP utilization with anoxic denitrification, and NO_3^- production from NO_2^- oxidation by NH_2Cl.

N_2. The rate of the release of N_2 gas is represented as equation 2.26:

$$\frac{dN_2}{dt} = \gamma_{NIN}\eta_{S,NiN}rutl_{H,NIN}X_h + \gamma_{NiN}\eta_{UAP,NiN}rutl_{H,UAP,NIN}X_h + \gamma_{NIN}\eta_{BAP,NIN}rutl_{H,BAP,NIN}X_h \quad (2.26)$$

From left to right, the terms in equation 2.26 are: accumulation of N_2 over time, release of N_2 from BOM utilization with NO_2^- respiration, release of N_2 from UAP utilization with nitrite respiration, release of N_2 from UAP utilization with NO_2^- respiration, release of N_2 from BAP utilization with NO_2^- respiration.

O_2. The rate of oxygen consumption is represented as equation 2.27:

$$\frac{dO_2}{dt} = -\left(Y_h(1-k_{ln}-K_{EPS})rutl_{H,AER} + (Y_{smp,h})rutl_{H,UAP,AER} + (Y_{smp,h})rutl_{H,BAP,AER}\right)X_h - Y_{n1}(1-k_{ns}-K_{EPS})rutl_{AOB,AER}X_{AOB} - Y_{n2}(1-k_{n2}-K_{EPS})rutl_{NOB,AER}X_{NOB} - f_d\left(b_h\left[\frac{O_2}{K_{O,h}+O_2}\right]X_h + b_{AOB}\left[\frac{O_2}{K_{O,ns}+O_2}\right]X_{AOB} + b_{NOB}\left[\frac{O_2}{K_{O,nb}+O_2}\right]X_{NOB}\right) \quad (2.27)$$

From left to right, the terms in equation 2.27 are accumulation of O_2 over time, O_2 consumption during heterotroph synthesis from BOM oxidation, O_2 consumption during heterotroph synthesis from UAP oxidation, O_2 consumption during heterotroph synthesis from BAP oxidation, O_2 consumption during NH_4^+ utilization, O_2 consumption during NO_2^- utilization, and consumption of O_2 during the endogenous decay of heterotrophic, AOB, and NOB biomass.

The model parameters used in all simulations are summarized in Table 2.2. These values are typical values from the literature, as noted in the table.

Table 2.2 Parameter Values used in CDWQ-E Model. All values are per hour.

Parameter	Units	H, aerobic	H, anoxic	AOB, aerobic	NOB, aerobic	Source(s)
b	h^{-1}	0.004	0.004	0.002	0.002	1
f_d	-	0.8	0.8	0.8	0.8	1
K_{BAP}	$\frac{\mu g\ COD}{L}$	30,000	30,000	n/a	n/a	1
K_{UAP}	$\frac{\mu g\ COD}{L}$	20,000	20,000	n/a	n/a	1
K_{BOM1}	$\frac{\mu g\ COD_{cell}}{\mu gCOD_S}$	15,000	15,000	n/a	n/a	1
K_{BOM2}	$\frac{\mu g\ COD_{cell}}{\mu gCOD_S}$	95,000	95,000	n/a	n/a	1
K_{NH4}^{+}	$\frac{mole\ N}{L}$	n/a	n/a	2.14E-06	n/a	1
K_{NO2}^{-}	$\frac{mole\ N}{L}$	n/a	n/a	n/a	5.36E-05	1
k_{UAP}	$\frac{\mu g\ COD_P}{\mu gCOD_S}$	0.2	0.2	1.54E06	4.20E05	1
k_{EPS}	$\frac{\mu g\ COD_P}{\mu gCOD_S}$	7.5E-03	7.5E-03	6.6E-03	1.8E-03	2, 3
$khyd_{EPS}$	h^{-1}	0.007	0.007	0.007	0.007	2
q_{BOM1}	$\frac{\mu g\ COD_S}{\mu gCOD_{Cell} - h}$	0.4	0.4	n/a	n/a	1
q_{BOM2}	$\frac{\mu g\ COD_S}{\mu gCOD_{Cell} - h}$	0.4	0.4	n/a	n/a	1
q_{NH4+}	$\frac{moleN}{\mu gCOD_{Cell} - h}$	n/a	n/a	4.76E-09	n/a	1
q_{NO2}^{-}	$\frac{moleN}{\mu gCOD_{Cell} - h}$	n/a	n/a	n/a	2.08E-08	1
q_{UAP}	$\frac{\mu g\ COD_P}{\mu gCOD_{Cell} - h}$	0.552	0.552	n/a	n/a	1
q_{BAP}	$\frac{\mu g\ COD_P}{\mu gCOD_{Cell} - h}$	0.0833	0.0833	n/a	n/a	1
Y	$\frac{\mu g\ COD_{cell}}{\mu gCOD_S}$	0.6	0.6	6.16E6**	1.68E6**	1
Yp		0.6	0.6	n/a	n/a	2

K_{O2}	$\frac{mg\ O}{L}$	0.2	n/a	0.2	0.2	4
K_{IDO}	$\frac{mg\ O}{L}$	n/a	0.05	n/a	n/a	4

**, µg CODcell/moleN; *, µg COD_p/moleN

Sources: 1, Woolschlager (2000); 2, Laspidou and Rittmann (2002); 3, Rittmann and McCarty (2001); 4, Bae and Rittmann (1996).

2.2 Numerical Method for Solving the CDWQ-E Model

All model differential equations are of the generic format t,y,y' = 0, where t is time, y is the concentration of each chemical species, and y' is the rate of loss or gain of the chemical species. From initial values for y and y', the model solves the system with Δt = 1 hour to $t = t_{end.}$ The differential equations are solved using a simple forward method, where $y_{i+1} = y_i + y'_I \Delta t$. The code was written in MATLAB 2000.

2.3 Justification for Developing CDWQ-E Model

To conclude this chapter I illustrate what distinguishes the CDWQ-E model from water quality models that came before and why this model is an effective tool for answering the research questions that I posed. As I noted earlier, first-order models lump all processes into single reaction parameters. This limits the usefulness of these models. Complex process models overcome this limitation. However, complex models have their own limitations. Most importantly, the majority of complex models were created for systems that use chlorine and do not address water decay issues associated with

chloramines such as nitrification and denitrification. Finally, none of the currently available complex water quality models combine issues of general bacteriological quality decay and pathogen growth. The CDWQ-E model advances beyond these existing models by modeling chloramine decay, nitrification and denitrification processes, and the growth of *Naegleria fowleri* within drinking water distribution systems.

Chapter 3

Assessing Key Features of the CDWQ-E Model

In Chapter 2, I described how I developed the CDWQ-E model. In this chapter, I describe key features of the CDWQ-E model including loss of residual chloramine, heterotroph synthesis, unified production of EPS and SMP, biological nitrification, and anoxic heterotrophic denitrification. Chapters 4 and 6 present more in-depth modeling results that address particular topics. In Chapter 4, I examine the trade off between BOM and chloramine for allowing or suppressing heterotroph growth. In Chapter 6, I use the CDWQ-E to analyze water quality deterioration and the growth of *Naegleria fowleri* in drinking water distribution systems.

3.1 Modeling Experiments

In order to highlight the key features of the CDWQ-E model, I simulated batch tests under two different sets of conditions.

Case I represents a scenario that is characterized by having significant chloramine, BOM, dissolved oxygen, and potential for nitrification. The model parameters I used in all simulations are summarized in Table 2.2. Table 3.1 shows the initial conditions for Case I, which I call the chloramination condition. While these conditions are not reflective of any real distribution system, they are typical of conditions reported in chloraminated distribution systems. My goal for running CDWQ-E under

these conditions was to show as much of the basic features of the model as possible. I simulated the model for 30 days.

Table 3.1 Initial conditions for Case I - Chloramination Conditions

Input	**Parameter Values**		
BOM1	900µg COD/L	EPS	0.0 µg COD/L
BOM2	4100 µg COD/L	X_i	0.0 µg COD/L
UAP	0 µg COD/L	CO_2	0.0 µg COD/L
BAP	0 µg COD/L	HOCl	0.0 mol N/L
$CtNH_3$	2.28E-05 mol N/L	OCl	0.0 mol N/L
NH_4	$(CtNH_3*H^+)/(H^++KNH_3)$	NH_2Cl	$4.4x10^{-5}$ mol N/L
NH_3	$(CtNH_3*KeNH_3)/(H+KeNH_3)$	$NHCl_2$	0.0 mol N/L
NO_2	$2.28x10^{-6}$ mol N/L	NHOHCl	0.0 mol N/L
NO_3	$3.80x10^{-5}$ mol N/L	Cl	0.0 mol N/L
X_h	0.4 µg COD/L	N_2	0.0 mol N/L
X_{AOB}	0. 04 µg COD/L	DO	8.38 mg O_2/L
X_{NOB}	0. 04 µg COD/L	K_La	10 day^{-1}

Case II, which I call the denitrification condition, represents a scenario that is characterized by having significant chloramine, BOM, limited dissolved oxygen, and potential for denitrification. To accentuate the effects of anoxic conditions and the switch from aerobic metabolism to denitrification, I made the DO mass-transfer coefficient lower, i.e., $K_La = 1.0\ day^{-1}$ instead of $10.0\ day^{-1}$ which I used in case I. A low K_La kept the DO low during the model run. I also lowered the input DO concentration to 4.0 mg O_2/L. All other inputs were the same as for case I scenario.

3.2 Results and Discussion

Case I scenario. Scenario I had chloramine, BOM, significant DO, and heterotrophic and nitrifying bacteria. This case demonstrates all of the features of the CDWQ-E with the exception of heterotrophic denitrification and *Naegleria fowleri* growth.

Figure 3.1 shows the modeled values of chloramine, ammonia, nitrite, nitrate, nitrogen, AOB, and NOB over a 30 day period. This figure shows three important trends: (i) During the simulated batch test, total ammonia increased considerably (~270%) throughout the 30 day period. The increase in ammonia corresponded with the projected release of ammonia from the decay of chloramine, oxidation of organic matter (BOM1, BOM2, UAP, BAP, EPS, X_i, and NO_2^-) by chloramine, and the utilization of organic matter by heterotrophic bacteria. All these reactions are represented in equation 2.23. (ii) Throughout the 30 day simulation the concentrations of nitrite and nitrate remained virtually the same. The changes to NO_2^- and NO_3^- concentrations were so small that they cannot be seen in the figure because of scale. (iii) AOB only grew modestly, halfway through the simulation, and NOB never grew.

To understand the three trends listed above I look at the construction of the CDWQ-E model as detailed in chapter 2. In the model chloramine is lost through autocatalytic decay, oxidation of organic matter, and biomass disinfection. All three reactions release ammonia and create potential for nitrification. This explains the correlation between chloramine depletion and the increase in ammonia concentration.

The stability of the nitrite and nitrate profiles indicate that nitrification was lacking or significantly minimal throughout the 30 day simulation. While chloramine

decay and biomass decay bolsters the pool of available ammonia, and by extension the potential for nitrification, in the CDWQ-E model the extent to which biological nitrification processes can occur depends on the balance between the availability of substrates (ammonia and nitrite) and the availability of residual chloramine, for disinfection. From figure 3.1 it is clear that net disinfection outpaced net AOB/NOB synthesis for most of the simulation time. The concentration of AOB steadily dropped from 100 cell equivalents/mL at day 1 to 2 cell equivalents/mL by day 18. AOB only showed net positive growth after day 18 when the chloramine concentration dropped below 0.8 mg/L as Cl_2. Still, the mass of AOB was too small to allow a noticeable increase in the NO_2^- concentration. Hence the NO_2^- profile did not show any significant change throughout the 30 day simulation. Unlike AOB, which recovered late the during simulation period, NOB remained in net decay for all 30 days. I expected NOB to lag AOB and be less than AOB, because NOB cannot grow until AOB produce enough NO_2^- to allow a net positive growth rate. The mass of AOB was too small to generate enough NO_2^- to support NOB growth. These results indicate that significant nitrification can be suppressed if the concentration of AOB is small at the time that chloramine decays enough for them to have a positive growth rate. The small changes in NO_2^- and NO_3^- concentration profiles were most likely due to chloramine oxidation of NO_2^- to NO_3^-, (equation 2.24), and not due to biological nitrification.

Trends similar to these have been reported in other works. Woolschlager (2000) reported that in batch tests, when biofilm kinetics are not accounted for, significant nitrification fails to occur even when the ammonia pool increases due to chloramine decay and biomass decay.

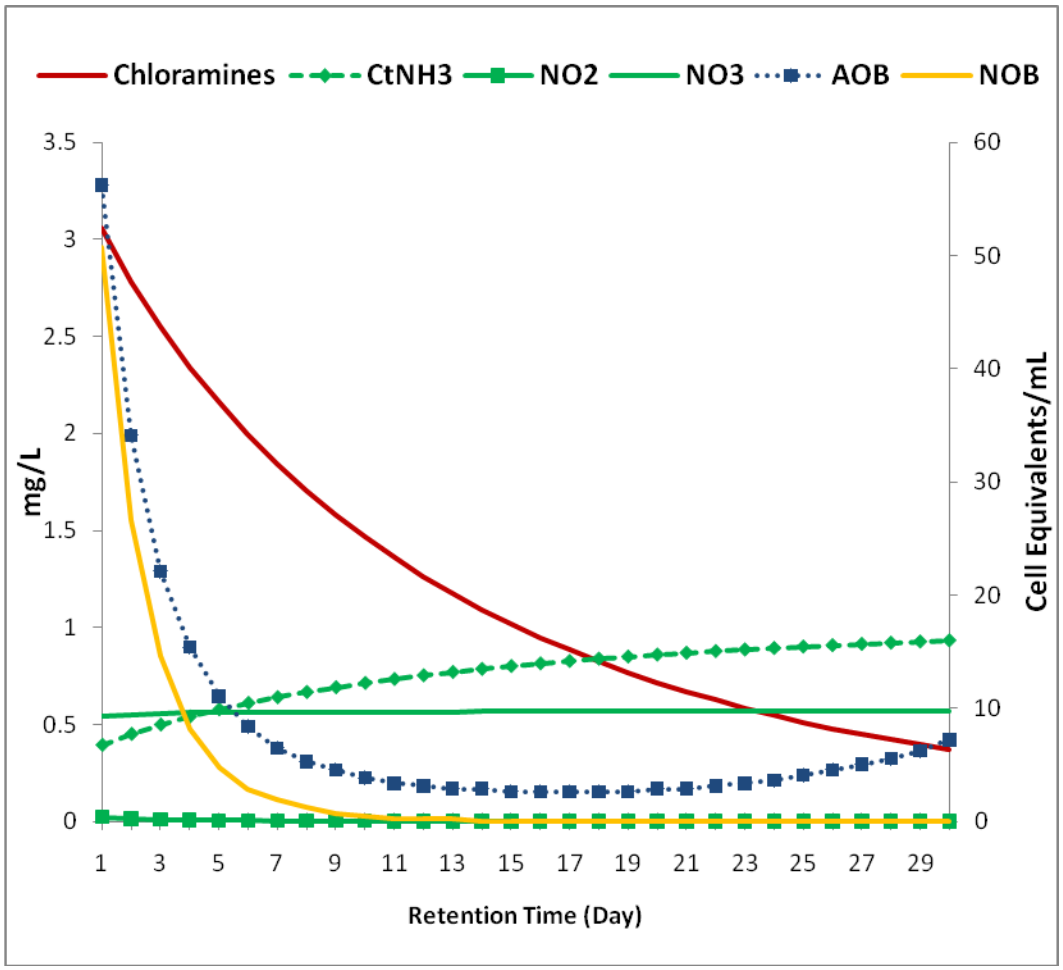

Figure 3.1 Effects of chloramine decay and nitrification for N and nitrifier species during the Scenario I simulation.

To explain why AOB grew while NOB remained in decline, I calculate the minimum substrate concentration (S_{min}) for AOB and NOB, based on the growth and decay parameters I used for scenario I. I derive S_{min} from the Monod equation as shown in Rittmann and McCarty (2001).

$$S_{\min} = K_S\left(\frac{b}{Yq_{\max} - b}\right) \tag{3.1}$$

For AOB ($CtNH_3$):

$$S_{\min} = 7.14*10^{-5} moleN/L\left(\frac{0.002h^{-1}}{6.16*10^{6}\mu gCOD_{cell}/\text{moleN}*4.76*10^{-9}\text{moleN}/\mu\text{gCODcell-h}-0.002h^{-1}}\right)$$

$$S_{\min} = 5.1*10^{-6} moleN/L$$

$$S_{\min} = 0.07 mgN/L$$

For NOB (NO_2^-):

$$S_{\min} = 7.14*10^{-5} moleN/L\left(\frac{0.002h^{-1}}{1.68*10^{6}\mu gCOD_{cell}/\text{moleN}*2.08*10^{-8}\text{moleN}/\mu\text{gCODcell-h}-0.002h^{-1}}\right)$$

$$S_{\min} = 4.3*10^{-6} moleN/L$$

$$S_{\min} = 0.06 mgN/L$$

Under chloraminating conditions, however, net biomass decay is the sum of decay from endogenous decay processes and disinfection. Therefore, the effective decay coefficient is $0.002h^{-1}$ plus the heterotroph disinfection rate coefficient: for chloramine, this is 150 L-mol^{-1}-h^{-1} (or 0.0021 L-μgCl_2^{-1}-h^{-1}) multiplied by the chloramine concentration. For example, if the residual chloramine concentration is 1 mg Cl_2/L, the net decay rate is 0.00410 h^{-1} and the new S_{min} values for AOB and NOB become 0.16 mg N/L and 0.13 mg N/L, respectively. For a residual chloramine of 3.2 mg Cl_2/L, the S_{min} values for AOB and NOB are 0.41 mg N/L and 0.34 mg N/L, respectively.

From minimum substrate concentrations, I can see that, in the absence of a residual disinfectant, AOB will need ammonia concentrations equal to or above 0.07 mg N/L and NOB will grow at NO_2^- concentrations equal to or above 0.06 mg N/L. The

presence of residual chloramine increases the required S_{min} for growth in both cases. For example, when the residual chloramine concentration is around 1.0 mg Cl_2/L, theoretical S_{min} values for AOB and NOB are 0.16 mg N/L and 0.13 mg N/L, respectively. For a residual chloramine concentration of 3.2 mg Cl_2/L, which is what the model predicted will be present immediately after the first day of simulation, S_{min} for AOB and NOB become 0.41 mg N/L and 0.34 mg N/L, respectively, although these values decline as residual chloramine is depleted. For AOB S_{min} is around or above the prevailing $CtNH_3$ concentration, predicted by CDWQ-E, for about the first half of the simulation time, but becomes significantly less than the prevailing $CtNH_3$ concentration around day 17, when AOB begin to have positive growth. For NOB, S_{min} remains significantly above the prevailing NO_2^- concentrations, predicted by CDWQ-E throughout the simulation, and the model predicted that NOB will not grow in 30 days.

Figure 3.2 shows BOM depletion, heterotroph growth, and microbial product formation for scenario I. Because the batch test had no advective losses, active biomass increased as long as substrate utilization was significant, and heterotroph growth corresponded to BOM depletion, which accelerated as total heterotroph biomass increased. The escalation of the rate of BOM depletion during heterotroph synthesis has been reported in other modeling and experimental studies (de Silva et al, 2000; Laspidou and Rittmann, 2002; Woolschlager et al., 2005). Overall, BOM1 was depleted much faster than BOM2, since its kinetics are much faster (Table 2.2).

Heterotrophs dominated active biomass throughout the simulation period, since heterotrophs can grow much faster than nitrifying bacteria. By the end of the simulation, the concentration of heterotroph bacteria was close to 63,000 cell equivalents/mL,

compared to ≤ 10/mL for the AOB (Fig. 3.1). A trend especially worth noting is that heterotrophs, unlike the nitrifiers, can grow when residual chloramine is present at a relatively high concentration, as long as their growth substrates, BOM1 and BOM2, are present in high enough concentrations. Figure 3.2 shows that their growth rate accelerated around day 18, when the chloramine concentration had decayed to about 0.8 mg/L as Cl_2. I dedicate Chapter 4 to evaluating the tradeoffs of BOM versus chloramine in controlling heterotroph growth in chloraminated water; thus, I do not discuss this at length here.

Since AOB growth was minimal, while NOB remained in net decline throughout the 30-day simulation, the nitrifiers contributed little to the production of SMP and EPS. Therefore, I can interpret that virtually all microbial product formation was due to heterotroph synthesis and BOM depletion. Panel B in Figure 3.2 shows that EPS accumulation tracked total heterotrophic-biomass accumulation, because EPS is produced in parallel to biomass synthesis. EPS was about 40 % of the heterotrophic biomass. Also evident in Panel B of Figure 3.2 is that UAP dominated soluble SMP throughout the simulation period. I also expected this, since UAP accumulation tracks substrate utilization, which is relatively fast, while BAP accumulation tracks EPS hydrolysis, which is relatively slow. If the simulation were run long enough to deplete most of the BOM, BAP eventually would overtake UAP as the major form of SMP.

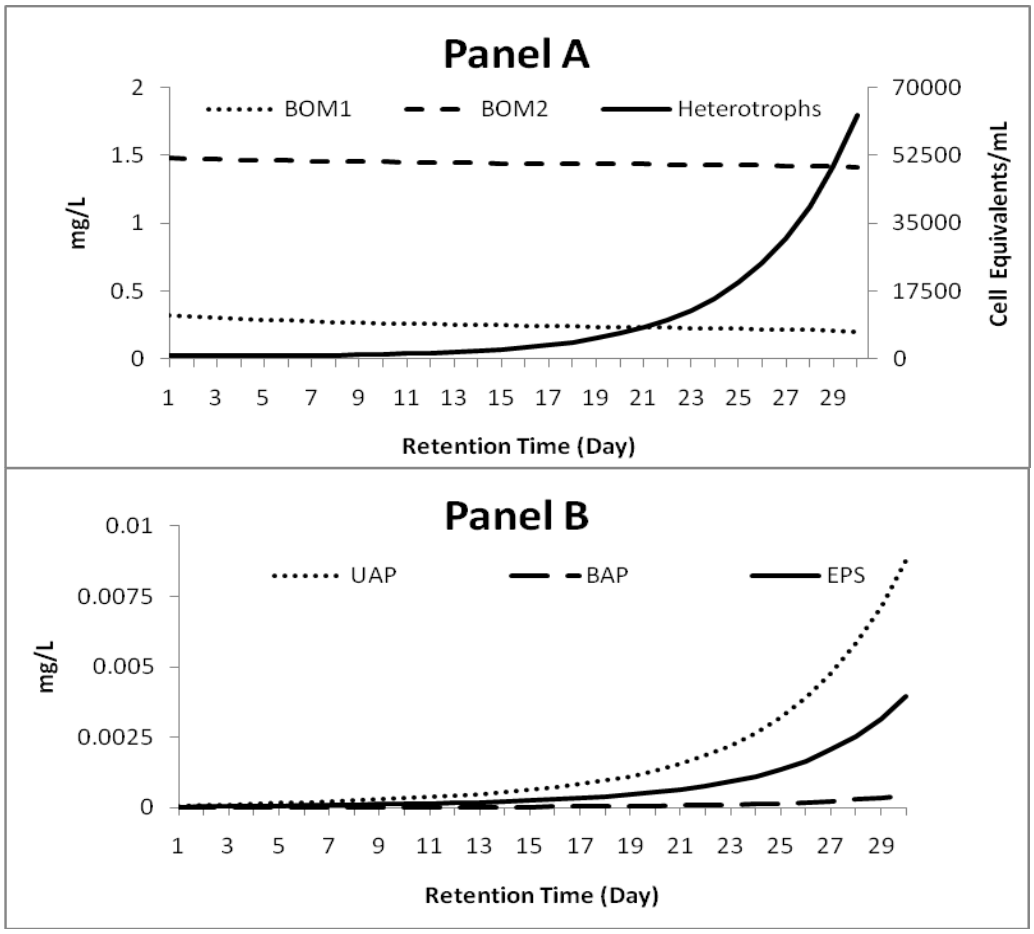

Figure 3.2 BOM depletion, heterotroph growth, and microbial product formation during the Scenario I simulation. Panel A highlights the relationship between BOM depletion and heterotroph growth. Panel B highlights relationship among the different types of microbial products.

Case II Scenario. Similar to scenario I, scenario II had chloramine, BOM, and heterotrophic and nitrifying bacteria, but scenario II had low DO, which accentuated the possibility of having denitrification and other dynamics of a low-oxygen environment.

Figure 3.3 shows the modeled values of chloramine, ammonia, nitrite, nitrate, nitrogen, AOB, and NOB over a 30 day period. This figure shows three important trends: (i) During the simulated batch test, total ammonia increased considerably (~270%) through the 30 day period. The increase in ammonia corresponded with the projected release of ammonia from the decay of chloramine, oxidation of organic matter (BOM1, BOM2, UAP, BAP, EPS, X_i, and NO_2^-) by chloramine, and the utilization of organic matter by heterotrophic bacteria. All these reactions are represented in equations 2.23. (ii) The concentrations of nitrite and nitrate both decreased while the concentration of nitrogen gas increased through the 30 day period. (iii) AOB and NOB growth was effectively suppressed throughout the 30 day period. As I did for scenario I, to understand the observed trends I look at the construction of the CDWQ-E model as detailed in chapter 2.

Again, the sustained increase in the $CtNH_3$ pool was due to chloramine decay and ammonia release from biomass decay. The inability of AOB and NOB to thrive was partly due to shortage of their electron acceptor, DO. Under conditions where ammonia is the most dominant form of dissolved nitrogen, as represented by scenario I, bacterial nitrification is controlled by the $CtNH_3$ concentration. AOB and NOB grow sequentially with AOB growing first by oxidizing ammonia. This ammonia oxidation creates a pool of NO_2^-, which has potential to support NOB synthesis. In this way the relationship is synergistic and in favor of NOB in the long term. But in the CDWQ-E model, AOB and NOB growth is not necessarily only donor limited. Acceptor concentration also plays an important role for bacterial growth. Since AOB and NOB use oxygen as their sole electron acceptor, one relationship between AOB and NOB is competition for DO. Because NOB have to "rely" on AOB growth for generation of their electron donor pool,

under low-oxygen conditions, as represented by scenario II, the relationship disadvantages NOB even more than AOB. In scenario II, the DO that was available at the start of the simulation dropped to sub-critical levels long before the chloramine concentration declined enough so that $CtNH_3 > S_{min}$ which is what happened in scenario I. To show that this was the case I estimate the theoretical minimum DO concentration (DO_{min}) required for aerobic growth using the same concept I employed to estimate S_{min} for electron donor substrates as follows:

$$DO_{\min} = K_{DO}\left(\frac{b}{Yq_{\min} - b}\right) \tag{3.2}$$

For AOB

$$DO_{\min} = 0.2 mgO/L\left(\frac{0.002h^{-1}}{6.16*10^{6}\mu gCOD_{cell}/\text{moleN}*4.76*10^{-9}\text{moleN}/\mu\text{gCODcell-h} - 0.002h^{-1}}\right)$$
$$DO_{\min} = 0.014\, mgO/L$$

For NOB

$$DO_{\min} = 0.2 mgO/L\left(\frac{0.002h^{-1}}{1.68*10^{6}\mu gCOD_{cell}/\text{moleN}*2.08*10^{-8}\text{moleN}/\mu\text{gCODcell-h} - 0.002h^{-1}}\right)$$
$$DO_{\min} = 0.012\, mgO/L$$

The DO concentration fell below these DO_{min} before the chloramine concentration declined enough to permit positive growth of AOB. In scenario I, I showed that the presence of residual chloramine increases the S_{min} required for growth in both cases. Here I re-calculate DO_{min} to see the effect that having a disinfectant residual will have on AOB and NOB growth under anoxic conditions. When the residual chloramine

concentration is around 1.0 mg Cl_2/L, theoretical DO_{min} for AOB and NOB are 0.03 mg O/L and 0.026 mg O/L, respectively. For a residual chloramine concentration of 3.2 mg Cl_2/L, DO_{min} for AOB and NOB become 0.085 mg O/L and 0.07 mg O/L, respectively, although these values decline as residual chloramine is depleted. DO reached 0.05 mg O/L by day 8, which is critically low. The chloramine concentration by day 8 was 2.2 mg Cl_2/L and required DO_{min} are 0.055 mg O/L and 0.044 mg O/L for AOB and NOB, respectively, and the DO already was below these values. Calculating DOmin and Smin for AOB and NOB helps me realize that the absolute, and sustained, suppression of nitrification, particularly the growth of AOB was mostly due to electron acceptor (DO) limitation that to electron donor limitation.

In scenario II, the decline in NO_3^- concentration was coupled with a commensurate increase in the concentration of N_2. This trend is indicative of denitrification, which can occur because the DO concentration is not high enough to totally inhibit nitrite respiration. The switching factor: $K_{I,\,DO}/(K_{I,\,DO} + DO)$ controls anoxic heterotrophic denitrification. If, the available concentration of DO is greater than the switching coefficient ($K_{I,DO}$) anoxic denitrification does not occur. For heterotrophs, $K_{I,DO}$ is 0.05 mg O/L. Noticeable denitrification can begin when $DO \leq \sim 10xK_{I,DO} = 0.5$ mg/L. When the initial DO concentration was set at 8.38 mg/L, DO never went below 6 mg/L, and denitrification was inhibited throughout the simulation. When the initial DO concentration was set at 4.0 mg/L for this scenario, DO dropped below 0.05 mg O/L by day 8 and below 0.5 mg/L by day 3, triggering significant denitrification. All in all, DO needs to be extremely low before denitrification takes place. This indicates that denitrification may not be important, if possible at all, within real distribution systems.

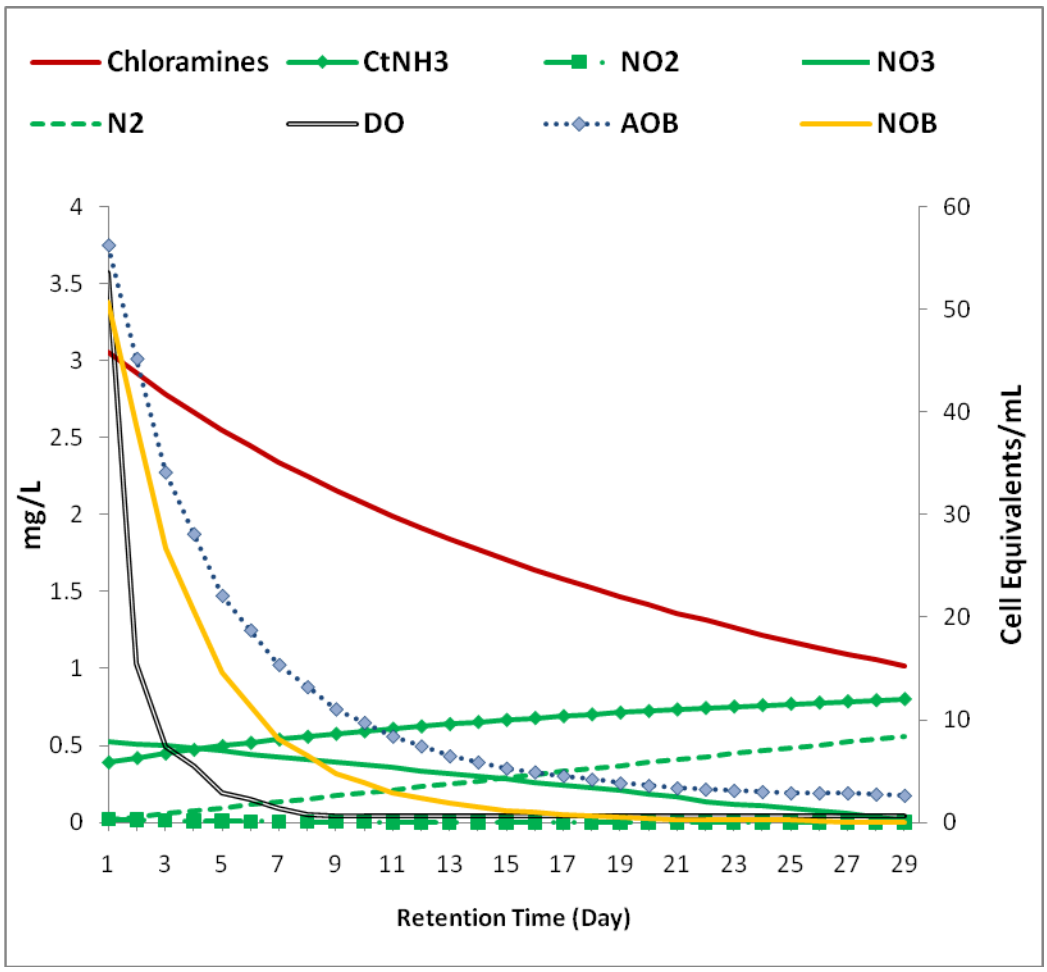

Figure 3.3 Effects of chloramine decay and nitrification for N and nitrifier species during the Scenario II simulation.

Figure 3.4 shows BOM depletion, heterotrophs growth, and microbial product formation for scenario II. The general trends for BOM depletion, heterotrophs synthesis and accumulation, and microbial product formation were all as reported for scenario I. However, at any given point in time, the actual concentrations of HPC, EPS, UAP, and BAP were all significantly lower for scenario II than for scenario I. By the end of the simulation, heterotroph concentration was almost 2,500 cell equivalents/mL, which is 75% lower than what I observed in scenario I for the same time period. Since scenarios I

and II had the same input concentrations for BOM1, BOM2, and NH_2Cl, the relative suppression of heterotroph accumulation in scenario II was most likely due to electron acceptor limitation. Low HPC synthesis and BOM depletion automatically resulted in reduced UAP and EPS production, because UAP production is linked to BOM depletion, while EPS production is linked to biomass synthesis. For example, EPS at the end of this simulation was $1.7*10^{-4}$ mg C/L, which is slightly less than 5% of the EPS concentration for scenario I.

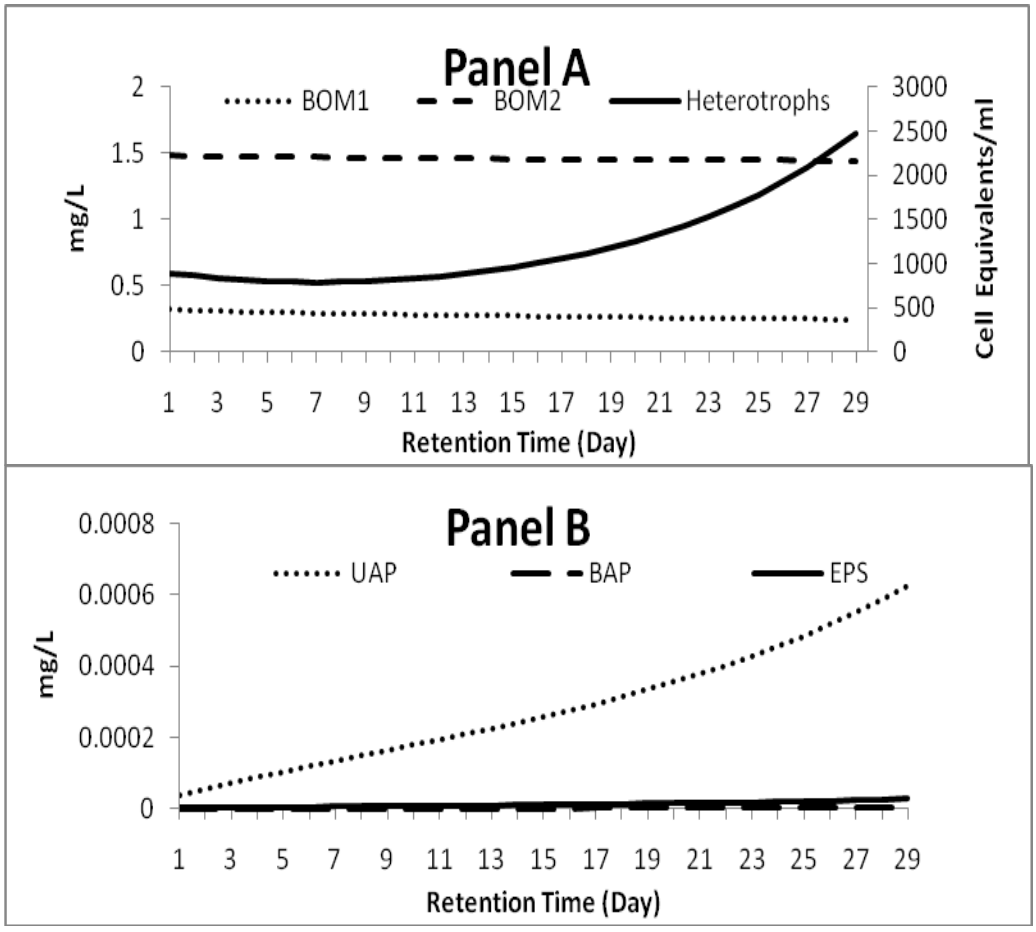

Figure 3.4 BOM depletion, heterotroph growth, and microbial product formation during the Scenario II simulation. Panel A highlights the relationship between BOM depletion and heterotroph growth. Panel B highlights relationships among microbial products

3.3 Testing the CDWQ-E Mass Balances

Numerically solving a mass balance model like CDWQ-E can lead to small gains or losses in the mass of the components being modeled due to numerical errors that build up over time. The build up of numerical errors is accentuated if the time step is too large. However, serious mass imbalances result from the use of incorrect equations, parameters, unit conversions, or coding. Woolschlager (2000) tested the original CDWQ model for mass balance closure, and all the major species - chlorine, nitrogen, and carbon -- converged. Due to the many additions and changes I made to create CDWQ-E I tested CDWQ-E for mass-balance closure. To test the equations for mass balance closure, I varied numerical time-steps, starting from 0.5 minutes and then decreasing to 0.05 minutes. For each time step, I ran the model for 30 days and then summed the mass of all the species containing each of the three major species at the end of each day. I used equations 3.1 through 3.3 to account for all form of Cl, N, and C.

$$\text{Total Mass of Cl} = NHCl_2 + NHCl_2*2 + NHOHCl + HOCl + OCl^- + Cl \quad (3.1)$$

$$\text{Total Mass of N} = CtNH_3 + NO_2^- + NO_3^- + N_2*2 + 6.24\times10^{-9}*(\text{BOM1}+\text{BOM2} + \text{Heterotrophs} + \text{AOB} + \text{NOB} + \text{EPS} + \text{Inerts} + \text{BAP}) \quad (3.2)$$

$$\text{Total Mass of C} = 3.12\times10^{-8}*(\text{BOM1} + \text{BOM2} + \text{Heterotrophs} + \text{AOB} + \text{NOB} + \text{EPS} + \text{Inerts} + \text{BAP} + \text{UAP}) \quad (3.3)$$

In these equations, 6.24×10^{-9} and 3.12×10^{-8} represent the number of moles of nitrogen per unit biomass (mole N/µg CODcell) and number of moles of carbon per unit biomass (mole C/µg CODcell), respectively; based on the biomass formula of $C_5H_7O_2N$. I computed the difference in total mass for each species from the time-0 values at the end of each 24-hour period, as well as the average difference in total mass over the entire 30-

day period. Table 3.2 presents the mass-balance errors for Scenario I using a time step of 0.05 minutes.

The largest mass-balance errors occurred for Cl, but never exceeded 0.003%, and the errors disappeared after 22 days. Errors for N and C always were less than 0.001%. Average errors were less than 0.001%. These results indicate that the CDWQ-E model did not have numerical or other mass-balance problems for Scenario I.

I followed the same procedure to test mass-balance closure for scenario II, and the results are shown in Table 3.3. Again, the largest mass-balance errors occurred for Cl, but never exceeded 0.003%, and the errors disappeared after 26 days. Errors for N and C always were less than 0.001%. These results indicate that the CDWQ-E model did not have numerical or other mass-balance problems for Scenario II, when denitrification was important.

Table 3.2 Results of mass-balance closure test for the CDWQ-E model showing percent change in total mass of chlorine, nitrogen, and carbon in a 30-day simulation of Case I

Mass Balance	**Mass Balance Change (Day)**		
Day	**Cl**	**N**	**C**
1	-0.003%	0.000%	0.000%
2	-0.002%	0.000%	0.000%
3	-0.001%	0.000%	0.000%
4	-0.001%	0.000%	0.000%
5	-0.001%	0.000%	0.000%
6	-0.001%	0.000%	0.000%
7	-0.001%	0.000%	0.000%
8	-0.001%	0.000%	0.000%
9	-0.001%	0.000%	0.000%
10	-0.001%	0.000%	0.000%
11	0.000%	0.000%	0.000%
12	0.000%	0.000%	0.000%
13	-0.001%	0.000%	0.000%
14	0.000%	0.000%	0.000%
15	0.000%	0.000%	0.000%
16	0.000%	0.000%	0.000%
17	0.000%	0.000%	0.000%
18	0.000%	0.000%	0.000%
19	0.000%	0.000%	0.000%
20	0.000%	0.000%	0.000%
21	0.000%	0.000%	0.000%
22	-0.001%	0.000%	0.000%
23	0.000%	0.000%	0.000%
24	0.000%	0.000%	0.000%
25	0.000%	0.000%	0.000%
26	0.000%	0.000%	0.000%
27	0.000%	0.000%	0.000%
28	0.000%	0.000%	0.000%
29	0.000%	0.000%	0.000%
30			
Mean % Change	-0.001%	0.000%	0.000%

Table 3.3 Results of mass-balance closure test for the CDWQ-E model showing percent change in total mass of chlorine, nitrogen, and carbon in a 30-day simulation of Case II

Mass Balance	**Mass Balance Change (Day)**		
Day	**Cl**	**N**	**C**
1	-0.003%	0.000%	0.000%
2	-0.003%	0.000%	0.000%
3	-0.002%	0.000%	0.000%
4	0.002%	0.000%	0.000%
5	-0.001%	0.000%	0.000%
6	-0.001%	0.000%	0.000%
7	-0.001%	0.000%	0.000%
8	-0.001%	0.000%	0.000%
9	-0.001%	0.000%	0.000%
10	-0.001%	0.000%	0.000%
11	-0.001%	0.000%	0.000%
12	-0.001%	0.000%	0.000%
13	-0.001%	0.000%	0.000%
14	-0.001%	0.000%	0.000%
15	-0.001%	0.000%	0.000%
16	-0.001%	0.000%	0.000%
17	-0.001%	0.000%	0.000%
18	-0.001%	0.000%	0.000%
19	-0.001%	0.000%	0.000%
20	-0.001%	0.000%	0.000%
21	-0.001%	0.000%	0.000%
22	-0.001%	0.000%	0.000%
23	-0.001%	0.000%	0.000%
24	-0.001%	0.000%	0.000%
25	-0.001%	0.000%	0.000%
26	-0.001%	0.000%	0.000%
27	-0.001%	0.000%	0.000%
28	0.000%	0.000%	0.000%
29	0.000%	0.000%	0.000%
30			
Mean % Change	-0.001%	0.000%	0.000%

3.4. Conclusions

To conclude this chapter, I address three questions: (i) How do results from the two simulated case scenarios validate CDWQ-E? (ii) What implications do simulation results bear for real distribution systems? (iii) What are the benefits of using CDWQ-E to analyze and interpret water quality trends?

The results from case scenarios I and II validate the CDWQ-E model. The nature and extent of all water quality decay trends observed from the two case simulations can be explained by looking at CDWQ-E process kinetics.

From the data obtained for case I scenario, I observed that, over time the concentration of ammonia increases, which represents nitrification potential, but no significant changes in nitrite and nitrate concentrations occurred throughout the simulation period. The increase in ammonia concentration matched the release of ammonia from chloramine decay and the oxidation of organic matter as presented in CDWQ-E model. AOB were in net decay until day 18 because in spite of the relative abundance of ammonia, the required S_{min} for AOB synthesis remained above the prevailing ammonia concentrations due to the presence of residual chloramine. In the absence of significant AOB growth, nitrite concentrations never reached the S_{min} required to support NOB growth and produce nitrate.

From the data obtained for case II scenario, I observed that over time the concentration of ammonia increases, which represents nitrification potential. I also observed significant declines in dissolved oxygen, nitrate and nitrite concentrations and an increase in the concentration of nitrogen. As was the case with scenario I, the increase in ammonia concentration matched the release of ammonia from chloramine decay and

the oxidation of organic matter as presented in CDWQ-E model. The depletion of dissolved oxygen, nitrate, and nitrite as well as the production of nitrogen all corresponded to the switch from aerobic heterotrophic respiration to anoxic denitrification. Oxygen depletion was also the reason why AOB and NOB never grew in this case scenario. The DO concentration dropped below the required DO_{min} long before the chloramine concentration declined enough so that prevailing ammonia concentration $> S_{min}$

The results from the projected case scenarios demonstrate two very important phenomena that have implications for water quality decay in real chloraminated distribution systems. First, over time nitrogen passes from chloramine to ammonia through chloramine decay and the oxidation of organic matter, creating potential for nitrification inside distribution systems. This demonstrates that reducing ammonia loading into the distribution system may not be enough to curtail nitrification inside distribution systems where chloramines are used. Nitrification can be more effectively controlled by reducing total organic loading rates and reducing the amounts of residual chloramines that are used throughout the distribution system. Second, while nitrification is a real threat for distribution systems where chloramines are used for disinfection, the potential for denitrification is very low because the level of oxygen depletion that is required to trigger anoxic heterotrophic denitrification is not likely to occur in distribution systems. The only exception to this could be deep biofilms and deep corrosion zones.

The main advantage of CDWQ-E is its predictive nature. In the real world, this will give water utility managers and treatment operators a chance to explore different options for alleviating water quality deterioration and select the one(s) likely to yield the

most wanted results. CDWQ-E can also be used to evaluate the efficacy of different treatment processes for example chlorination versus chloramination and give results that are specific for a particular source water quality.

Chapter 4

Modeling the Efficacy of Nutrient Substrate versus Disinfection in Controlling Heterotrophic Growth in Chloraminated Water

Bacterial growth is inevitable in drinking water distribution systems. On the one hand, bacteria present in source water can escape the treatment barrier and end up in distribution systems. On the other hand, bacteria can multiply inside distribution systems when electron donor substrates are present at concentrations high enough to support synthesis of new bacterial biomass. While there are many factors that affect bacterial growth, the extent to which bacteria accumulate within drinking water distribution systems rests upon two independent, but competing processes: bacterial growth related to the utilization of substrates and bacterial killing from disinfection (Block *et al.*, 1993; Servais *et al.*, 1993; Mathieu *et al.*, 1995; Dukan et al., 1996; Prevost *et al.*, 1997; Chandy and Angles, 1999; Ellis et al., 2000; Van Der Kooij, 2000; Le Puil, 2004, Llyod and Bartram, 1991, Momba et al., 2000, Woolschlager, 2000; Woolschlager et al, 2005; USEPA 2005). Several experimental and modeling studies of chlorine treated water have suggested that lowering substrate loading rates into the distribution system is a more effective strategy for controlling bacterial growth than maintaining a chlorine residual (Bourbigot *et al.*, 1984; LeChevallier *et al.*, 1991; Van Der Kooij, 1992; Block *et al.*, 1993; Servais *et al.*, 1993; Mathieu *et al.*, 1995; Prevost *et al.*, 1997; Chandy and Angles, 1999).

In order to assess the comparative efficacy of removing organic substrates versus disinfection in reducing the accumulation of heterotrophic bacteria in chloraminated drinking water I simulated batch tests under two different sets of conditions, with the batch version of the CDWQ-E model. In the first set, I simulated the model for different

BOM concentrations and without any chloramine. In the second set I simulated the model for different chloramine concentrations all with the same, non-growth-limiting, BOM concentration.

Here, I investigate three issues that can affect the quality of chloraminated water during distribution: the fate of biodegradable organic matter, the loss of chloramine residuals, and the accumulation of heterotrophic bacteria. I focused on heterotrophic bacteria because, although they do not necessarily pose a direct health risk, high levels of heterotrophic bacteria within a distribution system indicate that the network may be subject to a myriad of problems associated with water quality decay, e.g., rapid loss of residual disinfectants, extensive biofilm formation, protection of pollution indicator and pathogenic microorganisms, proliferation of predatory protozoa, the loss of oxygen and creation of anaerobic zones, and biologically produced tastes and odors (Dukan et al., 1996; Volk and LeChavallier, 1999; Zhang et al., 2004). I chose chloramine for two reasons. First, more utilities in the United States are choosing chloramine for secondary disinfection. This is because chloramines usually have better stability and a relatively lower disinfection byproduct formation potential than free chlorine. Second, and in spite of the previously stated fact, the bulk of studies that look at water quality decay during distribution have focused on free chlorine. By investigating the fate of biodegradable organic matter, the loss of chloramine residuals, and the accumulation of heterotrophic bacteria I want to quantify the relationship between BOM and chloramine in controlling heterotrophic bacteria. I also want to show the degree of disinfection required to suppress heterotrophic bacterial growth when BOM is abundant in treated water.

4.1 Model Simulations

4.1.1 Kinetic parameters

Values of all kinetic coefficients and input parameters used in the bacterial growth model are listed in Tables 2.1 and 2.2, respectively. Input and operational parameter estimates were based on the literature, current national drinking water quality standards, and results from two field studies that were recently conducted as part of the work reported in this dissertation (Chapter 5).

4.1.2 Run time

I simulated all case scenarios for 30 days. As stated in chapter 1, the average distribution system has a mean water retention time of 1.3 days and a maximum retention time of 3.0 days (AWWA, 2005). However, it is not unheard of for some sections of distribution systems to have water retention times as long as 24 days. Extremely long retention times are usually reported in small distribution systems and in areas where water stagnates, such as dead-ends (DiGiano et al., 2000; Prentice, 2000; Acker and Krasa, 2001; Vandermeyden and Hartman, 2001). In light of this, a retention time of 30 days represents a worst-case scenario in terms of bulk water age.

4.1.3 Selecting Key Inputs Parameter Values

To see the effect of disinfection on reducing the heterotrophic growth potential, I varied the initial chloramine concentration between 0.2 and 4 mg/L. The current USA maximum residual disinfectant level goals (MRDLGs) for free chlorine and chloramine are 4 mg/Las Cl_2 (USEPA, 2010). The minimum concentration of residual disinfectant that utilities must maintain at all points along the distribution network typically is 0.5 mg/L (USEPA, 2005). These guidelines are meant to strike a balance between

safeguarding against microbial growth and minimizing the formation of harmful disinfection by-products such as trihalomethanes and haloacetic acids within distribution systems.

The EPA has no standard for heterotrophic plate counts (HPC) in distribution systems. For all my simulations, I choose an initial heterotrophic concentration of 500 CFU/mL. This value is based on previous EPA recommendations in the Surface Water Treatment Rule (SWTR) of 1989, which recommended maintaining an HPC concentration below 500 CFU/mL as a substitute for maintaining a detectable chlorine residual (US EPA, 1989). In the 2001 National Primary Drinking Water Standards (NPDWS), the EPA sanctioned HPC enumeration as a method for measuring the variety of bacteria present in water, although without signifying any health significance. No MCL was set, but 500 CFU/mL was retained as the maximum level of HPC desirable in treated water (US EPA, 2001). A threshold of 500 CFU/mL is still used as an operational criterion when monitoring HPC in the US (USEPA, 2001).

Since all the recommended thresholds are on the CFU/mL basis, I converted CFU/mL to cells/mL (Appendix A) and then converted cells to COD equivalents in order to be consistent with the units in the model. To do these conversions, I used 4.3 cells to 1 CFU and $2{,}403 \times 10^3$ counts per μg COD. Using these conversions, 500 CFU/mL is equivalent to 0.89μg COD_{cell}/L. Derivation of all biomass and substrate unit conversions are shown in detain in appendix A.

To see the effect of biodegradable organic matter elimination on reducing the heterotrophic growth potential, I varied the initial DOC concentration between 0.5 and 5 mg C/L. The EPA does not regulate biodegradable organic matter as a 'contaminant.' Nevertheless, studies classify waters with the biodegradable organic carbon (BDOC)

concentrations above 0.5 mg C/L as having 'high' biodegradable organic carbon (Volk and LeChavellier, 1999). Since the consensus is that BDOC is about 10% of all the dissolved organic carbon in treated water, a BDOC concentration of 0.5 mg C/L roughly corresponds to a DOC concentration of 5 mg C/L. I used this cut-off to estimate input BOM1 and BOM2 concentrations. To reconcile an estimated maximum DOC concentration of 5 mg C/L to BOM1 and BOM2 concentrations, I assumed that DOC is 0.1 BOM1, 0.45 BOM2, and 0.45 ROM (refractory organic matter) (Woolschlager, 2000). Since the recommended threshold for DOC concentration is on mg C/L basis, I converted this to COD equivalents in order to input to the model. I used the ratio of 2.67 µg COD/µg C, which is based on an estimation of $3.12*10^{-8}$ mole C/µg COD, assuming that carbon has a zero oxidation state (Woolschlager, 2000).

Using these conversions, a DOC of 5 mg C/L is equivalent to 13.35 mg $COD_{substrate}$/L, with BOM1 and BOM2 fractions of ~1,340 and ~6,000 µg $COD_{substrate}$/L, respectively. This is equivalent to 2.75 mg C/L total biodegradable organic matter. I set the water temperature, which affects specific bacterial growth rate, the rate of residual chloramine decay, and rates of all oxidation reactions, at 25°C.

4.2 Results and Discussion

I assessed the heterotrophic growth potential of finished water by examining heterotrophic accumulation rates, substrate depletion rates, and the stability of residual chlorine in simulated batch tests. Figure 4.1 shows the general pattern of BOM depletion and heterotroph accumulation. Although the extent of BOM depletion and heterotroph accumulation varied with input BOM and chloramine concentrations, the trends in Figure

4.1 were true for all scenarios except those in which heterotrophs were in sustained decay throughout the simulation period. The three main trends in the figure can se summed as follows:

First, heterotroph accumulation tracked BOM depletion. I expected this because of the direct relationship between BOM utilization and heterotroph synthesis in the Monod equation (Eqn. 2.13). Throughout the simulation period, BOM depletion was most rapid during periods of increased heterotroph growth, a trend that has been reported in other modeling and experimental studies (De Silva et al, 2000; Laspidou and Rittmann, 2002; Woolschlager et al., 2005).

Second, BOM1 depletion was much faster than BOM2 depletion, as long as BOM1 was present. I also expected this because BOM1 is more readily degradable than BOM2. In the scenario presented by Figure 4.1, for example, BOM1 dropped by 80% by day 20, from 0.5 mg C/L at the start of the simulation to about 0.1 mg C/L. During the same time, BOM2 dropped from 2.25 mg C/L to 1.8 mg C/L, or only 20% depletion.

Third, BOM2 depletion was more rapid towards the end of the simulation, in this case represented in Figure 4.1 between days 21 and 30, BOM2 dropped from 1.8 mg C/L to 0.8 mg C/L. The more rapid biodegradation of BOM2 reflects that biomass concentration had increased from a combination of BOM1 and BOM2 utilization. While BOM1 had greater fractional removal than BOM2 due to its fast kinetics, BOM2 had greater absolute removal. This may indicate that that BOM2 grew more biomass than BOM1, increasingly so as the simulation time got longer.

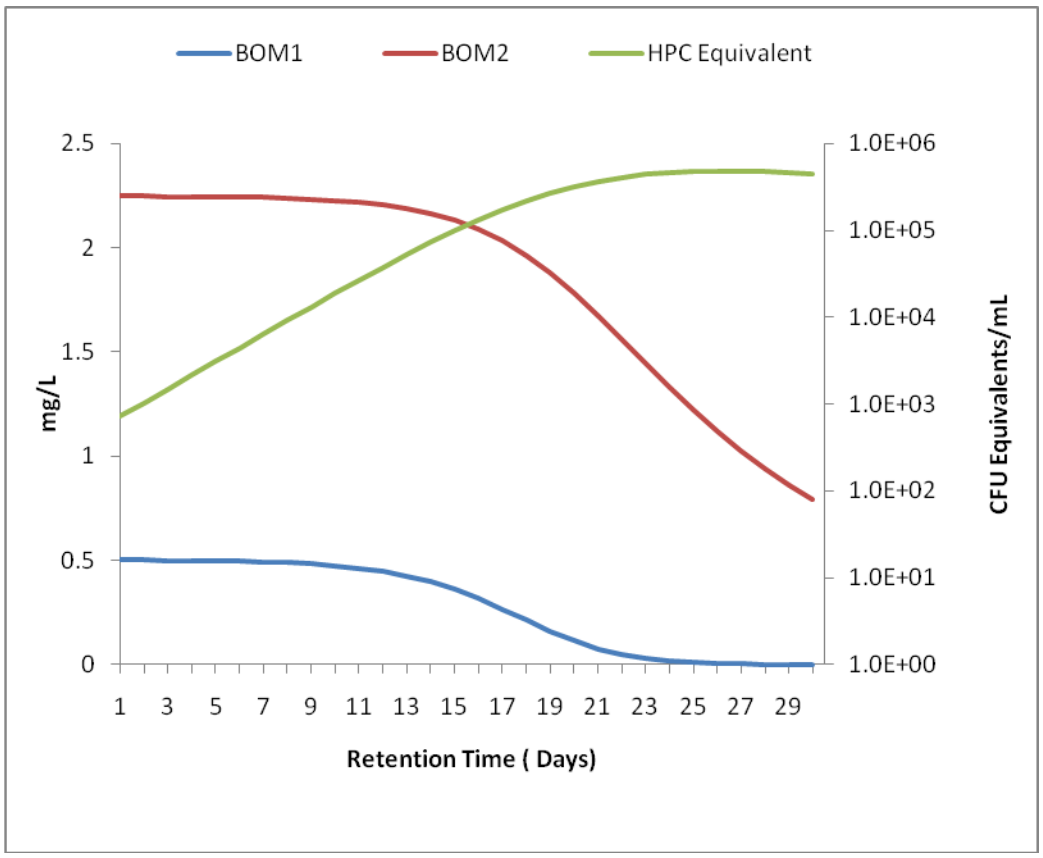

Figure 4.1 General trends for BOM depletion and heterotroph accumulation. This simulation had no chloramine residual and an initial HPC concentration of 500 CFU/mL.

4.2.1 Effect of varying substrate concentration on heterotrophic growth potential

In the absence of residual chloramine, heterotroph accumulation depends solely on the initial substrate concentration. To illustrate this I ran CDWQ-E for five combinations of input BOM1:BOM2. The input BOM1:BOM2concentrations were 0.050:0.225; 0.1:0.45; 0.2:0.910; 0.35:1.57; and 0.50:2.25 mg C/L which represent DOC concentrations of 0.5, 1.0, 2.0, 3.5, and 5.0 mg C/L respectively. Figure 4.2 shows selected results for this set of simulations.

In the scenarios I modeled here, the two lowest initial BOM concentrations (0.050:0.225, shown in Figure 4.2, and 0.1:0.45 mg C/L, not shown in the figure) led to

net decline in heterotrophic biomass from the start of the simulation. In contrast, initial BOM concentrations of 0.2:0.910 mg C/L and above yielded net heterotrophic growth. From this, I conclude that the minimum total BOM1:BOM2 concentration required for heterotroph growth is between 0.1:0.45 mg C/L and 0.2:0.910 mg C/L. I can estimate the theoretical minimum substrate concentration (S_{min}) based on the growth and decay parameters I use for these scenarios and equation 4.1 (Rittmann and McCarty, 2001).

$$S_{\min} = K_S\left(\frac{b}{Yq_{\max} - b}\right) \tag{4.1}$$

Since the CDWQ-E model separates BOM1 from BOM2, I can calculate S_{min} values for the two sub-types separately. Since the same microorganisms can use both BOM1 and BOM2 together, if either is above its S_{min}, I can get positive growth, and then both BOM types will be consumed.

BOM1:

$$S_{\min} = 15{,}000\mu gCOD/L\left(\frac{0.00417h^{-1}}{0.6\mu gCOD_{cell}/\mu gCOD * 0.417\mu gCOD/\mu gCODcell - h - 0.00417h^{-1}}\right)$$

$$S_{\min} = 255\,\mu gCOD/L$$

BOM2:

$$S_{\min} = 95{,}000\mu gCOD/L\left(\frac{0.00417h^{-1}}{0.6\mu gCOD_{cell}/\mu gCOD * 0.417\mu gCOD/\mu gCODcell - h - 0.00417h^{-1}}\right)$$

$$S_{\min} = 1{,}620\mu gCOD/L$$

In summary, net heterotroph synthesis will occur if (i) BOM1 is equal to or above 255 µg COD/L (0.10 mg C/L), (ii) BOM2 is equal to or above 1620 µg COD/L (0.60 mg C/L), (iii) both conditions are satisfied, or (iv) both BOM1 and BOM2 concentration are below S_{min}, but degradation of both together still gives a positive

growth rate. This means that the water is biologically stable only if both BOM1 and BOM2 concentrations are significantly below their S_{min} values. Looking at the results from the 5 simulations, I see that the S_{min} value estimated from the calculation correspond with the CDWQ-E simulations.

When input BOM1:BOM2 was 0.050: 0.255, heterotrophic biomass remained in sustained net decay for 30 days. This was expected, as BOM1 and BOM2 were well below the minimum concentrations of 0.10 and 0.6 mg C/L required to support net growth. For the highest three BOM1:BOM2 concentrations, 0.2:0.910; 0.35:1.57; and 0.50:2.25 mg C/L, the simulation yielded net positive growth. Again this was expected, as BOM1 and BOM2 were well above the calculated S_{min} values. Based on the S_{min} calculation alone, I might expect the second lowest input BOM1:BOM2 combination, 0.1:0.45 mg C/L, to yield net positive growth. While the input BOM2 concentration is less than calculated S_{min}, some growth from BOM1 utilization is possible because the input BOM1 concentration is right at S_{min}. Simulation results for this scenario, however, show negative net growth. Looking at the concentration profile of BOM1 (not shown), I can identify why BOM1 failed to sustain net positive growth. BOM1 quickly dropped below 0.10 mg C/L. By the end of the first day of simulation, BOM1 and BOM2 were well below their respective calculated S_{min} values.

For the three initial combinations of BOM1:BOM2 concentrations that supported positive net heterotrophic growth (0.2:0.910, 0.35:1.57, and 0.50:2.25 mg C/L), observed heterotrophic concentrations were 10^2 to 10^6 CFU/mL (Figure 4.2), with heterotroph concentration approaching10^6 for the largest input BOM concentration. Suspended heterotrophic bacterial counts in the range of 10^2– 10^6CFU/mL have been reported in

previous experiments (Reasoner and Gelderich, 1985; LeChavallier et al., 1987; Block et al., 1993; Gibbs et al., 1993; Prevost et al., 1998; Volk and LeChavallier, 1999; Woolschlager, et al., 2005) and modeling (Zhang et al., 2004; Woolschlager et al., 2005) studies. In field studies, heterotrophic plate counts up to 10^4 CFU/mL, for bulk water samples, are usually reported on occasions where residual disinfectant concentrations are low (Prevost et al., 1998; Volk and LeChavallier, 1999; Woolschlager, et al., 2005).

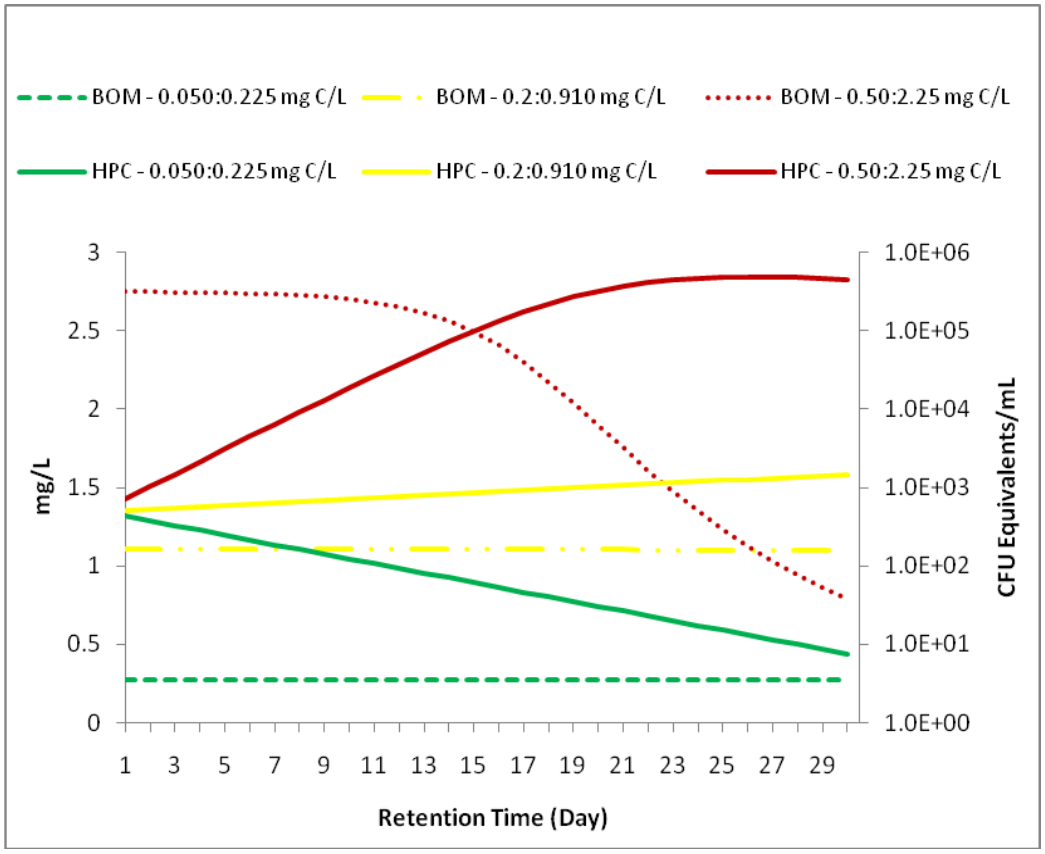

Figure 4.2 BOM depletion and heterotroph accumulation for various BOM1:BOM2 concentrations. Initial HPC concentration was 500 CFU/mL for all scenarios.

For the initial BOM concentration of 0.275 mg C/L (0.050:0.225), the lowest concentration tested, the net bacterial growth was negative, i.e., HPC declined from 500 CFU/mL to about 5 CFU/mL by day 30. When the initial BOM concentration was set at

2.75 mg C/L (0.50:2.25), the highest concentration tested the simulated bacterial concentrations increased to about $5x10^5$ CFU/mL after 30 days.

Thus, a tenfold increase in initial substrate concentration produced five orders of magnitude more bacterial concentration after 30 days. This underscores the importance of substrate concentration in controlling bacterial growth in drinking water (Dukan et al., 1996; Van Der Kooij, 1992; Volk et al., 1996; Woolschlager, 2000).

By looking at what happens over a 30 day period I am able to understand what could potentially happen under the worst case scenario. Because of the importance of retention time on all water quality decay trends forecast and analyzed here I want to highlight the extent of the observed trends at day 1 and 3, which represent the average and maximum retention times for most distribution systems in the US (AWWA, 2005).

For the initial BOM concentration of 0.275 mg C/L (0.050:0.225), HPC declined from 500 CFU/mL to about 400 CFU/mL after the first 24 hours dropping to 300 CFU/ml after 3 days. When the initial BOM concentration was set at 2.75 mg C/L (0.50:2.25), the simulated bacterial concentration was close to 700 CFU/mL after 24 hours, jumping up to 1500 CFU/mL after 3 days. Thus, in the absence of a disinfectant residual, increasing the input BOM concentration by one order of magnitude resulted in a fivefold increase in HPC over 3 days. This shows that the effect of initial substrate concentration on heterotrophic growth is evident even for short retention times.

4.3.2 Effect of varying residual disinfectant concentration on heterotrophic growth potential

To test the effect of disinfection on heterotrophic growth potential, I kept the input BOM1:BOM2 concentration constant at 0.50:2.25 mg C/L (total 2.75 mg C/L) and varied the input chloramine concentration between 0 and 4 mg Cl_2/L. Using these input BOM

concentrations made the water significantly biologically unstable, thus providing a strong test of the ability of chloramination to control bacterial growth.

The results are shown Figures 4.3. The general trends for bacterial growth accumulation and substrate utilization are similar to what I observed for 0.50:2.25 mg C/L in the absence of a residual disinfectant, but the chloramine residual had some impact on the rate of substrate utilization and bacterial accumulation: Increasing the initial chloramine concentration yielded a decline in the rates at which heterotrophic bacteria accumulated and the rate at which BOM was depleted over the duration of the simulation. However, the impacts were not large.

For the initial chloramine concentration of 0.2 mg Cl_2/L, the lowest non-zero concentration tested, the simulated heterotroph concentration was about $5x10^5$ CFU/mL at the end of the 30-day period, almost the same as for the no-chloramine simulation. Increasing chloramine concentration by an order of magnitude, to 2.0 mg Cl_2/L, resulted in only a small decrease in bacterial concentration, although the rate of increase was slower. Even an initial chloramine concentration of 4.0 mg Cl_2/L, the highest residual concentration that is allowed in distribution systems, decreased the HPC concentration only to about 50% of what the model predicted for lowest chloramine concentration.

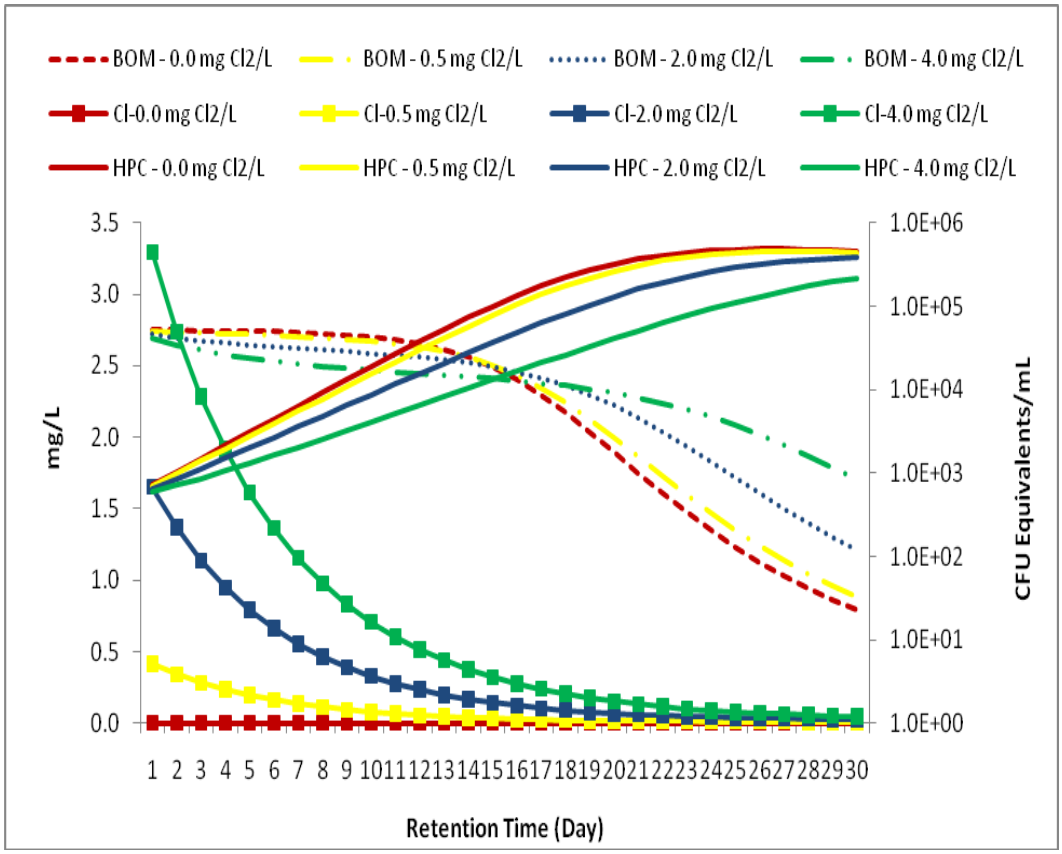

Figure 4.3 Heterotrophic accumulation, BOM depletion, and residual chloramine depletion. Initial BOM1:BOM2 concentration is 0.50:2.25 mg C/L with variations in input chloramine concentrations.

As expected, the loss of BOM correlated with the growth of HPC over the entire 30-day simulation. The highest chloramine concentration resulted in about 50% of the BOM loss seen for the no chloramine simulation. However, the results in Figure 4.3 also show that the rate of BOM was more rapid with higher chloramine concentration in the first half of the simulations. This rapid rate of BOM depletion was a result of the direct oxidation of substrate by residual disinfectants, not bacterial substrate utilization. The rapid loss of chloramine residuals is also shown in Figure 4.3. Similar trends were observed experimentally by Volk and LeChavallier (1999).

The loss of BOM accelerated around day 13 for the simulations with the lowest chloramine concentrations; by then, the chloramine concentration was less that 0.1 mg/L, while the HPC concentration was about $3x10^4$ CFU/mL. This combination allowed the BOM-utilization rate to increase. For initial chloramine concentrations of 2 and 4 mg/L, the time to accelerate the rate of BOM concentration was delayed to about 19 and 24 day, respectively, but the acceleration still took place.

Again, by looking at what happens over a 30-day period, I am able to understand what could potentially happen under the worst case scenario in terms of water residence time. The extent of water quality deterioration trends observed after the first 3 days are not as extreme as those observed after 30 days. When I simulated the model without any residual chloramine, HPC increased from 500 CFU/mL to about 700 CFU/mL after the first 24 hours. When the initial chloramine concentration was set at 0.5 mg Cl_2/L and 4.0 mg Cl_2/L, simulated bacterial concentrations were close to 700 CFU/mL and, 600 CFU/mL, respectively, after the first 24 hours. After the first 3 days, the simulated HPC counts were 1500 CFU/mL, 1400 CFU/mL, and 1100 CFU/mL for 0.0 mg Cl_2/L, 0.5 mg Cl_2/L, and 4.0 mg Cl_2/L respectively. These results clearly show that even over short retention times, when electron donor substrates are available at concentrations that are enough to support significant bacterial synthesis, high chloramine concentrations are required to effectively suppress growth.

The results in Figure 4.3 clearly demonstrate that a BOM1:BOM2 concentration of 0.50:2.25 mg C/L (total 2.75 mg C/L) presents so much biological instability that, even if the residual chloramine is 4 mg Cl_2/L, the highest concentration that the USEPA currently allows in drinking water, heterotrophic growth cannot be suppressed. Can more chloramine suppress the heterotrophs? Figure 4.4 shows that, at this BOM concentration,

the initial residual chloramine has to be between 12 and 15 mg Cl_2/L to suppress bacterial growth for 30 days.

The inability of residual disinfectants to effectively control the microbiological decay of finished water has been reported in other works. Earnhardt (1980) recovered coliform bacteria in samples containing 10 to 12 mg/L; free chlorine residuals as high as 15 mg/Liter were necessary to control bacterial growth inside the distribution system. Reilly and Kippen (1983) recovered coliform bacteria from 18% of chlorinated water samples from distribution systems. Olivieri and coworkers (1985) recovered coliform bacteria in 21% of the distribution system samples containing residual chlorine ranging from 1 to 3 mg/L. In the same study, coliform bacteria were also recovered from samples containing residual chlorine at concentrations as high as 8 mg/L. The relentless growth of bacteria in finished water is not limited to coliform bacteria. Numerous studies have shown that maintenance of disinfectant residuals does not always correlate with reduced HPC inside the distribution system (Goshko et al., 1983; LeChavallier et al., 1988; Momba et al., 2000; Woolschlager, 2000, 2005; LePuil, 2004).

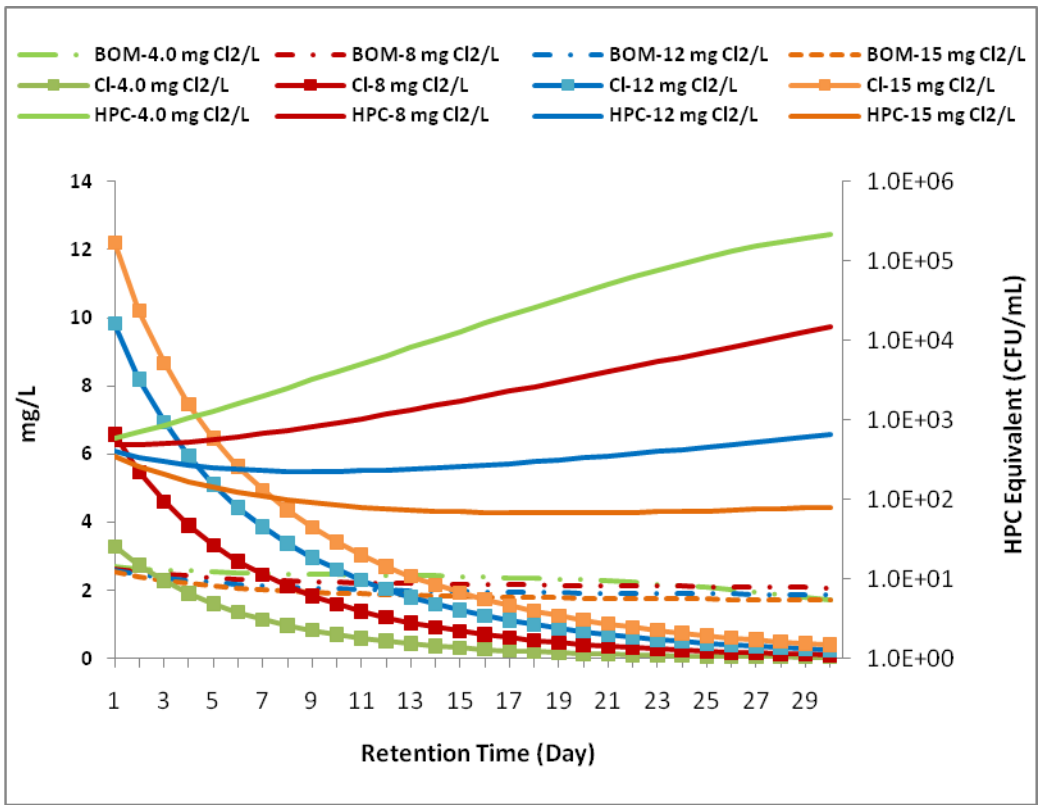

Figure 4.4 Heterotrophic bacterial accumulation for different chloramine concentrations when the water has a total BOM of 2.75 mg C/L.

In order to test the theoretical basis for heterotrophic growth rates under chloraminating conditions, I recalculate S_{min} by incorporating the decay effect from chloramine disinfection. In the absence of disinfection, I assume that biomass decay results solely from endogenous decay processes. The rate at which this happens depends on the concentration of biomass and the decay coefficient, for heterotrophs the decay coefficient is 0.00417 h^{-1}. Under chloraminating conditions, net biomass decay is the sum of decay from endogenous decay processes and disinfection. Therefore, the effective decay coefficient is 0.00417 h^{-1} plus the heterotroph disinfection rate coefficient, for chloramine this is 150 L-mol^{-1}-h^{-1} (0.0021 L-μgCl_2^{-1}-h^{-1}) multiplied by the chloramine concentration. For example, if the residual chloramine concentration is 1 mg

Cl_2/L, the net decay rate is 0.00628 h^{-1} and the new S_{min} values for BOM1 and BOM2 become 0.14 mg C/L and 0.90 mg C/L, respectively. For a residual chloramine of 4 mg Cl_2/L, the S_{min} values for BOM1 and BOM2 are 0.3 mg C/L and 1.96 mg C/L, respectively. Increasing the residual chloramine concentration to 8 mg Cl_2/L raises the S_{min} values for BOM1 and BOM2 to 0.41 mg C/L and 2.58 mg C/L, respectively. With my input concentrations of 0.50mg C/L for BOM1 and 2.25 mg C/L for BOM2, I still expect some degree of bacterial growth from the utilization of BOM1 when the input chloramine concentration is 8 mg Cl_2/L, as S_{min} still remains below 0.5 mg C/L. S_{min} declines as the residual chloramine decays. This explains why HPC decline before increasing in most scenarios in Figure 4.4.

4.3.3 Effect of residence time

As shown in table 1.3 prolonged water residence times can exacerbate most water quality decay trends. Table 4.1 compares BOM depletion, heterotroph growth, and chloramine decay for different water residence times. Results in this table clearly show that longer residence time exacerbates both the rates of heterotroph growth and residual chloramine depletion. If BOM is available at high enough concentrations, even the highest input residual chloramine concentration allowed by USEPA fails to effectively suppress heterotroph growth. Longer simulation times advance this, with HPC reaching 10^4/mL levels, even as chloramine residuals were available at or above maximum acceptable concentration. At high BOM levels, HPC suppression is only possible if chloramine is added at levels that far exceed the maximum recommended concentration. For relatively short simulation short times this leaves chloramine residuals at levels that violate the current regulations. Again, longer simulations time eventually lower

chloramine to levels that could not kill/inactivate bacteria at a rate higher than the rate at which synthesis occurred.

Table 4.1 Effect of water age on residual chloramine depletion and heterotroph synthesis

Water Age (Days)	**BOM: 0.275 NH_2Cl: 0.0**	**BOM: 2.75 NH_2Cl: 0.0**	**BOM: 2.75 NH_2Cl: 4.0**	**BOM: 2.75 NH_2Cl: 8.0**
1	HPC:10^2 Acceptable	HPC:10^2 Acceptable	HPC:10^2 Acceptable	HPC:10^2 Acceptable
	BOM:0.275 Acceptable	BOM :2.75 High	BOM:2.70 High	BOM:2.6 High
	NH_2Cl:N/A	NH_2Cl :N/A	NH_2Cl:3.3 Acceptable	NH_2Cl :6.6 Violation
3	HPC:10^2 Acceptable	HPC:10^3 High	HPC:10^3 High	HPC:10^2 Acceptable
	BOM:0.275 Acceptable	BOM:2.75 High	BOM:2.60 High	BOM:2.5 High
	NH_2Cl :N/A	NH_2Cl:N/A	NH_2Cl:2.2 Acceptable	NH_2Cl:4.6 Violation
5	HPC:10^2 Acceptable	HPC:10^3 High	HPC:10^3 High	HPC:10^2 Acceptable
	BOM:0.275 Acceptable	BOM:2.74 High	BOM:2.55 High	BOM:2.4 High
	NH_2Cl:N/A	NH_2Cl:N/A	NH_2Cl:1.6 Acceptable	NH_2Cl :3.33 Acceptable
10	HPC:10^2 Acceptable	HPC:10^4 High	HPC:10^3 High	HPC:10^3 High
	BOM:0.275 Acceptable	BOM:2.70 High	BOM:2.5 High	BOM:2.3 High
	NH_2Cl:N/A	NH_2Cl:N/A	NH_2Cl:0.7 Low	NH_2Cl:1.6 Acceptable
25	HPC:10^2 Acceptable	HPC:10^5 High	HPC:10^5 High	HPC:10^3 High
	BOM:0.275 Acceptable	BOM:1.23 High	BOM:2.1 High	BOM:2.1 High
	NH_2Cl:N/A	NH_2Cl:N/A	NH_2Cl:0.1 Violation	NH_2Cl: 0.2 Violation

*Concentrations are CFU/mL for HPC, mg/L as Cl_2 for NH_2Cl, and mg C/L for BOM. N/A, applicable i.e., parameter not measured for given set of conditions. All heterotrophic plate counts rounded off to the nearest 100.

4.3 Conclusions

Previous studies have suggested that substrate removal during drinking water treatment provides the most effective strategy for controlling bacterial growth and accumulation after treatment (Van Der Kooij, 1992; Dukan et al., 1996; Volk et al., 1996; Woolschlager, 2000; Zhang et al., 2004; Woolschlager et al., 2005). In this chapter, I have used the batch CDWQ-E model to quantify the effectiveness of substrate limitation versus disinfection on the heterotrophic growth potential of chloramine treated water. The results from the simulations illustrate important relationships among substrate concentration, residual disinfectant concentration, and water age in determining heterotrophic bacterial growth.

The results from the batch simulations show four important trends. First, BOM depletion matches well with heterotrophic growth and accumulation. Heterotrophic bacteria can grow to concentrations approaching 10^6 CFU/mL at the maximum residence time of 30 days if enough substrate is present in the water. Second, realistic chloramine concentrations cannot fully suppress the growth and accumulation of HPC when the water has a significant BOM concentration. This trend was evident even for shorter residence times. The only difference was the extent to which HPC accumulated. For example HPC tripled (from 500 CFU/mL to 1500 CFU/mL) after 3 days when the model was simulated under high BOM conditions. Even the highest allowable chloramine residual, 4 mg/L, merely slows HPC growth and reduces the final HPC concentration by about 50%. Third, maintaining a chloramine residual raises the minimum BOM concentration required for net bacterial growth. I showed this using simulation results and verified with S_{min} calculations. However, when BOM is available at high enough concentrations, the concentration of chloramine required to fully suppress bacterial

growth may be up to three times the maximum allowed by current drinking water regulations. Fourth, the natural loss of chloramine residual over time means that "old" water is naturally more susceptible to HPC growth unless the BOM concentration is below S_{min} with no chloramine present. Therefore, I conclude that maintaining low BOM concentrations is a more effective strategy to control heterotrophic levels in finished water than maintaining high chloramine residuals.

In this chapter I have addressed one key question, i.e., what causes prolific heterotrophic growth in finished water. I specifically looked at two major factors that control heterotrophic growth, availability of organic substrate and disinfection. While the data trends showed in Figures 4.2, 4.3, and 4.4 show the major trends for heterotrophic growth trends these figures alone do not show what the specific contributions of each of these factors (substrate availability and disinfection) towards heterotroph synthesis and or suppression are. To shed more light on this, I used S_{min} calculations to mathematically represent what takes place in the water under each of the simulated conditions. Net heterotrophic growth is only possible when the prevailing substrate concentration is equal to or higher than the required S_{min}. Because the S_{min} calculation includes the total decay term, in the presence of residual disinfectants, the required S_{min} increases. This is not fixed, as chloramine decays and the disinfection potential of the water decreases the required S_{min} also decreases and the substrate loading rate becomes more decisive in determining heterotrophic growth potential. The main conclusion here is that heterotrophic growth potential depends mostly on BOM loading. The importance of BOM in controlling distribution system heterotrophic growth is well recognized and widely reported (Block *et al.*, 199; Servais *et al.*, 1995; Woolschlager, 2000; Le Puil, 2004). However, by quantifying the relationship between BOM and disinfectant residual

through S_{min} calculations I show that minor boosts to the BOM pool require large increases in chloramine to maintain heterotrophic stability.

In real distribution systems, this means that when disinfectant concentrations are high, i.e., near the treatment plant or booster chlorination stations, the required S_{min} will be relatively high and disinfection is likely to outpace heterotroph synthesis. As the disinfectant residual decreases in the distribution system and over time, S_{min} decreases to levels equal to or less than prevailing concentrations, where net syntheses outpaces disinfection and heterotrophic growth occurs.

Chapter 5

Drinking water Distribution Systems as Potential Reservoirs of Infective *Naegleria fowleri*

Naegleria fowleri is acutely pathogenic to humans if it enters the brain. Most victims of *N. fowleri* infections are healthy children and young adults with a relatively recent history of exposure to warm, and often shallow, waters. *N. fowleri* flagellates can enter the central nervous system when contaminated water is drawn through the nose. Inside the nasal passage, the flagellates convert to the amoebic (trophozoite) form and travel up the olfactory mucosa, along olfactory nerve fibers, and through the cribriform plate into the brain. Once inside the brain, *N. fowleri* amoeba feed on red blood cells, white blood cells, and brain tissue causing a distinct type of meningitis. The disease advances rapidly, with upwards of 95% of reported cases ending in death within six days of the onset of symptoms (Fiordalisi et al., 1992; DeNapoli et al. 1996; Barwick et al., 2000; Lee et al., 2002; Gyori 2003; Marciano-Cabral et al., 2003; Craun et al., 2005; Blair et al., 2008; Morbidity Mortality Weekly Report 2008; Jamerson et al., 2009).

N. fowleri has been identified in recreational waters, thermally polluted run off, cooling water discharges from industries, and domestic water supplies (Wellings et al., 1977; Cabanes, 2001; Lee et al., 2002; Marciano-Cabral et al.,2003; Blair et al., 2008; CDC, 2008). *N. fowleri* is associated with warm waters, but the reasons why it thrives more in certain waters are not well understood. In this chapter, I evaluate the potential for drinking water distribution systems to act as reservoirs of infective *N. fowleri*.

I address the following questions: How can drinking water be a source of *N. fowleri*? What are the possible reservoirs for *N. fowleri* in a drinking water system? How can those reservoirs be eliminated? I use data from experimental studies conducted from two full scale distribution systems, two pipe loops, as well as the CDWQ-E model to answer these questions.

5.1 Background

5.1.1 General Introduction and Life Cycle

The genus *Naegleria* consists of six species of free-living amoebae widely distributed in soil and freshwater habitats. The different species can be distinguished on the basis of temperature tolerance, cyst morphology, immunologic criteria, and pathogenicity. *N. fowleri* which is primarily found in freshwater bodies and moist soils is the only species of Naegleria that is known to be pathogenic to humans (Marciano-Cabral, 1998).

The life cycle of *N. fowleri* has three stages: trophozoite, flagellate, and cyst (Figure 5.1). During the trophozoite stage, the organism measures 10 - 30 µm in diameter. This stage is characterized by a nucleus with a large centrally placed karyosome surrounded by a halo. Trophozoites are motile and move by using blunt pseudopodia and allowing the cell cytoplasm and contents to flow into the extension.

In the natural environment, trophozoites graze on bacteria, almost exclusively Gram-negative bacteria, and exhibit aerobic mitochondrial metabolism. Trophozoites replicate by binary fission.

Under severe environmental conditions, trophozoites may transmute to either the cyst or the flagellate stage. *N. fowleri* encysts in response to unfavorable environmental conditions, such as significant drops in temperature. *N. fowleri* cysts are spherical, have a nucleus surrounded by a thick cell wall, and measure 7-14 µm in diameter. The flagellate stage is more transient, and *N. fowleri* only enters this stage in response to changes in the ionic concentration of their immediate environment (Tyndall et al., 1989; Weisbuch, 2002; Marciano-Cabral et al., 2004; Blair and Gerba, 2006; Bennett et al., 2008; Blair et al., 2008; Jamerson et al., 2009; CDC, 2008).

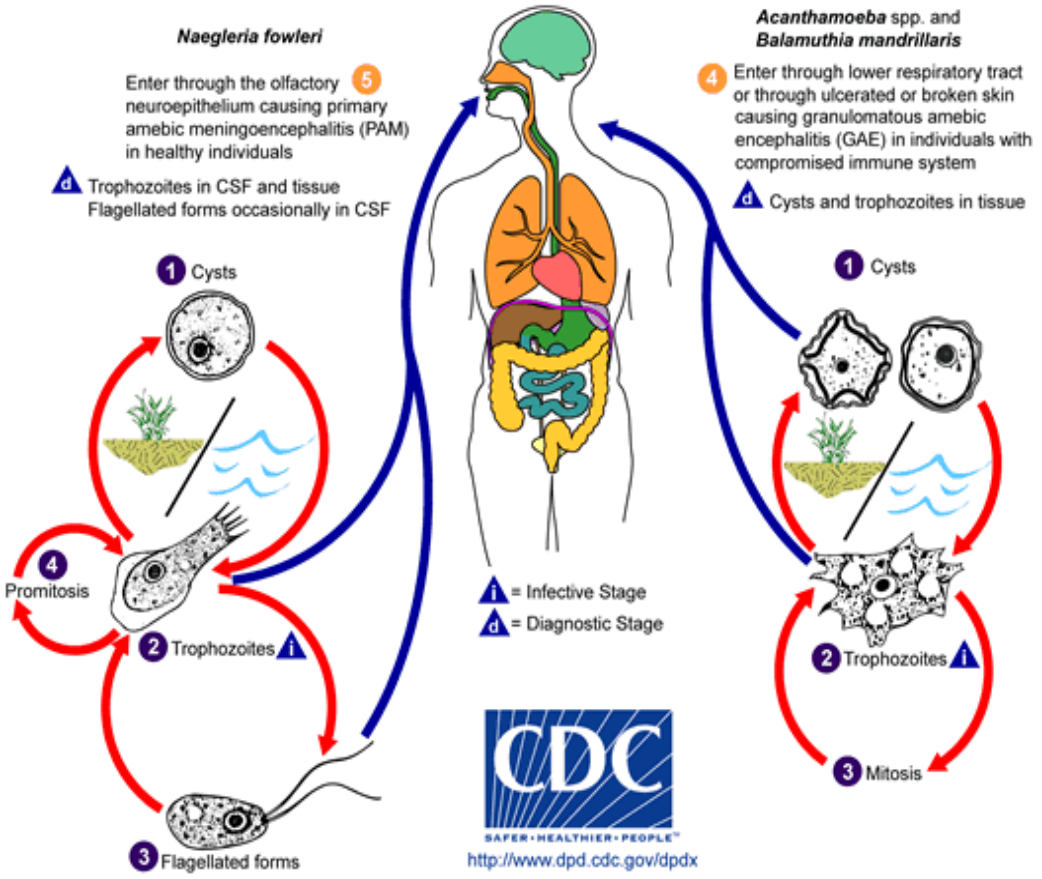

Figure 5.1 Life cycle of *Naegleria fowleri* (CDC, 2010)

5.1.2 Exposure and Pathogenesis

The disease most associated with *N. fowleri* infection is primary amoebic meningoencephalitis (PAM). *N. fowleri*-caused PAM disproportionately affects children and young adults. Most cases of *N. fowleri*-caused PAM occur during the warm summer months. This seasonal variation is most likely due to three reasons. First, being a thermophilic organism, *N. fowleri* thrives in warm waters. Second, *N. fowleri* cysts and trophozoites are usually present in higher numbers in the sediment than in the water. Because most natural water bodies have low water levels during the summer months, swimming or diving in shallow waters increases the likelihood of disturbing the sediment, thus releasing *N. fowleri* cysts and trophozoites that may be trapped in the sediment into the water. Third, increased participation in recreational water activities during the summer months raises the risk of exposure to contaminated waters. During infection, trophozoites enter the nose and invade the olfactory mucosa where they penetrate the sub-mucosal nervous plexus by crossing the cribriform plate to enter the subarachnoid space. The abundance of glucose and proteins, as well as the high oxygen content in the cerebrospinal fluid (CSF) and brain, sustains rapid growth and multiplication of the amoebae. Inside the brain, the trophozoites ingest red blood cells and white blood cells and destroy all tissue they come into contact with. This results in rigorous hemorrhagic necrosis of the brain.

Preliminary symptoms of PAM include sudden-onset headaches, fever, nausea, vomiting, and a stiff neck. These normally start between 1 to 4 days after infection. Secondary symptoms include puzzlement, lack of attention to people and surroundings, loss of balance, hallucinations, and seizures. *N. fowleri*-caused PAM progresses rapidly, with about 95% of all reported cases ending in death within 3 to 7 days of onset of

symptoms (Lozano-Alarcon et al., 1997; Cabanes et al., 2001; Marciano-Cabral et al., 2003; Bennett et al., 2008; Blair et al., 2008). By and large, death comes before the identification of *N. fowleri* as the disease agent.

5.1.3 *Naegleria fowleri* Prevalence in the United States and Arizona

The first case of *N. fowleri*-caused PAM was reported in 1965 in South Australia. Since then, incidences of *N. fowleri*-caused PAM have been reported from almost every continent. About half of all reported cases are from the United States (Marciano-Cabral, 1988; Cabanes et al., 2001; Schuster, 2002). In the United States, *N. fowleri*-caused PAM cases occur almost exclusively in the sun-belt states. The sun-belt region stretches across the south and southwest of the United States, below the 38th parallel north latitude (Figure 5.2). The region's definitive feature is its warm-temperate climate. Compared to the rest of the United States, this region has extended summers and brief, and often mild, winters. The extreme southern parts of this region are sub-tropical. The region covers roughly 15 states: Virginia, Oklahoma, Florida, New Mexico, Arizona, California, Georgia, South Carolina, Texas, Arkansas, Louisiana, Missouri, Mississippi, North Carolina, and Nevada. Of all these states, Arizona, Texas, and Florida lead in the number of reported cases of *N. fowleri* deaths (Lee et al., 2002; Marciano-Cabral et al., 2003; Blair et al., 2008; CDC, 2010).

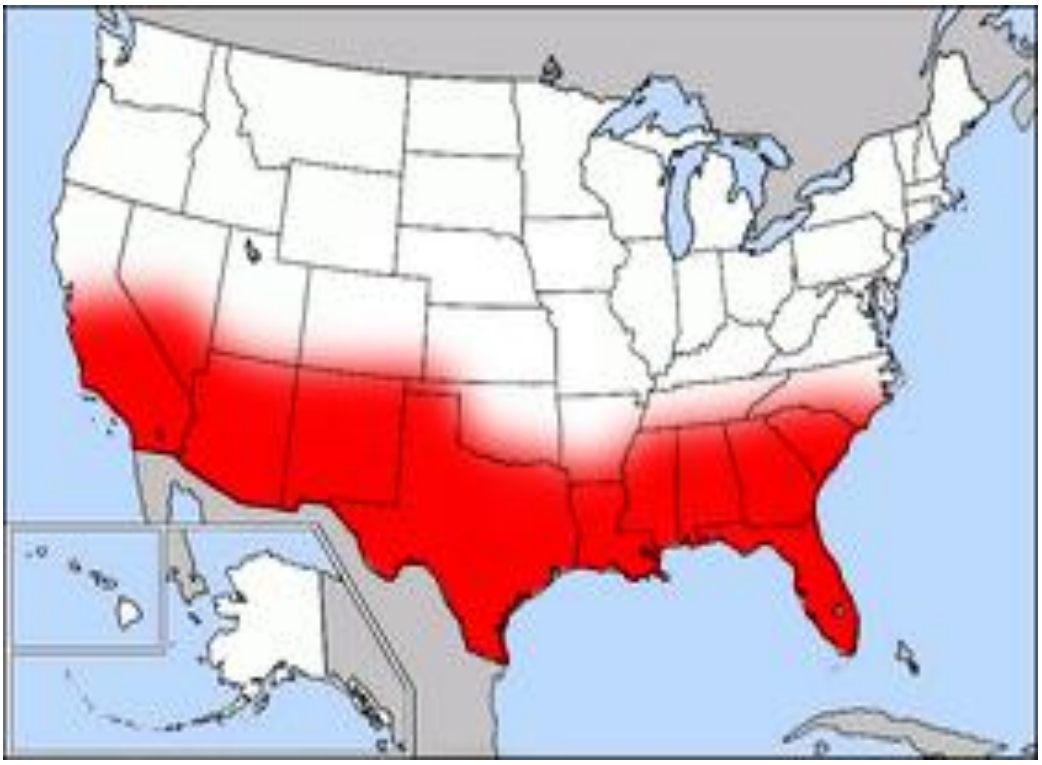

Figure 5.2 US map with Sun-Belt Region Highlighted (Wikipedia, 2010)

The first time that two cases of *N. fowleri*-caused PAM were reported in the same geographic area, at the same time, and linked to a single water source was in 2002 in Arizona (Weisbuch, 2002; *The Arizona Republic*, August 31, 2006), when two young boys died. In 2006, Blair and Gerba published a comprehensive study on the occurrence of *Naegleria* in Arizona's groundwater. This study showed *N. fowleri* to be present in 16% of 188 groundwater samples, including 8.3% of all drinking water wells sampled in this study, along with 7.2% of 97 samples collected from lakes, streams, and springs around Arizona. This study used molecular methods that targeted genomic *N. fowleri* DNA and did not employ any techniques to identify viable organisms. This study failed to show any correlation between the occurrence of *N. fowleri* and general water quality

indicators. This lack of correlation also was reported by Jamerson and co-workers (2009). One reason why *N. fowleri* occurrence is hard to correlate to water quality parameters stems mainly from the organism's ability to tolerate extremes of certain parameters. For example, the temperature at which *N. fowleri* grows ranges between 12 and 55 ^{o}C, and the pH ranges between 4.0 and 9.1 (Weisbuch, 2002, Blair et al., 2006; Blair et al., 2008; Jamerson et al., 2009). It is also possible that the most relevant water quality parameters may not have been measured. In the absence of disinfection guidelines and regulatory laws, *N. fowleri* remains a threat to Arizona and other communities where source waters might be contaminated, particularly if this organism finds its way to distribution systems (Marciano-Cabral et al., 2003).

5.1.4 Drinking water Distribution Systems as Reservoirs of *N. fowleri*

Within distribution systems, biofilms provide the most ideal micro-environment for the growth *N. fowleri*. Several factors support why biofilms potentially enhance the survival, growth, and dispersal of *N. fowleri* within drinking water distribution systems.

First, biofilms concentrate bacterial biomass. *N. fowleri* feeds almost exclusively on Gram-negative bacteria. In most distribution systems, the density of these bacteria in the water will be too low to sustain the growth of *N. fowleri*. Biofilm growth increases bacterial cell densities and by extension the potential for protozoan grazers to thrive (Camper et al., 1985; Newsome et al., 1985; Marshal et al., 1997; Murga et al., 2001; Banning et al., 2003; Blair and Gerba, 2006; Jamerson et al., 2009).

Second and of high importance here, biofilms offer protection from disinfection. Although *N. fowleri* can be inactivated by chlorine (Cassels, 1990), the efficacy of disinfection varies significantly depending on contact time and the available

concentration of chlorine. Chin (2000) recommends maintaining chlorine residuals of 1 – 2 mg/L to ensure the safety of swimming pool waters. Any factor that diminishes the concentration of the disinfectant can aid *N.fowleri* survival.

Third, successful attachment to the biofilm can enable *N. fowleri* to linger in the distribution system long after their initial introduction in the bulk water. Once inside the biofilm, *N. fowleri* can potentially act as long-term source of contamination through detachment and re-attachment (Donlan, 2002).

5.1.5. Objectives

The overall aim of the research that I am reporting in this chapter was to examine the ability of drinking water distribution systems to act as reservoirs of *N. fowleri*. The specific objectives were to determine: (i) if relationships exist among water chemistry, heterotrophic abundance, and the occurrence of *N. fowleri* and other amoeba, (ii) if operational practices such as flushing pipe networks and replacing distribution system fixtures, often employed to improve overall water quality, can reduce the occurrence of *N. fowleri* and other amoeba, and (iii) the ability of introduced *N. fowleri* to colonize and survive within distribution system biofilms.

5.2. Experimental Methods

5.2.1 Sampling

5.2.1.1 Field study

The two full-scale drinking water distribution systems identified for this study differed in type of source water, disinfection, size, and retention time. Table 5.1 summarizes the main differences between the relatively large system operated by the City of Peoria and the small system operated by the Maricopa Agricultural Center (MAC).

Table 5.1 Characteristics of the Two Full-Scale Distribution Systems

	City of Peoria	**MAC**
Source Water	Mixed: Ground and Surface Water	Ground Water
Disinfectant	Gaseous chlorine (Cl_2)	None
Client Population	City of Peoria Population ~ 145,000	Maricopa Agricultural Center population ~100
Retention time	~3 days	~5 days

Sampling sites reflecting variations in water chemistry, retention time, and biofilm-formation potential were identified across the two distribution systems. Each site was sampled twice, once before an operational intervention and once after the operational intervention. The operational intervention tested in both cases was unidirectional flushing. This was done for the main pipe network. Unidirectional flushing is one of the measures recommended to minimize potential for biofilm formation and help maintain desired levels of residual chlorine. The American Water Works Association (AWWA) recommends network wide unidirectional flushing every three years, with frequent flushing of dead-ends and other areas with persistently low residual chlorine, < 0.5 mg/L (AWWA, 2005). Two additional interventions were done by the City of Peoria: storage reservoirs were drained, pressure washed, disinfected, and then refilled with new water; water meters and fire hydrants were removed and replaced with new ones. Backflow preventer valves were taken apart and rebuilt in the field. Using biofilm control measures such as unidirectional flushing and cleaning reservoir tanks to avert the growth and spread of *N. fowleri* within distribution systems was first proposed by researchers from the Australian Water Quality Center (Robinson, 2005).

All samples for chemical analysis were collected in glass sample containers that had been previously sterilized in an oven at 500 ^{0}C for 2 hours. Where needed, 5 mL 0.1N sodium thiosulfate was added per liter of sample to neutralize chlorine. The

sampling points that had natural water flow, such as fire hydrants and faucets, were flushed until the water temperature stabilized; then, water samples were collected. Sample code, location, date, and time of sampling were recorded.

Samples were immediately placed on ice in a dark cooler box for transportation to the laboratory. Samples from the reservoir tank at the Maricopa Agricultural Center were collected with a Van Doren sampler, a mechanical sampling device that has a horizontal tube fitted with two plugs. The sampler is readied by pulling the plugs and locking them in a position that allows water to flow through the tube. The sampler is lowered to the reservoir by a cord. Once it had reached the bottom of the reservoir, the sampler was moved to allow the tube to fill with water and sediment. To collect only water and sediment from the bottom of the tank, a weight was dropped down the cord to snap the plugs into place on the ends of the tube. The Van Doren sampler was then hoisted to the top of the reservoir. The samples were then transferred to regular heat sterilized, sample collection bottles. The Van Doren sampler device was rinsed and disinfected between samples. Samples were stored on ice in a cooler box for transportation to the laboratory. Samples were transported to the laboratory and analyzed within 24 hours of collection.

At the laboratory, these samples (28 in total) were assayed for levels of heterotrophic bacteria, dissolved organic carbon (DOC), biodegradable dissolved organic carbon (BDOC), total nitrogen, total ammonia, ammonium, nitrate, nitrite, total chlorine, and free chlorine. Complementary water (8) and biofilm (20) samples were collected and taken to a collaborating laboratory for detection of general amoebic activity. Samples exhibiting amoebic activity were assayed for *N. fowleri*, *Acathamoeba*, and *Legionella*. These were very specific reasons why all samples tested for *N. fowleri* were

also tested for *Acathamoeba*, and *Legionella.* Like, *N. fowleri*, *Acathamoeba*, is a free living amoeba that is very widely distributed in soil and water and is pathogenic to humans. *Legionella*, a bacterial opportunist pathogen, is more often than not found in biofilms colonized by protozoa. Temperature, dissolved oxygen, and residual chlorine were measured for each set of samples collected.

5.2.1.2 Laboratory Study

For laboratory experiments, a dual-pipe loop system (Figure 5.3) was used. The system had two independent loops, one with cast-iron piping and the other with PVC piping. Each loop had a main pipe that is 5.5 m long and 5.1 cm in diameter, with a total volume of 50 liters. The main pipe was connected to a reservoir. A self-priming, thermally protected, magnetic-drive pump continuously re-circulated water between the main loop and the reservoir (Little Giant Pump Company, Oklahoma City, Oklahoma, USA). Water pressure, flow rate, and temperature (25 °C) were kept constant through external controls. Both pipe loops had been used continuously for the past 6 years and had well-established biofilm communities before the start of this study.

For these experiments, each pipe loop was fed with City of Tempe tap water that had been dechlorinated by aeration. In addition to the already established bacterial communities, the pipe loops were seeded with *N. fowleri* (ATCC 30894). In order to obtain the required dose before pipe loop inoculation, *N. fowleri* was cultured in Cline medium with sub-culturing every 4-5 days (Cline et al., 1983; Marciano-Cabral and Fulford, 1986; Page, 1988).

This stock culture was propagated until a concentration of $3.5x10^7$/mL median tissue culture infective dose ($TCID_{50}$) was reached. This concentration was enough to give an estimated *N. fowleri* concentration of 10^3 $TCID_{50}$/mL in the flowing water given

the volume of the pipe loop system. After inoculation with *N. fowleri*, the pipe loop was operated as batch systems for 5 months to track water quality and the fate of *N. fowleri*.

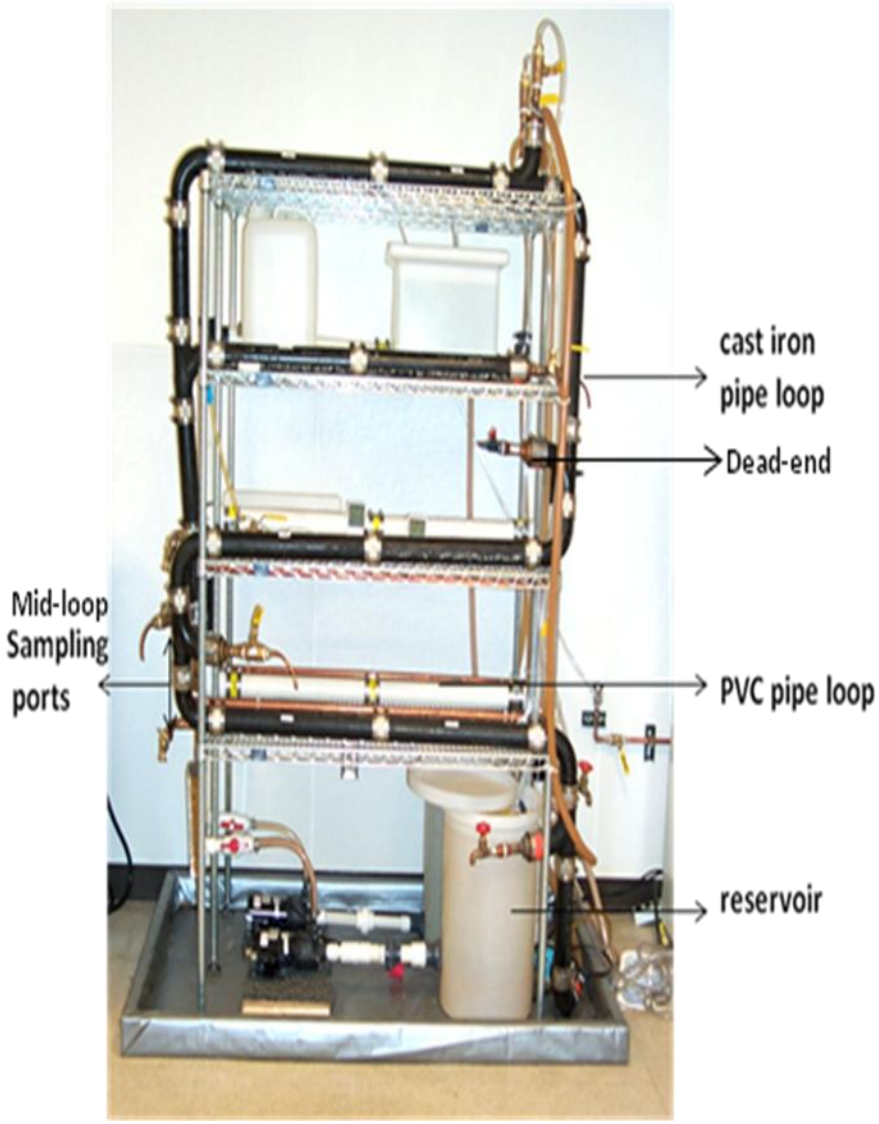

Figure 5.3 The Dual-Loop System with the PVC Loop is in the Back, and the Cast Iron Loop in the Front

At each sampling event, a water sample was collected from the reservoir, a dead end, and a sampling port in the middle of the loop. The two pipe loops were sampled at the same time, which means that six samples were collected each time. All samples for

chemical analysis were collected in glass sample containers that had been previously sterilized in an oven at 500 ^{0}C for 2 hours. Sampling ports were flushed for 3 seconds before sample collection. A total of 22 water samples were collected throughout the project: 18 small-volume samples (9 from each pipe loop) and 4 large-volume samples (2 from each pipe loop).

The small-volume samples were collected periodically through the duration of the study. Concentrations of DOC, total nitrogen, total ammonia, ammonium, nitrite, nitrate, and heterotrophic plate counts were measured for all small volume samples. The large-volume samples were collected only at the end of the study and assayed for concentrations of BDOC, plus all indicators measured in the small-volume samples. In addition to water samples collected for the analysis of chemical indicators, we collected additional weekly water samples from both pipe loops for use in viability assays. At the end of the 5-month simulation, biofilm samples were collected from the two pipe loops and assayed them for general amoebic activity and the presence of live *N. fowleri* and *N. fowleri* cysts.

5.2.2 Analytical Testing Methods

i. Temperature, pH, and Dissolved Oxygen

Temperature, pH, and dissolved-oxygen concentration were measured at the time of sample collection using a portable field meter (Accumet 13636AP84A, Fisher Scientific).

ii. Disinfectant Residuals

Measurements of total and free chlorine were taken at the time of sample collection using a HACH Chlorine Pocket Calorimeter™ II. The instrument uses AWWA standard methods 8021 (free chlorine) and 8167 (total chlorine).

iii. Dissolved Organic Carbon

DOC was measured using the combustion-infrared technique on a total organic carbon analyzer according to standard method 5310, a combustion-infrared technique. The biodegradable fraction of dissolved organic carbon was measured using a simplified version of the high-density BDOC test (Joret et al., 1991; Allegier et al., 1996; Woolschlager, 2000). This method uses a dense bacterial inoculum attached to sand and originally obtained from a biologically active drinking water filter. 100 g of sand was combined with sample water and incubated at room temperature until no further change in the DOC level was detected or until a minimum DOC value was reached, using AWWA Standard Method 5310, usually after 5-7 days (AWWA Standard Methods, 1995).

iv. Nitrogen Species

Total ammonium and total nitrogen were measured using calorimetric-based HACH methods 10031 and 10071, respectively. Concentrations of nitrite, nitrate, and ammonium were measured by ion chromatography using AWWA Standard Method 4110 (AWWA Standards Methods, 1995).

v. Heterotrophic Plate Counts

Our analysis for general bacteria solely focused on measurements of viable and culturable heterotrophic bacteria suspended in the water using heterotrophic plate counts (HPC). Since treated drinking water is generally considered a low-substrate

environment, a low-nutrient medium, R2A, was used. The plates were incubated at 28°C for 7 days AWWA Standard Method 9215 (AWWA Standards Methods, 1995).

vi. Detection of General Amoebic Activity and *N. fowleri*

Assays for the detection of general amoebic activity and the presence of *N. fowleri* were performed according to the techniques described in Marciano-Cabral et al (2003). Approximately 10 liters of each collected water sample were passed through a 1-µm-pore-size polypropylene disk filter (Cuno, Incorporated, Meriden, CT). The filter was then eluted in sterile Page's amoeba saline. Two 10-mL aliquots of the eluted sample were dispensed into individual 75-cm^2 tissue culture flasks. The samples were then incubated 2 days, one at 37°C and another at 44°C. Biofilm samples were centrifuged at 5,000 x g for 10 min and re-suspended in sterile Page's amoeba saline. Two 10-mL aliquots of the sample were dispensed into individual 75-cm^2 tissue culture flasks.

The samples were then incubated 2 days, one at 37°C and the other at 44°C. After incubation, tissue culture samples were observed for the presence of amoebae by light microscopy. If amoebic activity was detected, a small sub-sample was immediately transferred to Cline medium to hinder growth of bacteria and fungi present in the samples. After 10 days of further incubation in tissue culture flasks, a small aliquot of each sample was collected for PCR analysis. This was kept continuously cultured for 3 months. A second aliquot for PCR analysis was collected from each sample after 3 months. This aliquot was used for PCR analysis for the detection of *N. fowleri*.
For PCR analysis, DNA extraction was performed using the QIAamp DNA mini kit (QIAGEN, Valencia, California) according to the manufacturer's instructions. The eluates were stored at -20°C until used in the PCR assay. Nested PCR was performed by

amplifying a portion of a gene (*Mp2C15*) producing a protein unique to *N. fowleri* (Reveiller et al., 2002). The forward primer, *Mp2Cl5*.for (5'-TCTAGAGATCCAACCAATGG-3') and the reverse primer, *Mp2Cl5*.rev (5'-ATTCTATTCACTCCACAATCC-3'), were used to amplify a 166-bp fragment of the *Mp2C15* gene. The reaction was performed in a 50 µl volume consisting of 1x *Taq* DNA polymerase buffer (10 mM Tris-HCl [pH 8.3], 50 mM KCl, 2.5 mM $MgCl_2$), a 0.2 mM concentration of each deoxynucleoside triphosphate, 0.6 µM primer, 2.5 U of TaKaRa Ex Taq™ (Takara Bio Inc., Shiga, Japan) and 2 µl of DNA template using a Bio-Rad Tetrad2 Peltier Thermal Cycler (Bio-Rad, Hercules, CA, USA).

PCR amplifications were performed using a Bio-Rad Tetrad2 Peltier Thermal Cycler (Bio-Rad, Hercules, CA, USA) under the following cycling conditions: one cycle of an initial denaturation at 95°C for 5 min and 1 min at 95°C, 1 min at 65°C, and 2 min at 72°C for 35 cycles. To increase the sensitivity of the assay, nested primers, *Mp2Cl5*.for-in (5'-GTACATTGTTTTTATTAATTTCC-3') and *Mp2Cl5*.rev-in (5-GTCTTTGTGAAAACATCACC-3'), which amplified a 110-bp fragment of *Mp2Cl5*, were used in a second round of PCR. Amplification conditions were as follows: 35 cycles of 1 min at 95 ^{o}C, 1 min at 55 ºC, and 1 min at 72 ^{o}C. The presence of PCR products was visualized by 1.5% agarose gels using GelStar Nucleic Acid gel stain (Lonza, Rockland, ME, USA).

vii. PCR Detection of Bacteria and Acathamoeba

American Type Culture Collection (ATCC) strains were used to prepare positive controls and DNA standards for standard PCR. *Legionella sainthelensi* (ATCC 35248), was grown in BCYE agar medium supplemented with antibiotics. *Acanthamoeba*

castellanii (ATCC 50370) was maintained in axenic proteose-peptone-yeast-glucose (PYG) medium. DNA extraction was performed using Mo Bio PowerSoil kits (MO BIO Laboratories, Carlsbad, CA) according to the manufacturer protocol. DNA concentrations were measured with a NanoDrop ND-1000 UV spectrophotometer (NanoDrop Technologies, Wilmington, DE). DNA extracts were stored at –20°C until further processing.

Multiple PCR assays were performed targeting 16S and 18S rRNA genes for *Legionella* and *Acanthamoeba*, respectively. PCR amplifications were performed in 25 µl using the polymerase TaKaRa Ex Taq™ (Takara Bio Inc.) in a Bio-Rad Tetrad2 Peltier Thermal Cycler (Bio-Rad, Hercules, CA) under the following cycling conditions: one initial denaturation step at 95°C for 5 min and 35 cycles of 1 min at 95°C, 1 min at optimum annealing temperature (Table), and 1 min at 72°C. PCR products were visualized by 1.5% agarose gels using GelStar Nucleic Acid gel stain (Lonza, Rockland, ME, USA).

5.3 Results and Discussion

5.3.1 Field Study

The sampling locations for each distribution system were a point within the distribution system near the treatment plant or the wellhead, a point within the distribution system far from the treatment plant/wellhead, a water meter, a reservoir tank, a dead end, a fire hydrant, and a valve. Thirteen physical and chemical parameters known to affect microbial activity in water were measured and recorded for all field samples.

Overall, distribution system water quality parameters differed more between the two distribution systems than they did among samples taken from a single distribution system before and after the proposed operational practice. On average, water samples obtained from the Peoria (large and chlorine disinfected) distribution system had higher concentrations of DOC, BDOC, and residual chlorine and lower concentrations of heterotrophic bacteria than samples from the MAC (small and not disinfected) system. Of the 13 water quality parameters measured from all samples, only HPC concentrations differed significantly between samples collected before and after the proposed operational practices.

5.3.1.1 Depletion of Dissolved Organic Carbon, Depletion of Residual Chlorine, and Heterotrophic Abundance

Changes in DOC, residual chlorine, and HPC concentrations within a distribution system are related to the water's residence time. A longer residence times normally allows more heterotrophic growth. This in turn leads to the depletion of DOC and residual chlorine (Geldreich et al., 1972; LeChevallier et al., 1987; Maul et al., 1985; Zhang and DiGiano, 2002; Camper et al., 2003; AWWA, 2005). To demonstrate this trend for the two systems analyzed in this study, I compared the distribution of heterotrophic bacteria, residual chlorine, DOC, and BDOC at selected sites across the two distribution systems. As expected, samples taken from the sampling points close to the entrance of the distribution systems had high DOC and residual chlorine (for the Peoria system) concentrations and low HPC concentrations compared to corresponding samples taken from sampling points towards the end of the distribution system.

The variations in the concentrations of DOC, BDOC and HPC along the distribution network were more definite in samples from the MAC system. The

concentration of DOC dropped from 0.7 mg/L to 0.5 mg/L (-28%). It is important to note that the change in BDOC accounts for most of the difference in the concentrations of DOC measured at the entrance of the distribution system and those measured at sites far away from the entrance. While at the entrance of the distribution systems, BDOC was 0.2 mg C/L (29% of DOC), at the site furthest from the distribution system entrance BDOC was 0.01 mg C/L (<2% of DOC). This shows that, during residence within the MAC distribution system, BDOC was almost completely depleted. In parallel, HPC increased from 725 CFU/mL to 3270 CFU/mL (+350%) between the sampling site at the entrance of the distribution system to the site near the end of the distribution system for samples taken before the proposed best operational practice. Several studies have reported similar trends, i.e. more heterotrophic growth than can be accounted for by B/DOC depletion along the distribution system and concluded that the main source of HPC was the biofilm. Van de Wende and Characklis (1989) reported that biofilm growth and detachment accounted for almost all suspended bacteria in an unchlorinated potable water distribution system. Maul and co-workers (1991) reported that, in potable water distribution systems, the extent of bacterial growth in the bulk water is negligible. Camper and co-workers (1991) reported that, even in the absence of residual disinfectant, only biofilm-bound bacteria multiply when biodegradable organic matter is limited. This phenomenon of suspended bacteria originating from biofilms may explain the occurrence of high levels of heterotrophic place counts (HPC), coliforms, and pathogens inside distribution systems with no obvious breaching of treatment barriers.

After the proposed best operational practice, DOC dropped less -- from 0.6 mg/L to 0.54 mg/L (-10%), while BDOC increased from 0.1 – 0.2 mg C/L. The increase in the concentration in BDOC, which is equivalent to easily biodegradable organic matter

(defined as BOM1 in chapters 2, 3,and 4), could be due to the hydrolysis of other, hard to degrade, BOM (essentially BOM2 as defined in Chapters 2, 3, and 4). After the interventions, HPC increased less -- from 300 CFU/mL to 850 CFU/mL (+183%) -- between the entrance of the distribution system and the sampling point furthest from the treatment plant. The smaller changes after the operational practices may have been an outcome of biofilm removal.

Table 5.2 Distribution of Selected Water Quality Parameters at Selected Sampling Sites

Sampling Site	Operational Procedure	HPC (CFU/mL)	Cl (mg Cl_2/L)	DOC (mg C/L)	BDOC (mg C/L)
Entrance to Network (MAC)	Before	730	N/A	0.70	0.2
	After	300	N/A	0.60	0.1
End of Network (MAC)	Before	3300	N/A	0.50	0.01
	After	850	N/A	0.54	0.2
Dead-End (MAC)	Before	11000	N/A	0.50	0.2
	After	2200	N/A	0.60	0.3
Storage Reservoir (MAC)	Before	1200	N/A	0.78	0.3
	After	7200	N/A	0.50	0.0
End of Network (Peoria)	Before	-	-	-	
	After	550	0.93	0.96	0.4
Dead-End (Peoria)	Before	-	-	-	-
	After	2400	1	0.88	0.3
Storage Reservoir (Peoria)	Before	0	0.69	2.1	0.1
	After	38	0.90	1.6	0.7

The role that disinfection plays in determining heterotrophic abundance in finished water is also very clearly seen in these data. A comparison of data from the sampling points near the end of the two distribution systems revealed some interesting trends. In the MAC system (no chlorine disinfection), the measured DOC concentration was 0.54 mg/L and the BDOC concentration was 0.2 mg C/L, while the measured HPC concentration was 850 CFU/mL. By comparison, the corresponding sample from the

Peoria system (with chlorine disinfection) had a DOC concentration of 0.96 mg/L and BDOC of 0.4 mg C/L, both almost twice the concentration measured in the MAC system, but an HPC concentration of 550 CFU/mL, two thirds of the concentration measured in the MAC system. This general trend was also true for other sites such as dead-ends and storage reservoirs (all shown in Table 5.2). From this trend I can infer that, within the Peoria system, residual chlorine was partly suppressing bacterial growth in spite of a high growth potential.

The effect of a longer residence time on heterotrophic abundance and depletions of residual chlorine, DOC, and BDOC was also evident in other sites where water tends to stagnate (see Appendix B1 for results from all sampling sites). For example, Table 5.2 summarizes these parameters inside storage reservoirs and at dead-ends. On average, the concetrations of HPC bacteria measured at the dead-ends were higher than concentrations measured in samples from storage reservoirs and samples from the futherest point in the distribution systems. In contrast to storage reservoirs, dead-ends have high surface area to volume ratios. Coupled with the generally low flow rates, this makes the role of the exchange of biomass between the biofilm and bulk water significantly important in dead-ends. This may explain why HPC levels dropped significantly following the proposed best operational practice for the unchlorinated system after the operational practice. The measured HPC concentrations were 11,000 CFU/mL and 2,200 CFU/mL for the samples collected before and after the proposed best operational practice, respectively. Again, this observation underscores the role that biofilm-bound bacteria play in determining the bacteriological quality of potable water inside distribution systems. The high values in absolute terms underscore the escalated risks of biofilms in dead-ends.

5.3.1.2 Nitrification and Denitrification

Table 5.3 shows measured results for total ammonium, nitrite, and nitrate in samples from selected sites across the two distribution systems. On average, samples from the MAC system had higher concentrations of measured total dissolved nitrogen. Ammonia dominated dissolved nitrogen in both systems. Nitrate was generally present in the MAC system, with nitrite was detected only in trace quantities in both systems. On average, the samples from the Peoria system had almost twice as much ammonium and nitrate as samples from the MAC system.

Dissolved nitrogen species showed a significant spatial pattern within the distribution systems. This is best illustrated by a comparison of data from water samples collected from the sampling site near the entrance of the distribution system and the site furthest from the wellhead. In the MAC system, ammonium concentration decreased, while nitrate concentration increased. This indicates possible nitrification along the distribution system. Evidence of nitrification in the unchlorinated system was present before and after flushing, although the degree was lower after flushing. Nitrogen data were limited for the chlorinated system, but ammonium dominated the nitrogen content, while nitrate was detected only in the storage reservoir. Thus, the chlorine residual in the Peoria system largely suppressed nitrification.

Table 5.3 Distribution of Selected Water Quality Parameters at Selected Sampling Sites

Sampling Site	Operational Procedure	Ammonia (mg N/L)	Nitrate (mg N/L)	Nitrate (mg N/L)
Entrance to Network (MAC)	Before	0.3	0.002	0.5
	After	0.5	0.002	0.07
End of Network (MAC)	Before	0	0.003	1.3
	After	0.3	0.009	0.98
Dead-End (MAC)	Before	0	0.002	0.5
	After	0.004	0.002	0.001
Storage Reservoir (MAC)	Before	0.3	0	0.09
	After	-	0.001	0.01
End of Network (Peoria)	Before	-	-	-
	After	0.1	0.008	0.01
Dead-End (Peoria)	Before	0	0	0
	After	0.1	0	0
Storage Reservoir (Peoria)	Before	0.08	0.001	1
	After	0.1	0.002	0.05

5.3.1.3 Occurrence of Pathogens and Opportunistic Pathogens

Microscopic examination revealed amoebic activity in 54% of all samples collected, 13% of all water samples and 70% of all biofilm samples.

Samples that had amoebic activity were screened for two pathogenic species of amoeba, *N. fowleri* and *Acathamoeba* spp. as well as *Legionella* spp, an opportunistic pathogen. All results are shown in Table 5.4.

Overall, amoebic activity was similarly present in both systems and decreased after the operational practices for both systems. In the MAC system, 40% of the

locations that had tested positive before flushing tested negative after flushing. For the Peoria system, the reduction was 50%. Flushing the pipe network and replacing distribution system fixtures could have achieved the observed reduction of amoebic activity in two ways. The first mechanism is direct removal of biofilm that harbored amoeba. The second mechanism is indirect. Flushing and the other operational procedures tested in this study significantly reduced bacterial biomass, particularly the concentrated ready-to-graze biomass that biofilms provide. This lack of food material can limit the survival of live amoeba within distribution systems.

Despite some reduction in amoebic activity from the operational procedures, amoebic activity was present in both distribution systems in all cases. This was in spite of major differences in the DOC of the finished water, much higher in Peoria; residual chlorine, present in Peoria, but absent in MAC; and bacterial abundances, higher in MAC.

It is very important to note that while there was no significant difference in the percentage of samples that showed amoebic activity between the two distribution systems, both before and after operational procedures, there was a distinct spatial trend in the occurrence of amoebic activity within each distribution system. In both the MAC and Peoria systems samples taken from sites characterized by longer retention times i.e. dead-ends and storage reservoirs were more likely to show amoebic activity that samples taken from other sites in the distribution system. These were also sites characterized by low residual chlorine, low B/DOC, and high heterotrophic counts.

Table 5.4 Microbiaological Analysis of Water and Biofilm Samples from Field Samples

Sample ID **B – Before** **A – After**	**Microscopy**		**Standard PCR**	
	Amoebic activity	***Naegleria fowleri***	***Acanthamoeba* spp.**	***Legionella* spp.**
1. DS Entrance (MAC B)	-	N/A	N/A	N/A
2. DS Entrance (MAC A)	-	N/A	N/A	N/A
3. DS End (MAC B)	-	N/A	N/A	N/A
4. DS End (MAC A)	-	N/A	N/A	N/A
5. Reservoir (MAC B)	-	N/A	N/A	N/A
6. Reservoir (MAC A)	-	N/A	N/A	N/A
7. Reservoir Bf (MAC B)	+	–	–	+
8. Reservoir Bf (MAC A)	+	–	–	+
9. Dead-End Bf (MAC B)	–	–	–	+
10. Dead-End Bf (MAC A)	+	–	–	–
11. Hydrant Bf (MAC B)	+	–	–	–
12. Hydrant Bf (MAC A)	+	–	–	+
13. Valve Bf (MAC B)	+	–	–	–
14. Valve Bf (MAC A)	+	–	–	+
15. Meter Bf (MAC B)	–	–	–	+
16. Meter Bf (MAC A)	–	–	–	+
17. DS End (Peoria B)	N/A	N/A	N/A	N/A
18. DS End (Peoria A)	-	-	-	-
19. Reservoir Bf (Peoria B)	+	–	–	+
20. Reservoir Bf (Peoria A)	+	–	–	+
21. Dead-End Bf (Peoria B)	+	–	–	–
22. Dead-End Bf (Peoria A)	+	–	–	–
23. Hydrant Bf (Peoria B)	+	–	–	+
24. Hydrant Bf (Peoria A)	–	–	–	–
25. Valve Bf (Peoria B)	–	–	–	+
26. Valve Bf (Peoria A)	+	–	–	+
27. Meter Bf (Peoria B)	+	–	–	+
28. Meter BF (Peoria A)	–	–	–	–

All samples tested negetive for *N. fowleri* and for *Acathamoeba* spp. One reason why no *N. fowleri* was found is that they may never have been introduced. Although *N. fowleri* was never detected in field samples, a high potential for bacterial growth and by extension biofilm formation, the abundance of amoebic activity, as well as the abundance of *Legionella* spp., a bacterial species known for its affinity for growth in biofilm

communities where protozoa abound, are strong indications of a potential risk that *N. fowleri* could be harbored in the biofilm if introduced.

Legionella species were identified in 9 out 14, or 64%, of biofilm samples that had amoebic activity. This was in comparison to 3 out of 6, or 50%, of biofilm samples that did not have amoebic activity. The abundance of *Legionella* spp is another cause for concern, because a relationship between the abundance of *Legionella* and the occurrence of protozoa, including pathogenic species, has been established for distribution system environments (Newsome et al., 1985; Murga et al., 2001; Banning et al., 2003). When grown in model distribution systems, *Legionella* almost exclusively grew only in the presence of protozoa (Newsome et al., 1985; Murga et al., 2001; Banning et al., 2003).

As was the case with general amoebic activity, samples collected from sites characterized by longer retention times were overwhelmingly more likely to also contain Legionella spp. than samples collected from sites other sites in either distribution system.

The pervasiveness of amoebic activity and *Legionella* spp. in sites characterized by long retention times in both distribution systems is a serious cause for concern. Both observations support the conviction that while high heterotrophic counts do not represent a direct risk to public health, high heterotrophic growth within drinking water distribution systems is usually a reliable indication of a distribution system in which more serious water quality problems, such as rapid disinfectant depletion and pathogen growth, can also be expected.

5.3.2 Laboratory Study

The sampling locations for each pipe loop were a point halfway along the length of loop, a reservoir tank, and a dead-end. Within each pipe loop, differences in water

quality parameters in samples obtained from different sampling locations were minimal. Thus, the pipe loops behaved as completely mixed batch reactors.

When introduced to pipe-loop systems, *N. fowleri* successfully attached to biofilms and survived for extended periods of time. Live *N. fowleri* and *N. fowleri* cysts were detected from biofilm samples collected 5 months after initial inoculation of the laboratory pipe loops. This observation supports the role that biofilms can play in the protection and spread of *N. fowleri* if this pathogen finds its way across the treatment barrier or gets introduced to distribution system downstream of treatment processes. This is the most important finding from all the experimental work carried out as part of this dissertation.

First, this finding exposes a real challenge to utility managers in areas where source waters may be contaminated. Once established in biofilm-communities *N. fowleri* can be continuously released and spread throughout the distribution system through biofilm detachment and re-attachment. The detached microorganisms can subsequently infect bulk water or re-attach and colonize pipe surfaces downstream exposing consumers to a consistent source of infectious agents and potentially increase the likelihood of infection. The lack of federal guidelines for disinfection and regular monitoring of source waters for this organism further increases the risk associated with exposure from contaminated drinking water. Depending on the likelihood that a distribution system might be contaminated, utility managers may have to resort to such measures as shock chlorination or system-wide flushing, which can be expensive to carry out on a regular or semi-regular basis.

Second, this finding has serious implications for public health. Because *N. fowleri* infections have been invariably linked to exposure to contaminated recreational

waters, patients who present symptoms with no history of participating in recreational water activities could potentially be at risk of incorrect or delayed diagnosis and treatment. Needless to say, consequences for this could be dire as *N. fowleri* caused PAM advances very rapidly.

The observed water chemistry differed notably between the two pipe-loops, even though both loops had been fed the same tap water at the beginning of the experiment. Table 5.5 lists water quality trends observed trends. The trends in parameters clearly related to biological instability varied considerably due to the materials and prior biofilm accumulation in the two loops. In both pipe loops, DOC concentration decreased significantly over time. The rate at which DOC was depleted was much higher within the cast iron than within the PVC loop. Concentrations of heterotrophic bacteria increased during the first month then decreased. The concurrent drop in DOC concentration and increase in heterotrophic bacteria observed during the first month were expected, since the biodegradable fraction of DOC fuels heterotrophic metabolism. Interestingly, DOC levels continued to drop, although at reduced rates, beyond the first month, even though heterotroph levels did not continue to rise, but declined. It is likely that the growth of new bacterial biomass continued in parallel with the consumption of BDOC beyond the first month, but net bacterial growth remained negative due to predation by protozoa and other decay processes.

Table 5.5 Comparison of Water Quality Trends in the Pipe-Loops for Parameters Related to Biological Instability

Pipe-Loop	Time (weeks)	HPC (CFU/mL)	DOC (mg C/L)	Ammonia (mg N/L)	Nitrate (mg N/L)	Nitrate (mg N/L)
PVC	3	5.00E+04	7	0.1	0	0
	5	8.0E+05	4.4	0.2	0.03	0.03
	7	4.00E+05	3.3	0.13	0	0
Cast-Iron	3	2.0E+04	2.7	0.2	0	0.04
	5	3.0E+05	2.1	0.1	0	0
	7	2.0E+05	1.8	0.07	0	0

The PVC loop supported slightly more heterotroph growth than the cast iron loop. During the first few days, biological activity was faster in the cast iron loop, which showed more rapid depletion of DOC and accumulation of HPC. As the DOC (and BDOC) concentrations dropped, microbial activity became strongly dominated by decay and predation in the cast iron.

The PVC loop first had increases in the concentrations of ammonium, nitrate, and nitrite. This trend lasted for the first 5 weeks of the experiment. The increase in ammonium concentrations was most likely due to its release from decaying biomass that was present in the pipes from past experiments with them. The accumulations of nitrite and nitrate were results of nitrification, driven by the addition of ammonium into the system.

Results from the cast iron loop show an even stronger indication of nitrification. Ammonium declined steadily during the first 3 weeks of the experiment. This decline in ammonium was accompanied by a significant increase in the concentration of nitrate. While the ammonia concentration continued to decrease at more or less the same rate beyond the 3rd week of the simulation, the concentration of nitrate also dropped rapidly. This is some evidence that denitrification was occurring in parallel to nitrification. It

appears that conditions in the cast iron pipe loop were able to create anaerobic micro-environments for denitrification. Microenvironments may have been accentuated in the cast iron pipe due to it having thicker biofilm that the PVC pipe and localized corrosion and pitting. The release of reduced iron, Fe^{2+} from pipe corrosion most likely provided the much needed electron donor substrate to support further bacterial activity.

5.4 Conclusions

In this chapter, I have examined the potential role of drinking water distribution systems to act as reservoirs of infective *N. fowleri*. I addressed three essential questions: Can drinking water distribution systems harbor *N. fowleri*? What are the reservoirs for *N. fowleri* in a drinking water system? Can those reservoirs be eliminated? To draw some conclusions I re-iterate the key findings that can be inferred from the data presented in this chapter.

When introduced to pipe-loop systems, *N. fowleri* successfully attached to biofilms and survived for extended periods of time. Live *N. fowler* and *N. fowleri* cysts were detected from biofilm samples collected 5 months after initial inoculation of the laboratory pipe loops. This observation supports the role that biofilms can play in the protection and spread of *N. fowleri* if this pathogen finds its way across the treatment barrier or gets introduced to distribution system downstream of treatment processes. Biofilm-bound *N. fowleri* can then be continuously released and spread throughout the distribution system through detachment and re-attachment. The detached microorganisms can subsequently infect bulk water or re-attach and colonization pipe surfaces downstream. Thus, drinking water can be a source of *N. fowleri*, and the main reservoir appears to be biofilms dominated by bacteria.

Although *N. fowleri* was never detected in field samples, a high potential for bacterial growth and by extension biofilm formation, the abundance of amoebic activity, as well as the abundance of *Legionella* spp., a bacterial species known for its affinity for growth in biofilm communities where protozoa abound, are strong indications of a potential risk that *N. fowleri* could be harbored in the biofilm if introduced. Since there are no disinfection guidelines and no regulations, *N. fowleri* remains a threat to the State of Arizona, where source waters have been found to be contaminated and drinking water distribution system can act as reservoirs for this organism.

Bacterial growth and by extension biofilm formation are controlled by the water's residence time, chlorination, and the concentrations of DOC concentration in the finished water at the time that it enters the distribution system. A comparison of DOC depletion and HPC accumulation along the MAC distribution before and after flushing clearly showed this point. HPC increased from 725 CFU/mL to 3270 CFU/mL (+350%) between the sampling site at the entrance of the distribution system to the site near the end of the distribution system, while DOC only dropped from 0.7 mg/L to 0.5 mg/L (-28%) for the samples collected before the proposed best operational practice. Even after the proposed best operational practice, HPC increased from 300 CFU/mL to 850 CFU/mL (+183%) while DOC dropped from 0.6 mg/L to 0.54 mg/L (-10%) between the entrance of the distribution system and the sampling point furthest from the treatment plant.

The role that disinfection plays on heterotrophic abundance is clearly seen in these data. In the MAC system, the measured DOC concentration was 0.54 mg/L, while the measured HPC concentration was 850 CFU/mL. By comparison, the corresponding sample from the Peoria system had a DOC concentration of 0.96 mg/L, almost twice the

concentration measured in the MAC system), but the HPC concentration was 550 CFU/mL, only two thirds of the concentration measured in the MAC system. Thus, a chlorine residual counter-balance the growth potential from biodegradable organic matter in the water, although it could not eliminate HPC.

Different residence times created spatial variations in HPC concentrations along the two distribution systems. Almost without exception, samples collected from sites that generally experience longer residence times had elevated HPC, lower or no residual, and lower DOC concentrations than the average for each distribution system. This increase in HPC concentrations was coupled to a decrease in the concentrations of two chemical species that control HPC growth, DOC and residual chlorine. High HPC concentrations and low DOC and residual chlorine concentrations were also observed in storage reservoirs and dead ends, both locations where water tends to stagnate.

From field studies, the sites characterized by longer residence times, extreme heterotrophic growth, and DOC and residual chlorine depletion, were more often than not likely to test positive for amoebic activity and have *Legionella* spp. Temporal interventions in the full-scale distribution systems reduced HPCs and nitrification, but did not eliminate these water quality problems. Thus, the best-operational practices had only a modest impact on the biofilm reservoir. Large reductions in biofilm accumulation require that the main causes of bacteria growth be eliminated from the finished water. Those main causes are biodegradable DOC and ammonia, which fuel heterotrophic and nitrifier growth, respectively.

Chapter 6

Using CDWQ-E to Assess Distribution System Water Quality and the Growth of *Naegleria fowleri*

In Chapter 5, I evaluated the potential for drinking water distribution systems to act as reservoirs of infective *N. fowleri*.

Using data from two full scale distribution systems I showed five important water quality trends that occur during residence in the distribution system: (i) heterotrophic counts increase away from the treatment plant, (ii) organic substrates such as DBOC and ammonia decrease away from the treatment plant, (iii) disinfectant residuals decrease away from the treatment plant, (iv) prolonged residence within the distribution system exacerbates the extent of trends i, ii, and iii, (v) samples collected from sites where water is retained for long are most likely to test positive for amoebic activity and have *Legionella* spp. than samples collected from other sampling sites.

Needless to say, field data provides valuable insight into the evolution of water quality during distribution. Nevertheless, there are questions that all the data from experimental studies can not answer. For example, do heterotroph counts increase because residual chlorine levels drop along the Peoria system and because there is no disinfectant residual in the MAC system? Alternatively, are heterotroph counts high because of relatively high BOM levels in both the MAC and Peoria systems? Why are amoebic activity and the occurrence of *Legionella* more pervasive in sites with long water retention times? Looking at field data trends can not provide answers to these questions.

Using data from two pipe loops I showed two very important trends regarding the growth and survival of *N.fowleri* in distribution systems: (i) *N. fowleri* is able to attach to

distribution system biofilms (ii) inside distribution system biofilms *N.fowleri* can survive for extended periods of time. These data however does not show the reason(s) why *N. fowleri* is able to thrive in distribution system biofilms.

The CDWQ-E model comes in handy because I can use it to rank out individual influences of the processes of substrate utilization, chlorine decay, heterotroph synthesis, and *N. fowleri* growth on the observed water quality trends to answer all the questions I pose here and could not answer by looking at field and laboratory data. Hence, in this chapter I use the CDWQ-E model to interpret and analyze the water quality trends observed in field and laboratory studies presented in chapter 5.

6.1 Modeling Distribution System Water Quality Decay

For full scale distribution simulations I utilized the CDWQ-E model with input conditions similar to conditions observed in the MAC and Peoria systems. Table 6.1 highlights the key input parameter values for the simulations representing the two distribution systems. They are typical of the finished-water values I reported in Chapter 5, Tables 5.2 and 5.3. With the exception of K_{BOM1}, all kinetic parameters for bacterial growth and disinfection were as listed in Table 2.2. I used a K_{BOM1} value of 5 mg C/L to be representative of the BOM in these two systems. It is slightly lower than the value I used in Chapters 3 and 4, 15 mg C/L. This value gives good representation of the experimental results.

In Chapters 3 and 4, I assumed that DOC is 10% BOM1, 45% BOM2, and 45% non-degradable organic matter. Data from samples obtained from the MAC and Peoria systems (Table 5.2) indicated BDOC values that were 29% and 40% of the total DOC, respectively. To use this empirical information, I assumed that the BDOC is nearly

equivalent to BOM1. For the MAC system I assumed that, at the entrance of the distribution systems, DOC was 30% BOM1, 20% BOM2, and 50% non-biodegradable. For the Peoria system, I assumed that DOC was 40% BOM1, 10% BOM2, and 50% non-biodegradable.

Table 6.1 Key Input Conditions for Model Scenarios Representing MAC and Peoria Systems

Parameter	**MAC**	**Peoria**
DOC (BOM1:BOM2) mg C/L	0.70 (0.2:0.14)	2.0 (0.8:0.2)
Disinfectant Residual mg Cl_2/L	0	2.0
Heterotrophic cells/mL	310,000	860

I used the batch version of CDWQ-E model to forecast trends in water quality decay in the two distribution systems. In order to closely represent each system, I simulated the MAC and Peoria system for 3 and 5 days, respectively. These represent the actual water retention times of the two systems as shown in Table 5.1.

Using a suspended-growth batch model to represent a biofilm-dominated system has its limitations. Within biofilm-dominated systems, biofilm growth and detachment account for a larger proportion of the biomass in the bulk water than does synthesis of new biomass in the bulk medium itself. In other words, estimates based on the bacterial numbers in the bulk water underestimate microbial reactions, as accumulation in the biofilm retains biomass and creates a source of suspended biomass via biofilm detachment. A suspended-growth batch model is also likely to over-estimate the amount of residual disinfectant available for biomass disinfection. In real chloraminated distribution systems, total chloramine demand is a sum of the demand from auto-decay

reactions, oxidation reactions involving organic matter and inert biomass, and reactions that occur at the pipe surfaces. In a batch model with no biofilm, total chloramine demand is the sum of the demand from auto-decay reaction and oxidation reactions involving organic matter and inert biomass. Because the true amount of residual disinfectant is the difference between the amount of residual added and the total demand, underestimating the chlorine demand of water may result in over-estimating the amount of chlorine that is available for biomass disinfection.

Despite these limitations, the simulations I can carry out with the suspended-growth batch model do provide valuable insight to water-quality-decay trends within distribution systems. On the one hand, the batch model, with or without biofilm, is able to estimate the growth potential of the bulk water, i.e., the extent to which the water that enters the distribution system will be able to support new bacterial synthesis based on the balance of BOM concentrations and disinfectant residual. Likewise, the batch model represents the trends of disinfectant loss and its effect on releasing nitrogen and spurring the growth of nitrifying bacteria. On the other hand, I am able to include the impacts of the biofilm biomass by adjusting the amount of biomass in the system so that it includes the biomass in the biofilm. I explain how I do this in the next section.

The reality is that the experimental measurements were relatively sparse. This means that my goal is to use CDWQ-E to explain major similarities or differences in the trends of water quality decay in the distribution system studies. In this way, I can take advantage of CDWQ-E's ability to identify mechanisms that most strongly affect water quality, including the fate of *N. fowleri*. This strategy is especially effective because the MAC and Peoria systems were distinctly different in that the MAC system had no chlorine residual, while the Peoria system had a significant residual of free chlorine.

Figures 6.1 and 6.2 show the simulated water quality trends for the MAC and Peoria distribution systems, respectively. As I outline in the following paragraphs, the trends in water quality decay projected by CDWQ-E simulation were similar to trends observed from experimental data, as presented in Chapter 5 (Tables 5.2 and 5.3). This allows me to gain insights into the factors controlling water quality in these two quite-distinct distribution systems.

The MAC system, which had no chlorine residual, had relatively low DOC and BDOC concentrations at the time that the water entered the distribution system: 0.7 and 0.2 mg/L, respectively (from Table 5.2). In the model, I assumed an input DOC concentration of 0.7 mg C/L, corresponding BOM1 and BOM 2 concentrations of 0.2 mg C/L and 0.14 mg C/L, respectively. I calculate $S_{min, BOM1}$ and $S_{min, BOM2}$ as follows:

BOM1:

$$S_{\min} = 5{,}000 \mu gCOD / L \left(\frac{0.00417 h^{-1}}{0.6 \mu g COD_{cell} / \mu gCOD * 0.417 \mu gCOD / \mu gCOD cell - h - 0.00417 h^{-1}} \right)$$

$$S_{\min} = 85 \mu gCOD / L$$

$$S_{\min} = 0.032 mgC / L$$

BOM2:

$$S_{\min} = 95{,}000 \mu gCOD / L \left(\frac{0.00417 h^{-1}}{0.6 \mu g COD_{cell} / \mu gCOD * 0.417 \mu gCOD / \mu gCOD cell - h - 0.00417 h^{-1}} \right)$$

$$S_{\min} = 162 \mu gCOD / L$$

$$S_{\min} = 0.06 mgC / L$$

Based on the S_{min} values, I expected the water in the MAC system to support net positive heterotrophic growth, because the prevailing concentration of BOM1 (0.2 mg C/L) is significantly larger than the minimum concentration required to support growth

(0.032 mg C/L). Since S_{min} for BOM2 is also smaller than the initial concentration, BOM2 biodegradation is also possible.

Because the HPC data from field experiments (Table 5.2) were based on water sample analysis and did not include estimates of biofilm biomass, I assumed that biofilm biomass is 100 times the suspended biomass. Then, the model projected the total biomass, which is dominated by biofilm, but I converted back to suspended biomass by dividing the total biomass by 100.

Table 5.2 shows that HPC increased from 730 CFU/mL to 3,300 CFU/mL between the sampling point closest to the entrance of the distribution system and the one furthest from the distribution system entrance. Using the biomass conversion I show in Appendix A, I assumed that that these numbers are at least 4.3X less than the true estimates for all viable cells, because not all viable cells can be cultured on growth media. This changed bacterial concentrations to 3,100 cells/mL at the site close to the entrance of the distribution system and 14,000 cells/mL at the site furthest from the entrance of the distribution system. Using the ratio of 1:100 to account for biofilm in the model, I converted bacterial counts for the MAC system to 310,000 cells/mL at the site close to the distribution system entrance.

Figure 6.1 shows that, in the MAC system, HPC increased from 310,000 cells/mL at the start of the simulation to 410,000 cells/mL by the end of day 5. Adjusting for the 1:100 suspended growth to biofilm growth ratio this gives 4,100 cells/mL or 950 HPC/mL in the bulk water. This is equal to a 30% increase in heterotrophic biomass concentration. Although this is significantly lower than the 350% increase observed from field data, the ratio of suspended biomass to biofilm biomass is not necessarily a constant; it may go up downstream as detached biomass builds up in the water. So, 1:100

may become 1:30 or even 1:20 downstream, and these ratios would bring the model-predicted HPC results more line with the measured values.

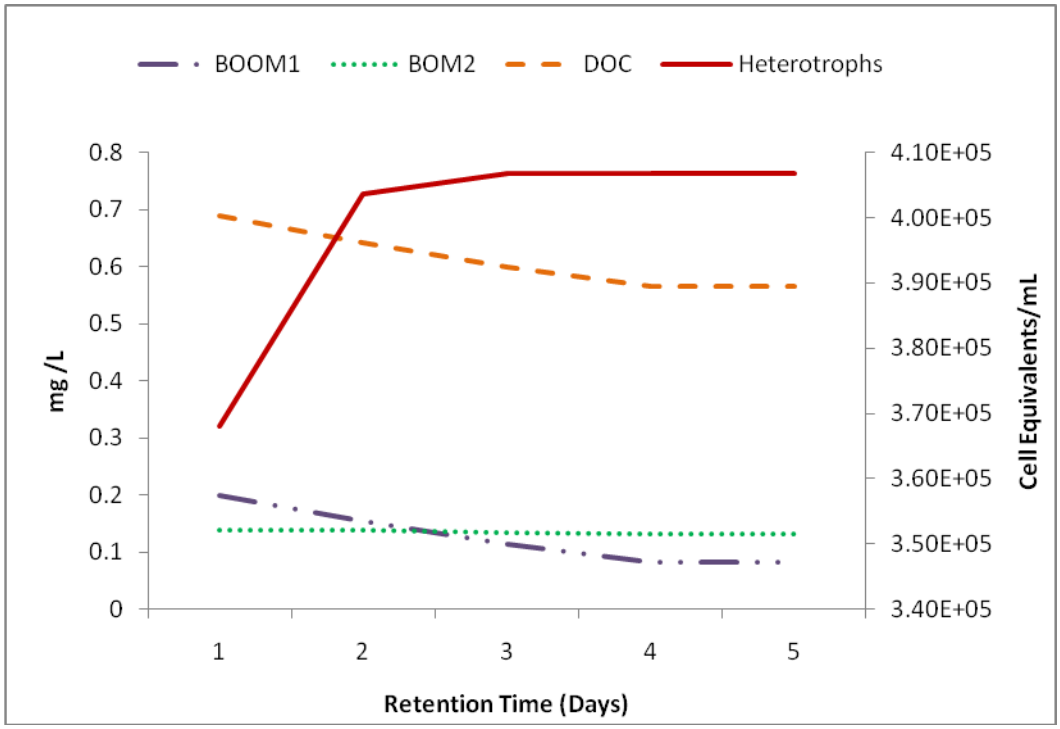

Figure 6.1 Selected Water Quality Parameters from CDWQ-E Batch Simulation of the MAC System. Retention time: 5 days. The heterotrophs represent the total biomass, which is dominated by the biofilm biomass.

Next, I compare BDOC and DOC depletion trends observed from field studies to those forecast by CDWQ-E. In the MAC system, DOC and BDOC were measured as 0.7 and 0.21 mg C/L, respectively, at the sampling site near the entrance of the distribution system. Corresponding samples taken at the site furthest from the entrance of the distribution system had DOC and BDOC at 0.5 and 0.01 mg C/L, respectively. This is equivalent to a 95% reduction in BDOC and 29% reduction in total DOC. CDWQ-E projected that BOM1 and BOM2 decrease from 0.21 to 0.008 mg C/L (BOM1) and 0.14 to 0.132 mg C/L (BOM2) from the start of the simulation to the end of 5 days. This is

equivalent to a 59 % and 20 % reduction for BDOC and DOC, respectively. These results compare very well to results from experimental studies. Again, these results show that the CDWQ-E model can generate reasonable trends of bulk water quality trends for real distribution systems.

The Peoria system had a high DOC concentration at the time that the water entered the distribution system, and this directly translates to a high heterotrophic growth potential. In the model, I assumed an input DOC concentration of 2.0 mg C/L, corresponding to BOM1 and BOM2 concentrations of 0.8 mg C/L and 0.2 mg C/L, respectively. Although BOM1 and BOM2 were above their respective S_{min} concentrations for non-disinfecting conditions, the Peoria system had residual chlorine. I adjusted the S_{min} values to account for disinfection as I did in eqn. 4.1 in Chapter 4. I started the simulation with 2.0 mg of chlorine, and it only dropped to 1.0 mg Cl_2/L by day 3. When residual chlorine was 2.0 mg CL_2/L, $S_{min,BOM1}$ was 0.06 mg C/L and $S_{min,BOM2}$ was 1.3 mg C/L. When residual chlorine dropped to 1.0 mg Cl_2/L, $S_{min,BOM1}$ dropped to 0.05 mg C/L while $S_{min,BOM2}$ dropped to 0.95 mg C/L. In other words, the prevailing BOM1 concentration was always above the disinfectant-adjusted S_{min} and could, therefore, support net heterotrophic growth. BOM2 concentrations could not support HPC growth alone, because they remained below the required S_{min} values. However, BOM2 still could be removed by the heterotrophic biomass grown through utilization of BOM1.

At the Peoria treatment plant, water was filtered and disinfected, and I expected this water to have very low bacterial levels at the time it entered the distribution system. Because I had to choose a non-zero value for heterotrophic bacteria for CDWQ-E simulation, I assumed that water had 1 CFU/mL at the point that is closest to the

distribution system entrance. This is equivalent to 4.3 cells/mL. As with the MAC system, I lumped biofilm and suspended biomass in CDWQ-E. But, I expected the ratio for suspended to biofilm bacteria to be low in this system because of continuous disinfection of detached biofilm biomass in the bulk water. Using a 1:200 ratio for suspended: biofilm bacteria, I used 860 cells/mL as a starting concentration for HPC. Model outputs presented in Figure 6.2 predicted that this water can support net heterotrophic growth, although modest compared to MAC. CDWQ-E predicted that HPC levels will increase from 860 cell/mL to 13,000 cells/mL by the end of day 3. Using the 1:200 suspended to biofilm bacteria, this is equivalent to 63 cells/mL or 15 CFU/mL in suspension. For the Peoria system, I had no field sample at the entrance of the distribution system. For CDWQ-E simulation I chose input DOC (BOM1 and BOM2) and HPC based on values measured at the sampling site furthest from the entrance of the distribution system. At this sampling site HPC were 2,400 cells/mL, or 550 CFU/mL.

Again, I had no BDOC and DOC data for the entrance of the distribution system. DOC and BDOC measured at the site furthest from entrance of the distribution system were 0.96 and 0.4 mg C/L respectively. In CDWQ-E, I assumed that input concentrations of DOC and BDOC are 2.0 mg C/L and 0.8 mg C/L respectively. This translates to 0.8 mg C/L BOM1 and 0.2 mg C/L BOM2. CDWQ-E simulation predicted that BOM1 and BOM2 will be reduced to 0.73 mg C/L and 0.197 mg C/L by the end of day 3. Since BOM is equivalent to BDOC, this is equivalent to 9 % and 3.5 % reductions in BDOC and DOC concentrations, respectively. Because this system had residual chlorine, I expected B/DOC utilization and heterotrophic growth to be modest, even though the BOM was relatively large in the Peoria water.

CDWQ-E predicted that residual chlorine decreases from 2.0 mg Cl_2 at the start of simulation to 1.15 mg Cl_2/L by the end of day 3. The chlorine concentration measured at the sampling site furthest from the entrance of the distribution system was 1.0 mg Cl_2/L. Again, I did not have field data for residual chlorine at any site close to the treatment plant.

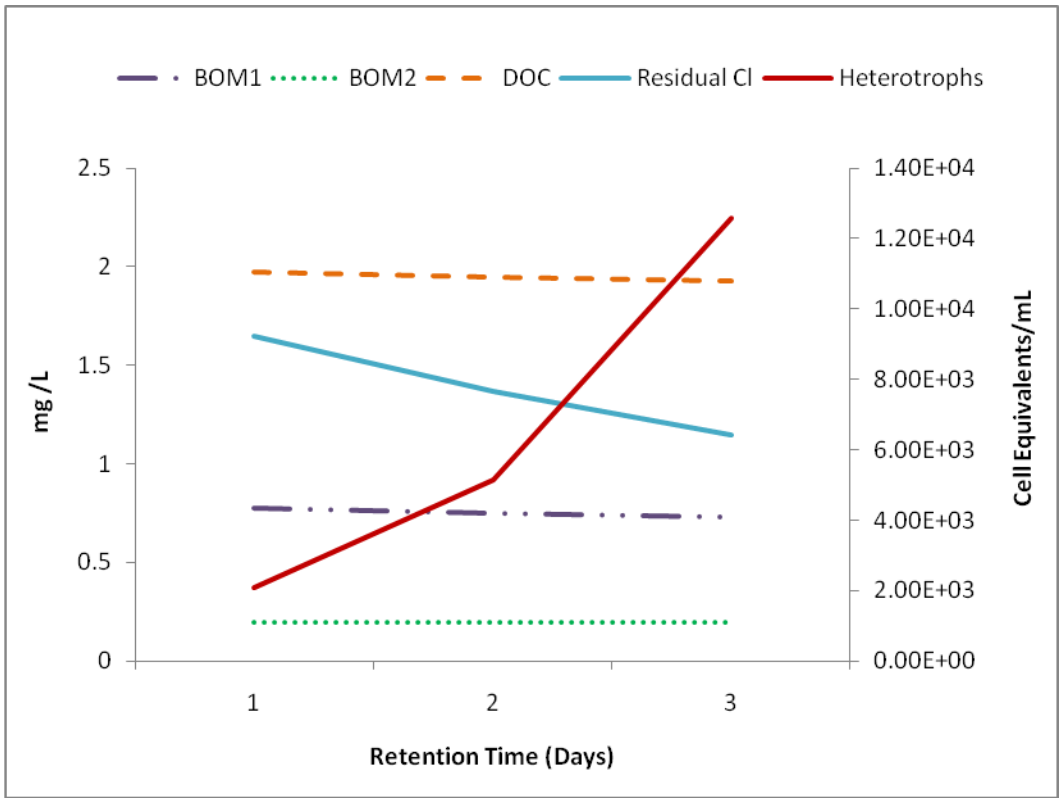

Figure 6.2 Selected Water Quality Parameters from CDWQ-E Batch Simulation of the Peoria System. Retention time: 3 days. Heterotrophs represent total biomass, which is dominated by biofilm biomass.

Finally, I compare, in Table 6.2, key model outputs and typical experimental results from the MAC and Peoria distribution systems and discuss what I learn from comparing model results to experimental results as well as comparing the two distribution

systems. The results obtained from field data and from CDWQ-E simulation highlight four key trends in water quality decay.

First, HPC increase with time, while B/DOC and residual chlorine decreased. I expect this because BDOC is the substrate fueling heterotrophic synthesis.

Second, in the absence of a disinfectant residual, HPC growth depends solely on the availability of substrate, i.e., BOM, at concentrations above the required S_{min}. The relationship between the degradation of organic matter and heterotroph growth was illustrated by the MAC system, in which HPC increased from 3,100 cells/mL to 14,000 cells/mL (+350%) between the sampling site at the entrance of the distribution system to the site near the end of the distribution system, while BDOC/BOM1 only dropped from 0.2 mg/L to 0.01 mg/L (-95%) for the samples collected before the proposed best operational practice. CDWQ-E captured the change in BDOC perfectly and gave the right trend for HPC. Changes in BDOC and DOC changes are much more reliable for comparisons than are changes in HPC. This is because changes in BDOC and DOC depend on total biomass concentration while HPC accumulation primarily depends on the exchange of biomass between the biofilm and bulk water. Other studies have also reported batch model projections of heterotrophic plate counts that were significantly less than what was projected by full-scale models and measured from field data (Woolschlager, 2000).

Third, the presence of a disinfectant residual suppresses HPC growth by increasing the required S_{min} concentrations for BOM1 and BOM2. The role that disinfection plays on heterotrophic abundance is clearly seen in the data from the Peoria system, which had higher BDOC and DOC concentrations than the MAC system. Although the water in the Peoria system had a higher heterotrophic growth potential than

the water in the MAC system HPC growth in the Peoria system was lower than in the MAC system. Having a disinfectant residual elevated the required S_{min} values for BOM1 and BOM2 in the Peoria system, thus suppressing the magnitude of HPC growth.

Fourth, bacterial growth (although modest) in the presence of 2.0 mg Cl_2/L of chlorine underscores the importance of substrate limitation in controlling bacterial growth. This concept is illustrated in detail in Chapter 4.

Without exception, the CDWQ-E model correctly simulated all water quality trends seen in the MAC and Peoria distribution systems. This is evidence that the CDWQ-E, even in batch mode, can be reliably used to forecast water quality trends that may occur in distribution systems.

Table 6.2 Selected Water Quality Parameters from CDWQ-E Simulation

		HPC (cells/mL)	DOC (mg C/mL)	BDOC (mg C/mL)	Cl_2 (mg Cl_2/mL)
MAC	In	CDWQ-E: 3100 Field: 3100	CDWQ-E: 0.7 Field: 0.7	CDWQ-E: 0.2 Field: 0.2	CDWQ-E: N/A Field: N/A
	Out	CDWQ-E: 4070 Field: 14,500	CDWQ-E: 0.56 Field: 0.5	CDWQ-E: 0.08 Field: 0.01	CDWQ-E: N/A Field: N/A
	Trend	Increase	Decrease	Decrease	N/A
Peoria	In	CDWQ-E: 90 Field: N/A	CDWQ-E: 2.0 Field: N/A	CDWQ-E: 0.8 Field: N/A	CDWQ-E: 2.0 Field: N/A
	Out	CDWQ-E:12600 Field: 2400	CDWQ-E: 1.92 Field: 0.96	CDWQ-E: 0.73 Field: 0.4	CDWQ-E: 1.15 Field: 1.0
	Trend	Increase	Decrease	Decrease	decrease

6.2 Modeling Survival of *N. fowleri*

In order to test if the CDWQ-E model can predict long-term survival of *N. fowleri*, as observed in pipe-loop experiments and reported in Chapter 5, I simulated the CDWQ-E model with input conditions similar to conditions observed in the pipe loops at the start of the *N. fowleri* survival experiments. All bacterial growth kinetic parameters were as listed in Table 2.2. Unlike bacteria, *N. fowleri* does not directly oxidize organic substrates; instead it grazes on bacterial biomass. Kinetic parameters used for the growth of *N. fowleri* in CDWQ-E are listed in Table 6.3. To the best of my knowledge, no previous studies have addressed the kinetics of *N. fowleri* growth. Due to lack of specific growth kinetic parameters, I chose *N. fowleri* parameters based on what has been reported for other protozoan studies (Marshall et al., 1997; Murga et al., 2001; Banning et al., 2003; Jamerson et al., 2009).

Table 6.3 Parameters for the Growth of *N. fowleri* by Predation of Bacteria and Its Decay

Parameter	Value
$K_{Bacteria}$ (µg $COD_{N.fowleri\ cells}$/µg $COD_{Bacteria}$)	10,000
$q_{Bacteria}$ (µg $COD_{Bacteria}$/µg $COD_{N.fowleri\ cell}$-h)	0.38
$Y_{N.fowleri}$ (µg $COD_{N.fowleri\ cell}$/µg $COD_{Bacteria}$)	0.06
$b_{N.fowleri}$ (h^{-1})	0.00042

I assumed that the pipe loops were not biofilm dominated. The pipe loops were batch, not flow through; thus, washout for suspended bacteria did not occur, as it would in a full-scale distribution system. I simulated CDWQ-E with a high, 10^5 CFU/mL, starting HPC concentration. While these bacterial densities are typical of the HPC levels observed in the bulk water in the two pipe-loops during laboratory experiments (Table 5.4), bacterial densities this high are generally found in biofilms in distribution systems. The results I presented in Chapter 5 identified biofilms as the main reservoir of *N. fowleri* within distribution systems. Thus, I assumed that the fate of *N. fowleri* was the same in the biofilms and in the suspended phase. To assess the effect of protozoan grazing on bacterial abundance and BOM depletion, I also ran a scenario with the same initial conditions, but no *N. fowleri*. Key input parameter values for the pipe-loop simulation are outlined in Table 6.4.

Table 6.4 Key Starting Conditions for Pipe-Loop Simulation

Parameter	Value
DOC--BOM1:BOM2 (mg C/L)	7.0--0.7:3.15
Disinfectant Residual (mg Cl_2/L)	0.0
HPC (CFU/mL)	$5x10^5$
N. fowleri (cell equivalents/mL)	40
Retention time Days	60

Projected results for DOC utilization, HPC growth, and *N. fowleri* growth are shown in Figure 6.3. As expected, DOC was depleted during the simulation, with BOM1 and BOM2 declining in parallel with the growth of heterotrophs. With or without *N. fowleri*, HPC increased over the first ~ 10 days and then slowly declined for the rest of the simulation period. In the presence of *N. fowleri*, the rate at which HPC accumulated was slightly less than what was observed without *N. fowleri*, and BOM consumption rates also were slightly slower. The difference was due to *N. fowleri* grazing on bacteria, which gives a lower net HPC growth rate and HPC concentration.

N. fowleri increased over the first ~10 days, similar to bacterial mass. The rate of *N. fowleri* growth decreased after about 15 days, when the HPC concentration was less than 10^5 CFU/mL. To test the theoretical basis for this, I estimate the minimum concentration of bacterial biomass, B_{min}, that is required to support positive *N. fowleri* growth using the kinetic parameters listed in Table 6.2:

$$B_{min} = K_{Bacteria}\left(\frac{b_{N.fowleri}}{Y_{N.fowlericel}^{*}q_{Bacteria} - b_{N.fowleri}}\right)$$

$$B_{min} = 10{,}000\,\mu gCOD_{Bacteria}/L\left(\frac{0.000417\,h^{-1}}{0.06\mu gCOD_{N.fowleri}/\mu gCOD_{Bacteria}*0.38\mu gCOD_{Bacteria}/\mu gCOD_{N.fowleri}*h-0.000417\,h^{-1}}\right)$$

$B_{min} = 190\ \mu gCOD_{Bacteria}/L$

$B_{min} = 4.6*10^5\ cells/mL$

From this calculation, I see that positive *N. fowleri* growth requires bacterial concentrations equal to or above $4.5*10^5$ cells/mL (as appendix A1, 1 µg COD/L = 2,400 cells/mL). Since I assume that the ratio of colony forming units per respiring viable cells is 1:4.3, B_{min} is $1.0*10^5$ CFU/mL. Since HPC levels this high are very rarely reported in bulk water, the only exceptions being dead ends and other sites where water stagnates, I deduce that HPC levels normally available in the bulk water are not enough to support active *N. fowleri* growth. Biofilms, on the other hand, can provide high HPC densities, easily upwards of the 10^5/mL mark; thus, biofilms can sustain *N. fowleri* for extended periods of time in the distribution system. Biofilm growth increases bacterial cell densities and by extension the potential for protozoan grazers to thrive.

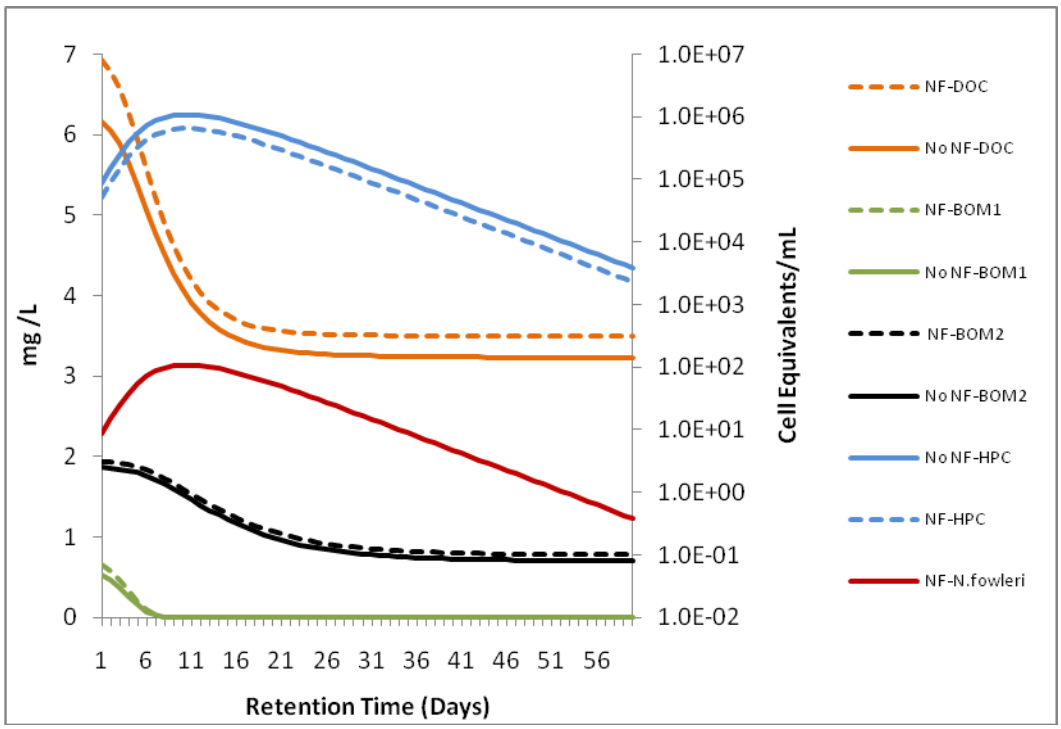

Figure 6.3 Batch CDWQ-E Simulation of Pipe-Loop Showing BOM depletion, heterotrophic growth, and *N.fowleri* growth.

In general, all water quality trends predicted by CDWQ-E for the pipe-loop were similar to trends observed from measured data. First, data from the cast iron and PVC loops showed that HPC increased as DOC was depleted and that the rate at which HPC increased slowed down with decreasing DOC concentrations (Table 5.4). As shown in Table 5.4, measured HPC concentrations in the PVC loop were $4.8x10^4$ CFU/mL, $8.1x10^5$ CFU/mL, and $4.0x10^5$ CFU/mL at weeks 3, 5, and 7 respectively. For the same loop, corresponding DOC measurements were 7, 4.4, and 3.3 mg C/L. During the same time period, the HPC in the cast iron loop were $1.6x10^4$ CFU/mL, $3.2x10^5$ CFU/mL, and $1.7x10^5$ CFU/mL for weeks 3, 5, and 7, and the corresponding change DOCs were 2.7, 2.1, 1.8 mg C/L. HPC densities from both pipe loops increased and then decreased, but remained above the 10^4 CFU/mL through the first 7 weeks. Both trends coincide with

what the CDWQ-E model predicted (Fig. 6.3). The lowest concentration of DOC recorded from pipe-loop data, at the end of week 7 was 1.8 mg C/L in the cast iron loop and 3.3 mg C/L in the PVC loop. CDWQ-E predicted that DOC will drop to 3.2 mg C/L by the end of 8 weeks.

Live *N. fowleri* were detected in both loops 5 months after the start of the laboratory experiment. Data from model simulations showed long-term survival of *N. fowleri*, at least up to 57 days, is possible.

Because *N. fowleri* data from laboratory experiments were limited to presence/absence data based on microscopy, I do not know if *N. fowleri* sustained a net positive growth throughout the first few days, as is shown in Fig. 6.3.

6.3 Summary and Interpretation

In this chapter, I have used the batch version of the CDWQ-E model to simulate water quality decay trends and the growth and survival of *N. fowleri* within distribution systems. The CDWQ-E model explains how bacterial growth depends on organic substrate loading rates, disinfection, and the length of time that treated water is retained within the distribution system. Bacterial counts increase with long residence time, since their growth is coupled to depletion of residual chlorine and DOC. Both trends are similar to what was observed from experimental studies as detailed in Chapter 5. CDWQ-E also predicts that, when introduced to pipe-loops, *N. fowleri*, can survive for at least up to 2 months, as long as bacterial densities are maintained at high concentrations, around 10^5/mL. Linking this finding to the CDWQ-E estimates for heterotrophic abundance in the MAC and Peoria systems, I expect *N. fowleri* to be able to survive in the MAC biofilms (HPC = $4.1*10^5$ cells/mL), but not in bulk water (HPC = 4,100

cells/mL). The Peoria system has low biomass, 12,600 cells/mL in the biofilm and 65 cells/mL in bulk water, and I do not expect *N. fowleri* to thrive in this system even if introduced.

Chapter 7

Summary and Recommendations for future work

7.1 Summary

In this chapter, I summarize the major contributions of this research and make recommendations for future research. Since individual chapters have conclusions/summaries, I only cover the overarching issues here. I list the major contributions of this work in the order of presentation.

The development of CDWQ-E represents a major contribution to the field of water quality modeling in general and to the advancement of understanding of water quality decay in chloraminated systems. One of the main goals of this research was to create a model that represents and relates processes of bacterial growth, disinfectant decay, nitrification, denitrification, and pathogen survival in finished water. The CDWQ-E model successfully accomplishes this goal. This is a major advancement over most water quality models that often separate the issues associated with general bacterial growth and disinfection from pathogen survival.

The CDWQ-E model represents major water quality trends that can be expected in chloraminated water, including but not limited to bacterial growth, depletion of organic matter, disinfectant decay, nitrification, depletion of oxygen, and denitrification. The model fits these trends and offers specific connections between water quality decay trends and chemical and or biological processes behind the trends.

When used to assess the efficacy of substrate limitation versus disinfection in controlling heterotrophic growth, CDWQ-E quantitatively demonstrated that bacterial growth is more effectively controlled by lowering substrate loading into distribution systems than by adding disinfectant residual. High BOM concentrations supported

extensive bacterial growth even in the presence of high levels of chloramine. Model results also showed that total ammonia increases with chloramine decay and the oxidation of organic matter. Within distribution systems high ammonia concentration represent potential for nitrification provided that other conditions necessary for nitrification such as availability of dissolved oxygen and the presence of nitrifying bacteria are met. In principle, a combination of significant nitrification and oxygen depletion may lead to denitrification in distribution system. Results from CDWQ-E simulation showed that in order for heterotrophic denitrification to occur, dissolved oxygen has to be available at a concentration equal to or less than 0.5 mg O/L. Within distribution systems, dissolved oxygen seldom gets below 0.5 mg O/L, thus denitrification is seldom important.

When used to explore water quality decay in full-scale distribution systems, CDWQ-E showed that the extents of bacterial growth and by extension biofilm formation are controlled by organic substrates concentration in the finished water at the time that it enters the distribution system, the presence of disinfectant residuals, and the water's residence time. Bacterial counts increased inside the distribution system. This increase was coupled with the depletion of organic matter and disinfectant residuals. All these trends were exacerbated by longer retentions times. Without exception, water quality trends predicted by CDWQ-E matched trends observed from field and laboratory data.

Another major goal of this research was to evaluate the role of drinking water distribution systems as reservoirs of *N. fowleri*. This goal was accomplished through the use of experimental methods and modeling. Controlled laboratory experiments showed that drinking water can be a source of *N. fowleri*, and the main reservoir appears to be biofilms dominated by bacteria. When introduced to pipe-loop systems, *N. fowleri* successfully attached to biofilms and survived for up to 5 months. Although *N. fowleri*

never was detected in field samples, a high potential for bacterial growth and biofilm formation, the abundance of amoebic activity, and the presence of *Legionella* spp., which is known for its affinity for growth in biofilm communities where protozoa abound, are strong indications of a potential risk that *N. fowleri* could be harbored in the biofilm if introduced. Since no disinfection guidelines and regulations are in force for *N. fowleri*, it remains a threat to the state of Arizona and other locations where source waters have been found to be contaminated and water temperatures are high.

When CDWQ-E was used to evaluate the ability *N. fowleri* to survive in finished drinking water, the model showed that *N. fowleri* can survive for extended periods of time in distribution system environments. Model results also showed that the survival of *N. fowleri* depends on the availability of high bacterial densities in the 10^5/mL range. Since HPC levels this high are rarely reported in bulk water, it is clear that biofilms are the prime reservoirs for amoeba, since biofilm densities are high and, therefore, can sustain *N. fowleri* growth for extended periods of time in a distribution system.

7.2 Future Research

This project has uncovered two new ideas about distribution system biofilms in general and the survival of *N. fowleri* in distribution systems in particular: (1) Distribution systems, dominated by bacterial biofilms, can act as reservoirs of *N. fowleri*. (2) Temporal interventions only have a modest impact on the biofilm reservoirs, since large reductions in biofilm accumulation require that the main cause of bacterial growth, biodegradable organic substrates, be eliminated from the finished water. Carefully planned laboratory and pilot-scale studies should be performed to examine both areas in a controlled environment in more detail.

Another area of future research is motivated by limitations of this project. All kinetics parameters for *N. fowleri* growth were chosen based on studies of other protozoa since no modeling studies have been done on *N. fowleri* in general and within distributions system environments in particular. Once precise laboratory and pilot scale tests on *N. fowleri* survival have been accomplished, CDWQ-E can be re-run with kinetic parameters for *N. fowleri*.

Finally, a full-scale version of CDWQ-E should be developed to account for complex biofilm processes.

REFERENCES

Acker C and Kraska D. 2001. Operation and Maintenance of Water Distribution Systems during and After Conversion to Chloramine Disinfection. Proceedings: American Water Works Association Annual Conference. Denver, CO.

Allegier SA, Summers RS, Jacangelo JG, Hatcher VA, Moll DM, Hooper SM, Swertfeger JW, and Green RB. 1996. A Simplified and Rapid Method for Biodegradable Dissolved Organic Carbon Measurement. Proceedings: American Water Works Association, Water Quality Technology Conference. Boston, MA.

American Water Works Association (AWWA). 1990. Water Quality Modeling in Distribution Systems. Edited by Grayman WM, Clark RM, and Males RM. AWWA, Denver, CO.

American Water Works Association (AWWA). 2005. Computer Modeling of Water Distribution Systems, AWWA Manual M-32, Denver, CO.

Appenzeller BMR, Yanez C, Jorand F and Block C-J. 2005. Advantage Provided by Iron for Escherichia coli Growth and Cultivability in Drinking Water. Applied and Environmental Microbiology 71(9): 5621-5623.

Bae W and Rittmann BE. 1996. A structured Model of Dual-Limitation Kinetics. Biotechnology and Bioengineering 49: 683-689.

Banning N, Toze S, and Mee BJ. 2003. Persistence of biofilm-associated *Escherichia coli* and *Pseudomonas aeruginosa* in Groundwater and Treated Effluent in a Laboratory Model System. Microbiology 149: 47-55.

Bennett NJ, Domachowske J, Khan A, King J, and Cross JT. 2008. Naegleria. The Medscape Journal of Medicine. 28:07-28.

Blair B, Sarkar P, Bright KR, Marciano-Cabral F, and Gerba CP. 2008. Emerging Infectious Diseases 14(9): 1499-1500

Blair BA and Gerba CP. 2006. Occurrence of *Naegleria fowleri* in Well Water in. Arizona. Department of Soil, Water and Environmental Science, University of Arizona, Tucson Arizona (unpublished research report).

Block J-C, Haudidier K, Paquin J, Miazga J, and Levi Y. 1993. Biofilm accumulation in drinking water distribution systems. Biofouling 6:333-343.

Bourbigot, MM, Dodin A, and Lheritier R. 1984. Bacteria in distribution systems. Water Research 18:585-591.

Brent W. 2006. The Arizona Republic, August 30, 2006. Amoeba related Illness Causes death of Six-Year Boy.

Cabanes P, Wallet F, Pringuez E, and Pernin, P. 2001. Assessing the Risk of Primary Amoebic Meningoencephalitis from Swimming in the Presence of Environmental Naegleria fowleri. Applied and Environmental Microbiology 67(7): 2927–2931.

California Department of Health Services. http://www.dhs.cahwnet.gov/ps/ddwem/chemicals/NDMAindex.htm (retrieved May 2008).

Camper AK, Brastrup K, Sandvig A Clement J, Spencer C, and Capuzzi AJ. 2003. Impact of distribution system materials on bacterial regrowth. American Water Works Association 95(7):107-121.

Camper AK, Jones WL, AND Hayes JT. 1996. Effect of Growth Conditions and Substratum Composition on the Persistence of Coliforms in Mixed-Population Biofilms. Applied and Environmental Microbiology 62 (11):4014–4018.

Camper AK, Lechevallier MW, Broadaway S, and McFeters GA. 1985. Growth and Persistence of Pathogens on Granular Activated Carbon Filters. Applied and Environmental Microbiology 50(6): 1378-1382.

Camper AK, McFeters GA, Characklis WG, and Warren LJ. 1991. Growth Kinetics of Coliform Bacteria under Conditions Relevant to Drinking Water Distribution Systems. Applied and Environmental Microbiology 57(8): 2233-2239.

Camper AK. 1996. Factors limiting microbial growth in distribution systems: Pilot Experiments. American Water Works research Foundation, Denver CO.

CDC. 2008. http://www.ama.cdc.gov/amax (retrieved May 2008).

CDC. 2010. http://www.dpd.cdc.gov/dpdx (retrieved January 2010).

Chandy JT, and Angles ML. 1999. Significance of limiting nutrients on biofilm formation in drinking water distribution systems. Proceedings: International Water Association Biofilm Systems Conference. London, United Kingdom.

Characklis WG. 1981. Fouling biofilm development: a process analysis. Biotechnology and Bioengineering 23: 1923–1960.

Chen, C-I, Griebe T, and Characklis WG. 1993. Biocide action of monochloramine on biofilm systems of *Pseudomonas aeruginosa*. Biofouling 7: 1-17.

Clark BH. 2001. Microbiologically Influenced Corrosion in Fire Sprinkler Systems. Fire Protection Engineering 9: 14-22.

Clark RM, Grayman WM, and Males RM. 1988. Contaminant Propagation in Distribution Systems. Environmental Engineering 114:(2).

Clark RM, Grayman WM, Goodrich J, Deininger RA, and Hess A. 1991. Field-testing distribution water quality models. American Water Works Association 83(7): 67-75.

Cline M, Marciano-Cabral MF, and Bradley SG. 1983. Comparison of *Naegleria fowleri* and *Naegleria giruibeni* Cultivated in the Same Nutrient Medium. Protozoology 30: 387-391.

Craun GF, Calderon RL, and Craun MF. 2005. Outbreaks associated with recreational water in the United States. International Journal of Environmental Health Research 15: 243–262.

Craun, M.F. 2006. Waterborne outbreaks reported in the United States. Water and Health.04 (l2): 19-30.

Cunliffe DA. 1991. Bacterial nitrification in chloraminated water supplies. Applied Environmental Microbiology 57: 3399-3402.

D'Souza CD and Kumar MSM. 2010. Comparison of ANN Models for Predicting Water Quality in Distribution Systems. American Water Works Association 102(7): 92-106.

De Silva DG and Rittmann BE. 2000. Nonsteady-State Modeling of Multispecies Activated-Sludge Processes. Water Environment Research 72 (5): 554-565.

DeNapoli TS, Rutman JY, Robinson JR, and Rhodes MM. 1996. Primary Amoebic Meningoencephalitis after Swimming in the Rio Grande. Texas Medical Association 92:59-63.

DiGiano FA, Travaglia A, and Zhang W. 2000. Water Age (EPANET) and Mean Residence Time of Fluoride Tracers in Distribution Systems. In Proceedings of American Water Works Association Water Quality Technology Conference. Denver, CO.

Donlan R M. 2002. Biofilms and Device-Associated Infections. Centers for Disease Control and Prevention Atlanta, Georgia, US.

Dukan S, Levi Y, Pirious P, Guyon F, and Villion P. 1996. Dynamic modeling of bacterial growth in drinking water networks. Water Research 30(9): 1991-2002.

Earnhardt KB Jr. 1980. Chlorine resistant coliform-the Muncie, Indiana, experience. Proceedings of the American Water Works Association Water Quality Conference. American Water Works Association: 371-376.

Ellis BD, Butterfield P, Jones WL, McFeters GA, and Camper AK. 2000. Effects of Carbon Source, Carbon Concentration, and Chlorination on Growth Related Parameters of Heterotrophic Biofilm Bacteria. Microbial Ecology 38: 330-347.

Emde KM, Smith DW, and Facey R. 1992. Initial investigation of microbially influenced corrosion (mic) in a low temperature water distribution system. Water Research 26: 169-175.

Fair GM and Geyer JC. 1971. Water Supply and Waste-Water Disposal. John Wiley and and Sons, Inc,NY.

Fiordalisi I, Christie J, and Moffitt C. 1992. Amoebic meningoencephalitis-North Carolina 1991. Morbidity and Mortality Weekly Report Center for Disease Control. 41:437-439.

Geldreich EE, Nash H, Reasoner DJ, and Taylor R. 1972. The necessity of controlling bacterial populations in potable waters: Community water supply. American Water Works Association 64: 596-602.

Goshko MA, Minnigh HA, Pipes WO, and Christian RR. 1983b. Relationships between standard plate counts and other parameters in water distribution systems. American Water Works Association 75:568-571.

Goshko MA, Pipes WO, and Christian RR. 1983a. Coliform occurrence and chlorine residual in small water distribution systems. American Water Works Association75:371-374.

Grayman WM, Clark RM, and Males RM. 1988. Modeling distribution system water quality: Dynamic Approach. American Water Works Association 85(7): 67-77.

Grayman WM, Rossman LA Deininger RA, Smith CD, Arnold CN, and Smith JF. 2004. Mixing and Aging of Water in Distribution System Storage Facilities. American Water Works Association 96(9):70-80. 2.

Grigorescu AS and Hozalski RM. 2010. Modeling HAA Biodegradation in Biofilters and Distribution Systems. American Water Works Association 102(7): 67-79.

Gullick RW, Grayman WM, Deininger RA, and Males RM. 2003. Design of Early Warning Monitoring Systems for Source Waters. American Water Works Association 95(11):58-72.

Gyori E. 2003. 19 Year Old Male with Febrile Illness after Jet-Ski Accident. Brain Pathology 13: 237–239.

Hack DJ. 1984. State regulation of chloramine. American Water Works Association 77(1): 46-49.

Hall EL and Dietrich AM. 1999. A brief history of drinking water. Openflow 26(6): 46-51.

Hobie JE, Daley RH, and Jasper S. 1977. Use of nucleopore filters for counting bacteria by fluorescence microscopy. Applied and Environmental Microbiology 33:1225-1228.

Insurance Services Office (ISO). 2003. Fire Suppression Rating Schedule. Insurance Services Office, NY.

Jacobs S, Reiber S, and Edwards M. 1998. Sulfide-induced copper corrosion. American Water Works Association 90(7): 62-73.

Jamerson M, Remmers K, Cabral G, and Marciano-Cabral F. 2009. Survey for the Presence of *Naegleria fowleri* Amebae in Lake Water Used to Cool Reactors at a Nuclear Power Generating Plant. Parasitology Reviews 104:969–978.

Joret J, Levi Y, and Volk C. 1991. Biodegradable Dissolved Organic Carbon (BDOC) Content of Drinking Water and Potential Regrowth of Bacteria. Water Science and Technology 24(2): 95-100.

Kiene L, Lu W, and Levi Y. 1998. Relative importance of the phenomena responsible for chlorine decay in drinking water distribution systems. Water Science and Technology 38(6): 219-227.

Krasner SW, Weinberg HS, Richardson SD, Pastor SJ, Chinn R, Sclimenti MJ, Onstad G and Thruston AD. 2006. Occurrence of a new generation of disinfection by-products. Environmental Scieince and Technology 40:7175–7185

Laspidou CS and Rittmann BE. 2002. Non-steady state modeling of extracellular polymeric substances, soluble microbial products, and active and inert biomass.Water Research 36:1983–1992

Le Dantec C, Dugust J-P, Montinel A, and Dumoutier N. 2002. Occurrence of Mycobacteria in Water Treatment Lines and in Water Distribution Systems. Applied and Environmental Microbiology 68(11): 5318-5325.

Le Puil M. 2004. Biostability in drinking water distribution systems: A study at pilot scale. Ph.D. dissertation, University of Central Florida, Orlando Florida.

LeChevallier MW and McFeters GA. 1985. Enumerating injured coliforms in drinking water. American Water Works Association 77(6): 81-87.

LeChevallier MW and McFeters GA. 1985. Interactions between heterotrophic plate count bacteria and coliform organisms. Applied and Environmental Microbiology 49: 1338-1341.

LeChevallier MW, Babcock T, and Lee RG. 1987. Examination and characterization of distribution system biofilms. Applied and Environmental Microbiology 53: 2714-2724.

LeChevallier MW, Schulz W, and Lee RG. 1991. Bacterial nutrients in drinking water. Applied and Environmental Microbiology 57: 857-862.

LeChevallier MW, Welch NJ, and Smith DB. 1996. Full-scale studies of factors related to coliform regrowth in drinking water. Applied and Environmental Microbiology 62: 2201-2211.

Lee, SH, O'Connor JT, and Banerji SK. 1980. Biologically mediated corrosion and its effects on water quality in distribution systems. American Water Works Association 72(11): 636-645.

Little B, Wagner P, Hart K, Ray R, Lavoie D, Nealson K, and Aguilar C. 1998. The role of biomineralization in microbiologically influenced corrosion. Biodegradation 9:1-10.

Lozano-Alarcorn E, Bradley GA, Houser BS, and Visvesvara GS. 1997. Primary Amebic Meningoencephalitis Due to *Naegleria fowleri* in a South American Tapir. Veterinary Pathology 34: 239-243.

Marciano-Cabral F and Fulford DE. 1986. Cytopathology of Pathogenic and Nonpathogenic *Naegleria* Species for Cultured Rat Neuroblastoma Cells. Applied and Environmental Microbiology 51: 1133-1137.

Marciano-Cabral F, MacLean R Mensah A, and LaPat-Polasko L. 2003. Identification of *Naegleria fowleri* in Domestic Water Sources by Nested. Applied and Environmental Microbiology 69(10): 5864–5869.

Marciano-Cabral F. 1988. Biology of *Naegleria* spp. Microbiological Reviews: 114-133.

Marciano-Cabral F. 2004. Introductory remarks: Bacterial Endosymbionts or Pathogens of Free-Living Amoebae. Eukaryotic Microbiology 51: 497–501.

Mathieu L, Block J-C, Prevost M, Maul A, and DeBischops R. 1995. Biological stability of drinking water in the city of Metz distribution system. Water Services Research. Technology 44(5): 230-239.

Maul A, El-Shaarawi AH, and Block J-C. 1985. Heterotrophic bacteria in water distribution systems, part 1: Spatial and temporal variation. Science of the Total Environment 44: 201-214.

Mays LW. 2001. Water Resources Engineering. John Wiley and Sons Publishing Inc. New York, NY.

Momba MNB, Kfir R, and Cloete TE. 2000. An overview of biofilm formation in distribution systems and its impact on the deterioration of water quality. Water SA, 26(1): 59-66.

Center for Biofilm Engineering, Montana State University (MSU-CEB). www.msu.edu/cbe (retrieved July 2010).

Morbidity and Mortality Weekly Report. 2000. Surveillance for Waterborne-Disease Outbreaks—United States, 1997-1998. Center for Disease Control Summer Surveillance 49:1-21. Report by Barwick RS, Levy DA, Craun GF, Beach MJ, and Calderon RL.

Murga R, Forster TS, Brown E, Pruckler JM, Fields BS, and Donlan RM. 2001. Role of Biofilms in the Survival of *Legionella pneumophila* in a Model Potable-Water System. Microbiology 147: 3121–3126.

Neden DG, Jones RJ, Smith JR, Kirmeyer GJ, and Foust GW. 1992. Comparing chlorination and chloramination for controlling bacterial regrowth. American Water Works Association 84(7): 80-88.

Newsome AL, Baker RL, Miller RD, and Arnold RR. 1985. Interactions between *Naegleria fowleri* and *Legionella pneumophila.* Journal of Infections and Immunity 2(50): 449-452.

Norton CD and LeChevallier MW. 2000. A pilot study of bacteriological population changes through potable water treatment and distribution. Applied and Environmental Microbiology 66(1): 268-276.

Odell LH, Kirmeyer GJ, Wilczak A, Jacangelo JG, Marcinko JP, and Wolfe RL. 1996. Controlling nitrification in chlorinated systems. American Water Works Association 88(7): 86-96.

Oliveri VP, Bakalian AE, Bossung KW, and Lowther ED. 1985. Recurrent coliforms in water distribution systems in the presence of free residual chlorine. In Jolley R, Bull W. Davis, Katz M, Roberts W, and Jacobs V (Editors). Water chlorination – Chemistry, environmental impact, and health effects (pp. 651-656). Chelsea, Michigan: Lewis Publishers, Inc.

PL107-188. Public Bioterrorism Act. 2002.

Prentice M. 2001. Disinfection Modeling Study for the Owen Sound Water Distribution System. Proceedings: American Water Works Association Annual Conference. Denver, CO.

Prevost M, Gauthier C, Hureiki L, and Servais P. 1998. Removal of amino acids, biodegradable organic carbon and chlorine demand by biological filtration in cold water. Environmental Technology 19: 903-911.

Reasoner DJ, and Geldreich EE. 1985. A new medium for enumeration and subculture of bacteria from potable water. Applied Environmental Microbiology 49: 1-7.

Regan JM, Harrington GW and Noguera DR. 2002. Ammonia and Nitrite-Oxidizing Bacterial Communities in a Pilot-Scale Chloraminated Drinking Water Distribution System. Applied and Environmental Microbiology 68(1): 73-81.

Regli S. 2007. A Public Health Perspective on Distribution Systems TCR/DS Stakeholder Workshop January 30, 2007.

Reilly KJ and Kippin JS. 1983. Relationship of bacterial counts with turbidity and free chlorine in two distribution systems. American Water Works Association 75(6): 309-312.

Richardson SD. 2005. New Disinfection By-product Issues: emerging DBPs and Alternative Routes of Exposure. Global NEST Journal 7(1):43-60,

Rittmann BE and McCarty PL. 2001. Environmental Biotechnology: Principles and Applications. McGraw-Hill Book Company, New York.

Rittmann BE and Snoeyink VL. 1984. Achieving Biologically Stable Drinking Water. American Water Works Association 76(10): 106-114.

Rittmann BE, and Huck PM. 1989. Biological Treatment of Public Water Supplies. CRC Critical Reviews in Environmental Control 19(2): 119-184.

Rittmann BE, Regan JM, and Stahl DA. 1994. Nitrification as a Source of Soluble Organic Substrate in Biological Treatment. Water Science and Technology 30 (6): 1–8.

Rose JB. 1997. Environmental ecology of Cryptosporidium and public health implications. Annual Reviews in Public Health 18:135-161.

Rossman LA and Boulos PF. 1996. Numerical methods for modeling water quality in distribution systems: a comparison. Water Resources Planning and management 4: 137-146.

Rossman LA, Clark RM, and Grayman WM. 1994. Modeling chlorine residuals in drinking water distribution systems. Environmental Engineering 120: 803-819.

Schuster FL. 2002. Cultivation of Pathogenic and Opportunistic Free-Living Amebas. Clinical Microbiology 15(3): 342–354.

Servais P, Laurent P, and Randon G. 1995. Comparison of the bacterial dynamics in various French distribution systems. Water Services Research and Technology 44(1): 10-17.

Sibille I, Sime-Ngando T, Mathieu L, and Block JC. 1998. Protozoan Bacterivory and *Escherichia coli* Survival in Drinking Water Distribution Systems. Applied and Environmental Microbiology 64(1): 197–202.

Standard Methods for the Examination of Water and Wastewater, 19th Edition. 1995. Published jointly by the American Public Health Association (APHA), American Water Works Association (AWWA), and the Water Environment Federation (WEF), Washington.

Szewzyk U, Szewzyk R, Manz W, and Schleifer K-H. 2000. Microbiological Safety of Drinking Water. Annual Reviews in Microbiology 54:81-127.

Tuovinen OH and Hsu JC. 1982. Aerobic and anaerobic microorganisms in tubercles of the Columbus, Ohio, water distribution system. Applied and Environmental Microbiology 44: 761-764.

Tuovinen OH, Button KS, Vuorinen A, Carlson L, Mair DM, and Yut LA. 1980. Bacterial, chemical, and mineralogical characteristics of tubercles in distribution pipelines. American Water Works Association 72(11), 626-635.

Tyndall RL, Ironside KS, Metler PL, Tan EL, Hazen TC, and Fliermans CB. 1989. Effect of Thermal Additions on the Density and Distribution of Thermophilic Amoebae and Pathogenic *Naegleria fowleri* in a Newly Created Cooling Lake. Applied and Environmental Microbiology 55:722–732.

U.S. Environmental Protection Agency. 1999. EPA Guidance Manual Alternative Disinfectants and Oxidants. Washington, DC.

Uber J, Shang F, Polycarpou M, and Wang Z. 2003. Feedback Control of Booster Chlorination Systems. AwwaFR, Denver, CO.

US- Environmental Protection Agency. 1998. National Drinking Water Regulations: Disinfectants and Disinfection By-Products. Final Rule. EPA 815-F-98-010, Washington, DC.

US- Environmental Protection Agency. 2002. The Clean Water and Drinking Water Infrastructure Gap Analysis, Washington, DC.

US- Environmental Protection Agency. 2003. Stage 2 Disinfection By-Product Rule, Initial Distribution System Evaluation Guidance Manual, Washington, DC.

US- Environmental Protection Agency. 2010. National Primary Drinking Water Regulations. EPA 816-F-09-004, Washington, DC.

US-Environmental Protection Agency. 1974. Safe Drinking Water Act (SDWA), Public Law 93-523, Washington, DC.

US-Environmental Protection Agency. 2001. National Primary Drinking Water Regulations: Draft Stage 2 Disinfectants and Disinfection By-Products Preamble, Washington, DC.

US-Environmental Protection Agency. 2005. Water Distribution Systems: Field Studies, Modeling, and Management – A reference Guide for Utilities. Washington, DC.

Van der Kooij D and Veenendaal H. 1992. Assessment of the biofilm formation characteristics of drinking water. Paper presented at the Water Quality Technology Conference, American Water Works Association, Denver, CO.

Van Der Kooij D. 2000. Biological Stability: A Multidimensional Quality Aspect of Treated Water. Water, Air, and Soil Pollution 123:25–34.

Van der Wender E and Characklis WG. 1990. Biofilms in potable water distribution systems. In: McFeters GA (ed) Drinking Water Microbiology: Progress and Recent Developments 249-268.

Vandermeyden C and Hartman D. 2001. Water Quality Modeling of a Complete Distribution System Development, Results, and Practical Applications. Proceedings: American Water Works Association Annual Conference. Denver, CO.

Vasconcelos JJ, Rossman L A, Grayman WM, Boulos PF, and Clark RM. 1997. Kinetics of chlorine decay. American Water Works Association 89(7): 54-65.

Videla HA. 1989. Metal dissolution/redox in biofilms. In W. G. Characklis and P. A. Wilderer (Eds.), Structure and function of biofilms (pp. 301-320). John Wiley & Sons, New York, NY.

Wajon JE, Kavanagh B, Kagi R, Rosich R., and Alexander R. 1988. Controlling swampy odors in drinking water. American Water Works Association 80(6): 77-83.

Walski TM, Chase DV, Savic DA, Grayman W, Beckwith S, and Koelle E. 2003. Advanced Water Distribution Modeling and Management. Haestad Press, Waterbury, CT.

Weisbuch JB. 2003. *Naegleria Fowleri* in Arizona: Tracking a Deadly Ameba (unpublished report).

White GC. 1986. Handbook of Chlorination and Alternative Disinfections. Van Nostrand Reinhold, New York.

Whiting Brent. 2006. *The Arizona Republic*, August 31, 2006. Amoeba Related Illness Causes Death of Six-Year old Boy.

Wikipedia. https://wikipedia.org/wiki/Sun_Belt (retrieved February 2010).

Williams MM and Braun-Howland EB. 2003. Growth of *E.coli* in model distribution systems exposed to hypochlorous acid and monochloramine. Applied and Environmental Microbiology 69(9): 5462-5271.

Wolfe RE, Lieu NI, Izaguire G, and Means EG. 1990. Ammonia-oxidizing bacteria in a chloraminated distribution system: Seasonal occurrence, distribution, and disinfection resistance. Applied and Environmental Microbiology 56(2): 451-462.

Wolfe RL and Lieu NI. 2001. Nitrifying Bacteria in Drinking Water. Encylopedia of Environmental Microbiology (4). Wiley and Sons, New York NY.

Wolfe RL, Means EG III, Davis MK, and Barrett SE. 1988. Biological nitrification in covered reservoirs containing chloraminated water. American Water Works Association 80(9)): 109-114.

Woolschlager JE, Rittmann BE, and Piriou P. 2005. Water quality decay in distribution systems-problems, causes and new modeling tools. Urban Water Journal 2(2): 69-79.

Woolschlager JE. 2000. A comprehensive disinfection and water quality model for drinking water distribution systems. Ph.D. Dissertation, Northwestern University, Evanston, IL.

World Health Organization (WHO). 2000. Disinfectants and Disinfectant By-products: Environmental Health Criteria 216, International Program on Chemical Safety. Geneva, World Health Organization.

Zhamg Y and Edwards M 2010. Nutrients and Metals Effects on Nitrification in Drinking Water Systems. American Water Works Association 107(7): 56-65.

Zhang W, and DiGiano FA. 2003. Comparison of Bacterial Regrowth in Distribution Systems Using Free Chlorine and Chloramine: A Statistical Study of Causative Factors. Water Research 36(6):1469-1482.

Zhang W, Miller CT, and DiGiano FA. 2004. Bacterial re-growth models for water distribution systems incorporating alternating split-operator solution technique. Environmental Engineering (ASCE) 130(9): 932-941.

Zhang Y, Griffin A, and Edwards M. 2008. Nitrification in Premise Plumbing: Role of Phosphate, pH, and Pipe Corrosion. Environmental Science and Technology 42(12): 4280-4290.

Zhang Y, Love N, and Edwards M. 2009. Nitrification in Drinking Water Systems. Environmental Science and Technology 39(3):153-161.

APPENDIX A

DERIVATIONS OF CONVERSIONS USED IN CDWQ-E

A.1 Organic Matter and Biomass as Chemical Oxygen Demand (COD)

In line with the original CDWQ model (Woolschlager, 2000), in the CDWQ-E all organic matter and biomass are converted to chemical oxygen demand (COD). COD is the theoretical grams of O_2 used in a redox reaction in which all electrons contained in the carbon are removed and transferred to O_2. This is done to maintain consistent units and track the oxidation state of carbon in the model. The conversion factors used for organic matter is 2.67 μg COD/μg C and for biomass is 4.16 x 10^{-7} μg COD/cell (Woolschlager, 2000). There are two on which the conversions are based, (i) All organic matter was assumed to have the chemical equation as biomass – $C_5H_7O_2N$ (Hoover and Porges 1952; Woolschlager, 2000), and (ii) All organic matter carbon was assumed to have an oxidation state of zero.

Half reactions used in formulation of conversions are as follows:

Bacterial cell synthesis with ammonia as the nitrogen source.

$$\frac{1}{20}C_5H_7O_2N + \frac{9}{20}H_2O = \frac{1}{5}CO_2 + \frac{1}{20}HCO_3^- + \frac{1}{20}NH_4^+ + H^+ + e^-$$

Reaction for oxygen as an electron acceptor:

$$\frac{1}{2}H_2O = \frac{1}{4}O_2 + H^+ + e^-$$

Conversion derivation is as follows:

Organic matter as C to COD (2.67μg COD/μg C):

$$\left(\frac{\frac{1}{4}mole\,O_2}{1e^-eq.}\right)\left(\frac{32g\,O_2}{mole\,O_2}\right) = 8g\,O_2 \Big/ e^-eq.$$

$$\left(\frac{\frac{1}{20}mole\,C_5H_7O_2N}{1e^-eq.}\right)\left(\frac{60g\,C}{mole C_5H_7O_2N}\right) = 3.0gC \Big/ e^-eq.$$

$$\left(\frac{8g\,O_2}{1e^- eq.}\right)\left(\frac{1e^- eq.}{3.0g\,C}\right) = 2.67g\,O_2/g\,C \; or \; 2.67\mu g\,COD/\mu g\,C$$

Cells to COD (4.16 x10^{-7} μg COD/cell):

Assuming that cells to have a carbon content of 1.56 $\times 10^{-7}$ μg C/cell, gives:

$$\left(\frac{8g\,O_2}{1e^- eq.}\right)\left(\frac{(4-0)\,e^- eq.}{mole\,C}\right) = 32g\,O_2/mole\,C$$

$$\left(\frac{32\mu g\,O_2}{\mu mole\,C}\right)\left(\frac{1.56\times10^{-7}\,\mu g\,C}{cell}\right)\left(\frac{\mu mole\,C}{12\mu g\,C}\right) = 4.16\times10^{-7}\,\mu g\,COD/cell$$

A.2 Moles of Carbon and Nitrogen in Biomass and Organic Matter.

CDWQ tracks carbon in BOM and biomass as μg COD/L, CO_2 as mole/L of C, and nitrogen species (e.g., NH_3, NO_2^-, NO_3^-) as mole/L of N. The incorporation of carbon and nitrogen in biomass and the release of carbon and nitrogen from organic matter and biomass reactions requires the following conversions: $\lambda_C = 3.12 \times 10^{-8}$ mole of C per μg COD and $\lambda_N = 6.24 \times 10^{-9}$ mole of N per μg COD. These conversions are derived as follows:

Mole of C per μg COD (assuming all carbon in COD is at an oxidation state of zero):

$$\left(\frac{\mu g\,C}{2.67\mu g\,COD}\right)\left(\frac{moleC}{12\times10^6\,\mu gC}\right) = 3.12\times10^{-8}\,moleC/\mu g\,COD$$

Mole of N per μg COD (assuming that organic matter and biomass is $C_5H_7O_2N$):

$$\left(\frac{3.12\times10^{-8}\,moleC}{\mu g\,COD}\right)\left(\frac{\frac{1}{5}moleN}{moleC}\right) = 6.24\times10^{-9}\,moleN/\mu g\,COD$$

A.3 Cells per mL per μg COD/L.

CDWQ-E tracks carbon in biomass as μg COD/L. To compare the CDWQ-E model to measured cell count requires the following conversion: 2,404 cells per μg COD/L. This conversion is derived below:

Cells/mL per μg COD/L:

$$\left(\frac{cell}{4.16\times10^{-7}\ \mu g\ COD}\right)\left(\frac{liter}{1000ml}\right) = 2{,}404 cells\ per\ ml \Big/ \mu g\ COD\ per\ L$$

Assuming that the ratio of cells/mL to colony forming units (CFU) is 4.3:1 (Woolschlager, 2000), 2404 cells/mL = 559 CFU/mL.

APPENDIX B

CHEMICAL AND MICROBILOGICAL WATER QUALITY DATA FOR ALL FIELD AND LABORATORY WATER AND BIOFILM SAMPLES

B1. Summary of chemical water quality data for field and laboratory studies. Total Number of samples = 28.

Sample ID	Chemical Data				
	Chlorine (mg /L)	**DOC (mg /L)**	**Ammonia (mg N/L)**	**Nitrate (mg /L)**	**Nitrate (mg /L)**
DS Entrance (MAC B)	N/A	0.7	0.3	0.002	0.5
DS Entrance (MAC A)	N/A	0.6	0.5	0.002	0.07
DS End (MAC B)	N/A	0.5	0	0.003	1.3
DS End (MAC A)	N/A	0.54	0.3	0.009	0.98
Reservoir Bf (MAC B)	N/A	0.78	0.3	0	0.09
Reservoir Bf (MAC A)	N/A	0.5	-	0.001	0.01
Dead-End Bf (MAC B)	N/A	0.5	0	0.002	0.5
Dead-End Bf (MAC A)	N/A	0.6	0.004	0.002	0.001
Hydrant Bf (MAC B)	N/A	-	0	0	0
Hydrant Bf (MAC A)	N/A	0.5	0	0	0.01
Valve Bf (MAC B)	N/A	-	0	0	0
Valve Bf (MAC A)	N/A	0.7	0.2	0.003	0.09
Meter Bf (MAC B)	N/A	0.6	0.5	0.002	0.08
Meter Bf (MAC A)	N/A	0.5	0.5	0.002	0
DS End (Peoria B)	N/A	N/A	N/A	N/A	N/A
DS End (Peoria A)	0.9	0.96	0.1	0.008	0.01
Reservoir Bf (Peoria B)	0.7	2.1	0.08	0.001	1
Reservoir Bf (Peoria A)	0.9	1.6	0.1	0.002	0.05
Dead-End Bf (Peoria B)	-	-	0	0	0
Dead-End Bf (Peoria A)	1	0.88	0.1	0	0
Hydrant Bf (Peoria B)	0.3	3.6	0.1	0.002	0.1
Hydrant Bf (Peoria A)	0.1	3	0.5	0.06	0.03
Valve Bf (Peoria B)	0.8	1.3	0.3	0.009	2.5
Valve Bf (Peoria A)	0.9	1.4	0	0.001	0.1
Meter Bf (Peoria B)	1	1.9	0	0	0
Meter BF (Peoria A)	0.8	1.7	0	0	0.07

B2. Summary of microbiological water quality data for all field and laboratory studies. Total no. of samples = 28.

Sample ID	Microbiological Data				
	Amoebic activity	***N. fowleri***	***Acanthamoeba* spp.**	***Legionella* spp.**	**HPC CFU/mL**
DS Entrance (MAC B)	-	N/A	N/A	N/A	730
DS Entrance (MAC A)	-	N/A	N/A	N/A	300
DS End (MAC B)	-	N/A	N/A	N/A	3300
DS End (MAC A)	-	N/A	N/A	N/A	850
Reservoir (MAC B)	-	N/A	N/A	N/A	
Reservoir (MAC A)	-	N/A	N/A	N/A	
Reservoir Bf (MAC B)	+	–	–	+	1200
Reservoir Bf (MAC A)	+	–	–	+	7200
Dead-End Bf (MAC B)	–	–	–	+	11000
Dead-End Bf (MAC A)	+	–	–	–	2200
Hydrant Bf (MAC B)	+	–	–	–	-
Hydrant Bf (MAC A)	+	–	–	+	500
Valve Bf (MAC B)	+	–	–	–	-
Valve Bf (MAC A)	+	–	–	+	3100
Meter Bf (MAC B)	–	–	–	+	1770
Meter Bf (MAC A)	–	–	–	+	700
DS End (Peoria B)	N/A	N/A	N/A	N/A	N/A
DS End (Peoria A)	-	-	-	-	550
Reservoir Bf (Peoria B)	+	–	–	+	0
Reservoir Bf (Peoria A)	+	–	–	+	38
Dead-End Bf (Peoria B)	+	–	–	–	-
Dead-End Bf (Peoria A)	+	–	–	–	2400
Hydrant Bf (Peoria B)	+	–	–	+	710
Hydrant Bf (Peoria A)	–	–	–	–	550
Valve Bf (Peoria B)	–	–	–	+	550
Valve Bf (Peoria A)	+	–	–	+	2000
Meter Bf (Peoria B)	+	–	–	+	4000
Meter BF (Peoria A)	–	–	–	–	1000